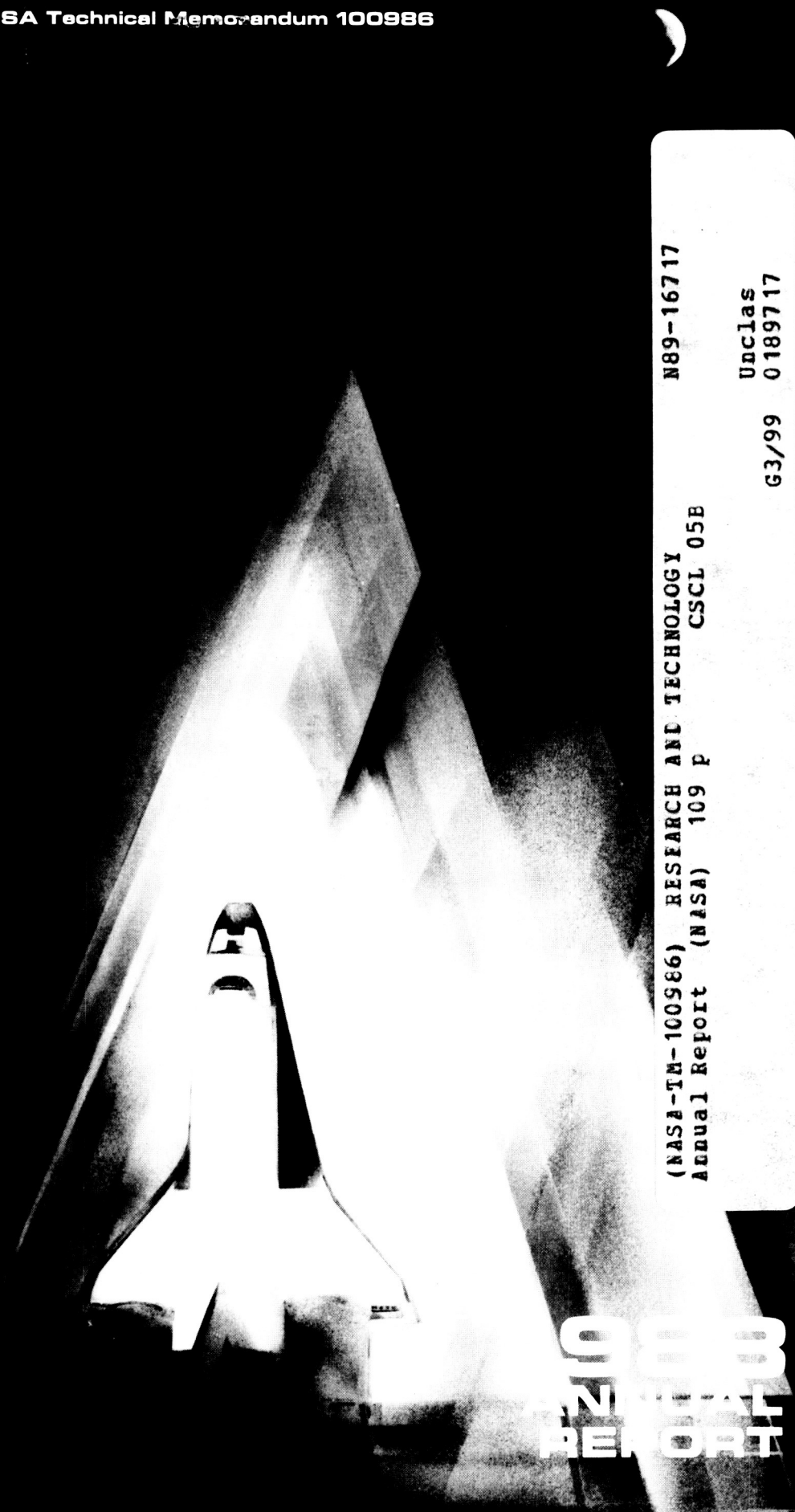


RESEARCH AND TECHNOLOGY



210
REPORT

John F. Kennedy
Space Center

N89-16717

(NASA-TM-100986) RESEARCH AND TECHNOLOGY
Annual Report (NASA) 109 P CACL 05B

G3/99 Unclass
0 189717

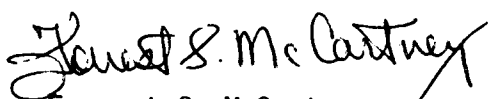
"Cathedral" - mixed media by Sara Larkin, is part of the NASA art collection. The original is currently on display in the Galaxy gallery, Spaceport USA.

**Research and Technology
1988 Annual Report
of the John F. Kennedy
Space Center**

FOREWARD

As the NASA Center responsible for assembly, checkout, servicing, launch, recovery, and operational support of Space Transportation System elements, and payloads, Kennedy Space Center is placing increasing emphasis on the Center's research and technology program. In addition to strengthening those areas of engineering and operations technology that contribute to safer, more efficient, and more economical execution of our current mission, we are developing the technological tools needed to execute the Center's mission relative to future programs. The Engineering Development Directorate encompasses most of the laboratories and other Center resources that are key elements of research and technology program implementation, and is responsible for implementation of the majority of the projects in this Kennedy Space Center 1988 Annual Report.

For further technical information about the projects, contact David A. Springer, Projects Management Office, DE-PMO, (407) 867-3035. Thomas M. Hammond, Technology Utilization Officer, PT-PMO, (407) 867-3017, is responsible for publication of this report and should be contacted for any desired information regarding the Center-wide research and technology program.


Forrest S. McCartney
Director

AVAILABILITY INFORMATION

For additional information on any summary, contact the individual identified with the highlight. Commercial telephone users may dial the listed extension preceded by area code 407. Telephone users with access to the Federal Telecommunications System may dial the extension preceded by 823.

CONTENTS

FOREWORD	i
AVAILABILITY INFORMATION	ii

INSTRUMENTATION AND HAZARDOUS GAS

The Test and Evaluation of a Chemiluminescent Propellant Vapor Detection System	1
Remote Analysis of Monomethylhydrazine Using High-Flow Sampling	5
Evaluation of Electrochemical Hypergolic Fuel Vapor Detector Cells	7
Color Chemistry for Hydrazine Detection	8
Field Evaluation of a Quantitative Hydrazine Sampler	10
Detection of Hypergolic Vapors Using Ion Mobility and Field Domain Ion Mobility Spectrometry	11
Hydrogen Laser Monitoring System (HLMS)	12
Multispectral Imaging of Hydrogen Fires	13
Remote Detection and Characterization of Fugitive Hydrogen by a Raman LIDAR System	14
Characterization of a Turbomolecular-Pumped Magnetic Sector Mass Spectrometer	15
Advanced Hazardous Gas Detection System (AHGDS)	17
Bidirectional Flow Meter	19
Chemiresistors for the Detection of Hydrazine and Nitrogen Dioxide	19
Toxic and Flammable Gas Detectors	21
Colorimetric Hydrazine Dosimeter Badge for Personnel Monitoring	21
Fast-Response Instrumentation Van	23

MATERIALS SCIENCE

Protective Coating Systems for Repaired Carbon Steel Surfaces	24
Study of Thermal Sprayed Metallic Coatings for Potential Application on Launch Complex 39 Structures	24
Development of New Flooring Materials for Clean Rooms and Launch Site Facilities	25
Conductive Organic Polymers As Corrosion Control Coatings	25
Protective Coating Systems for the Space Transportation System (STS) Launch Environment	26
Ignition of Metals in High-Pressure Oxygen	26
Permeability of Polymers to Organic Liquid and Condensable Gases	27
Improved Bubble-Point Test Method	27
Electrically Conductive Polymer Applications	28
Thermal Sprayed Cathodic Protection for Steel Structures	29
Corrosion of Convolute Metal Flexible Hoses	30

ROBOTICS

Six-Degree-of-Freedom (6-DOF) Robot Target Tracking in KSC's Robotic Applications Development Laboratory	31
Robotic Automation in the Controlled Ecological Life Support System (CELSS)	32
Robotics Applications Development Laboratory (RADL)	33

ATMOSPHERIC SCIENCE

Thunderstorm Weather Forecasting Expert System	36
Atmospheric Science Instrumentation Laboratory (ASIL)	37
Clear-Air Wind-Sensing Doppler Radar	37
Lightning Tower Measurements System	40
Lightning Hazard Detection and Warning	41
Rocket-Triggered Lightning	42
Lightning-Induced Effects	44
Electric Field Measurements Aloft	46
Numerical Weather Modeling	47
Measurement of Electromagnetic Enhancement Due to Site Nonuniformities	49
Atmospheric Science Field Laboratory (ASFL)	50
Solid State Instrumentation for Electric Field Detection of Lightning Potential	51

ARTIFICIAL INTELLIGENCE

Checkout, Control, and Monitor Subsystem (CCMS) Operations Analyst (OPERA) Expert System	54
Remote Maintenance Monitoring System	57
Expert Mission Planning and Replanning Scheduling System	59
Automatic Test Expert Aid System Environment (AT-EASE)	60

BIOMEDICAL

Biological Flight Research Program: Chromosomes and Plant Cell Division in Space	62
Muscle Exercise Machine for Concentric Only Exercise	62
Human Physiology Research Projects: Blood Pressure Control	63
Controlled Ecological Life Support System (CELSS) Breadboard Project	63
Environmental Monitoring Program	65
Controlled Animal Nutrients Delivery System (CANDS)	66

OPERATIONS

Telemetry Data Processing Using Microcomputers	68
Expendable Launch Vehicle (ELV) Payload Processing Historical Data Retrieval Study	68
Orbiter Spare Quantification Methods	69
Certification of a Microwave Landing System Using the Global Positioning System	71

FIBER OPTICS AND COMMUNICATIONS

Hydrogen Detection Television Camera	73
DC to 150-Megabits-per-Second Fiber Optic Link Development	73
Microwave Fiber Optic Link Study	75

TECHNOLOGY UTILIZATION

Alarm Processing and Diagnostic System Using NASA's Knowledge-Based Autonomous Test Engineer (KATE) Technology	77
Feasibility Analysis of a High-Efficiency Dehumidifier/ Air Conditioner Using Heat Pipes	78
Development of a Digital Hearing Aid	79
EPCOT Project	81

CRYOGENICS

Two-Phase Pressure Drops in Developing and Fully Developed Pipe Flow of Dispersed Liquid/Vapor Mixtures Under Zero-Gravity Environment	82
Clamshell Bellows Repair Technique With Hastelloy C-22 Material	83
Temperature-Sensitive Variable-Area Joule-Thomson Expansion Nozzle and Cryocooler Development Program	84

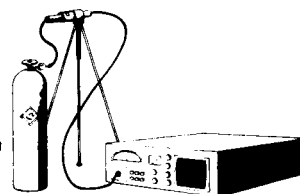
DIGITAL ELECTRONICS

Partial Payload Checkout Unit	85
High-Speed Data Filter	86
Generic Checkout System (GCS)	87
High-Speed Pulse Code Modulation (PCM) Processing System	88
Manchester Interface for VME Bus	89

MECHANISMS

Telescoping Tube	90
------------------------	----

INSTRUMENTATION AND HAZARDOUS GAS



The Test and Evaluation of a Chemiluminescent Propellant Vapor Detection System

Objective: To evaluate a modified chemiluminescent hydrazine detection system.

Background: To provide the best protection for personnel and equipment against the adverse effects of hydrazines, NASA and the Air Force Space Division tasked the Naval Research Laboratory (NRL) to test and evaluate a hydrazine monitoring system. This system is based on a design originally built for Titan II missile silos, modified for the Titan 34D system, and again modified for Shuttle operations.

The system measures hydrazine, monomethylhydrazine (MMH), unsymmetrical dimethylhydrazine (UDMH), and nitrogen tetroxide (N_2O_4) in air or nitrogen atmospheres. The system, called the Propellant Fixed Vapor Detection System (PFVDS), was manufactured by Thermedics, Inc., and consists of a multiple sampling module, analyzer, electronics console, and two remote panels. The sample system has nine sample inlets. The points being sampled are connected to the console using 1/4-inch inner diameter lines. The instrument continuously draws sample vapors down all the sample lines. The sample lines are connected to a manifold within the instrument where one of the lines is selected for analysis. The instrument can be operated in three modes: (1) cycles through all the sample lines, (2) looks at a combined sample from all nine lines, or (3) only samples one line. The system uses two calibrated gas mixtures of nitric oxide (NO). One is a calibration gas to span the analyzer, and the other is a test gas to verify the accuracy of the analyzer.

The PFVDS system detects light from the chemiluminescent reaction that occurs between NO

and ozone. This detection method used in the PFVDS requires that the fuel and oxidizer vapors in the sample be converted to NO, which is then measured. The N_2O_4 is thermally decomposed to NO. UDMH is thermally oxidized to produce NO. Hydrazine and MMH cannot directly be converted to NO. They are first reacted with acetaldehyde in the gas stream to form azine and hydrazone derivatives. The azine and the hydrazone compounds are thermally oxidized to produce NO. The reaction between the fuel and acetaldehyde is unique to hydrazines and makes the system highly selective.

The selectivity is achieved by using a three-channel system. The first channel, called the oxidizer channel, is used to measure the oxidizer. The other two channels are identical except acetaldehyde is added to one. Interfering compounds will produce an NO signal in both channels; therefore, the net differential signal is zero. Hydrazine and MMH only produce a signal in the channel containing the aldehyde. UDMH produces twice the signal with aldehyde than without it. The three outputs are called the fuel channel, the amine channel, and the oxidizer channel. The instrument is highly automated and designed to operate unattended for several days. It has significant self-checking capabilities.

Approach: Controlled test gas streams were sampled. A 16-foot length of Teflon tubing was connected to sample port 1 and a 42-foot length of Bev-a-line tubing was connected to sample port 2. The other seven sample ports were not used. Each sample line was connected to a solenoid valve. The solenoid valve, located between two gas manifolds, directed either clean air or a test gas to the PFVDS system. Both sample lines simultaneously draw about 2 liters per minute to the instrument. Little difference was observed using either sample line; this was consistent with previous experiments at NRL. Slight differences in response times at the lowest concentrations were expected. These differences were masked by the instrument's response time.

After daily automatic calibration with the calibration gas, the instrument was exposed to known concentrations of hydrazine, MMH, and UDMH in air humidified at 45 percent relative humidity. The response and recovery times were measured for the entire gas flow system beginning at the sample line and were also measured after switching the gas flow system at the sample manifold internal to the instrument. The accuracy and linearity of the instrument were determined. The stability of the response without the daily calibration was measured. In addition, the functionality of the instrument was observed.

The noise level of the instrument is about ± 50 parts per billion (ppb) for hydrazine and MMH and ± 150 ppb for UDMH; therefore, the limit of detection (three times the signal-to-noise) is near the threshold limit value (TLV) for all the fuels.

The instrument was exposed to hydrazine, MMH, and UDMH. The accuracy of the instrument is shown in Table 1. As MMH sampling progressed, instrument response decreased. Although no error messages were displayed on the console, the aldehyde addition system was suspect. The aldehyde container was removed and found to contain only 40 milliliters. After filling, the accuracy of the instrument was restored. UDMH produced a response in both the fuel channel and the amine channel. The amine channel produced one-half the signal of the fuel channel. The response of the instrument to hydrazine was 25 percent below the calibrated value, the response to MMH was within 10 percent below the calibrated value, and the response to UDMH was about 65 percent below the calibrated value.

The response and recovery times for low concentrations were slow for all the vapors, but were worse for MMH. The lag time for MMH was between 4 and 32 minutes for concentrations below 1 part per million (ppm). A quick response time was observed at high concentrations. Linearity of the MMH response was good; however, reliability of the measurement below 0.5 ppm was poor due to the noise and slow response time. The response and recovery in the amine channel were much faster than in the fuel channel.

During stability tests in which the instrument was exposed to the test gas (NO) once a day for

Table 1. PFVDS Accuracy to Fuels

Test Vapor	Actual Concentration (ppm)	Fuel Channel Response (ppm)	Amine Channel Response (ppm)
hydrazine	.41	.31	
hydrazine	1.11	.74	
MMH	.69	.8	
MMH	.65	.75	
MMH	3.3	4	
MMH	3.3	3	
MMH	2.9	1.9	
MMH	2.9	1.65	
MMH	5.6	2.65	
MMH	5.6	2.38	
MMH	11	2.63	
MMH	11	2.52	
MMH	2.8	.74	
*	*	*	
MMH	3	3.3	
MMH	11	12	
MMH	11	13	
MMH	11	12	
UDMH	13.7	4.85	2.5
UDMH	13.7	4.74	2.4
UDMH	5.4	2.1	1
UDMH	5.4	2.2	1
UDMH	24.8	8.2	4.4
UDMH	24.8	8.2	4.4
UDMH	1.66	.7	.24
UDMH	1.66	.8	.28
UDMH	1	.35	.13
UDMH	1	.25	.17
UDMH	3.8	1.42	.69
UDMH	3.8	1.4	.7

*Acetaldehyde replenished.

one week (no auto-calibration was performed), the instrument was stable and accurate to within 5 percent; however, the response to fuel dropped to 50 percent after the first day and settled at about 33 percent of the known concentration in a week.

The response of the instrument in the combined and scanning modes was tested with 3.8 ppm of UDMH. The combined sample lines resulted in a nine-fold dilution of the sample. The response time of the combined sample was slow, and the change in magnitude of the signal was small. The instrument was tested in the scan mode after being programmed to all nine sample ports, switching sample lines every 24 seconds. The maximum response of the instrument was one-third the actual concentration. Longer sample time is needed; however, the maximum amount of time that can be programmed into the system is 2 minutes. The optimum sample time is dependent upon sample concentration.

Table 2. Response and Recovery Time of the PFVDS

Test Vapor	Actual	Response Time			Recovery Time			Exposure of Day
	Conc (ppm)	Lag	50%	90%	Lag	50%	90%	
			(minutes)			(minutes)		
Hydrazine	.2	3	5	8	.3	1.5	8	1
Hydrazine	.2	3	5	8	.3	1.5	5	2
Hydrazine	.4	3	5	8	.3	1	10	1
Hydrazine	.4	2	4	10	.5	1.5	10	2
Hydrazine	.2	10	15					
Hydrazine	.2	10	15					
Hydrazine	.4	3	5	7	.5	1.5	8	3
Hydrazine	.4	5	8.5	2	10	4		
Hydrazine	1.1	13	15	25	1	3		1
MMH	.69	5	9	16	2	5	22	1
MMH	.69	32	34	42	1.5	3.5	10	1
MMH	.65	15	20	40	1	3	23	2
MMH	.65	4	5	10	1	2	10	3
MMH	.65	7	9	15	2	3	10	1
MMH	.2	16	25	35		2		
MMH	.2	11	21	25	3	8	15	1
MMH	3	5	81.5	2	9	2		
MMH	3	2	3	7	.5	1.5	7	3
MMH	3	3	5	10	1	3	40*	1
MMH	3	2	3	5	1	*	•	2
MMH	5.6	1	1.5	5	.5	1	12*	3
MMH	5.6	1	2	7	.5	*	*	4
MMH	3	5	7	15	1	2	7	1
MMH	11	.5	1	1.5	.25	.5	6	3
MMH	11	.75	1	5	.5	1	11	1
UDMH	13.7	.5	.5	3.5	.5	.5	2.5	1
UDMH	13.7	.5	1	1.5	.25	.5	2	2
UDMH	5.4	1	1.5	4	.5	1	3	3
UDMH	5.4	1	1.25	3	.5	1	12	4
UDMH	24.8	.5	.5	1	.5	.5	5	1
UDMH	24.8	.5	.5	2	.25	.25	3	2
UDMH	1.7	2	3	7	1	6	16	3
UDMH	1.7	2	4	11	2.5	6	26	4
UDMH	1	5	7	17	2.5	5	20	1
UDMH	1	5	7	13	2	3	11	2
UDMH	3.8	1.5	2.5	10	.5	1	11	3
UDMH	3.8	1	2	4	.5	1		4

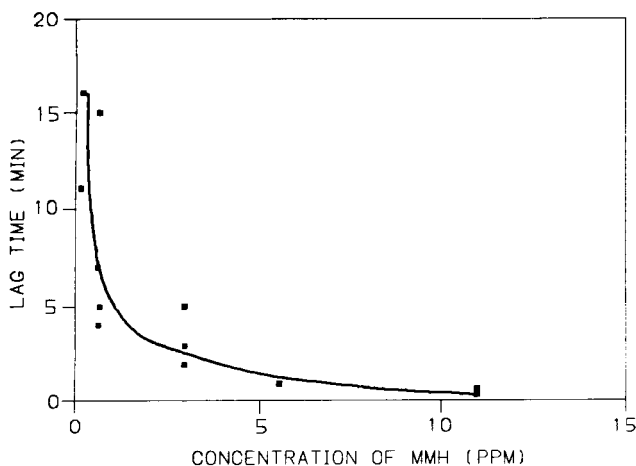
*Never reached actual value.

Table 3. Response and Recovery Time of the UDMH in Amine Channel

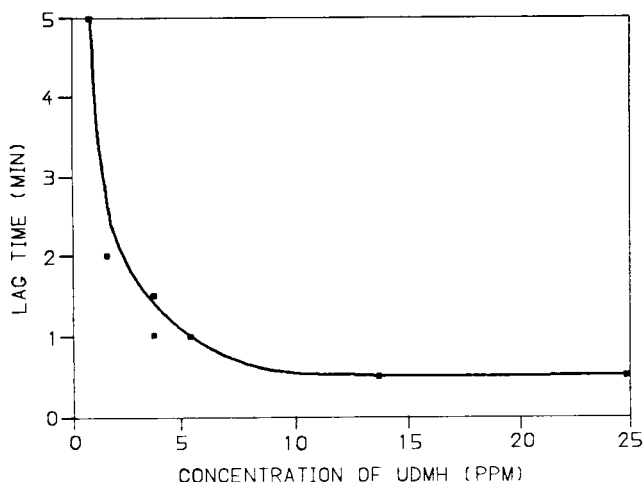
Test Vapor	Actual	Lag	Response Time		Lag	Recovery Time		Exposure
	Conc (ppm)		50%	90%		50%	90%	
			(minutes)			(minutes)		
UDMH	13.7	-	-	-	.5	.5	1	1
UDMH	13.7	.5	.5	.5	.5	.5	.5	2
UDMH	5.4	1	1	1.5	.25	.25	.5	3
UDMH	5.4	.5	.5	.5	.3	.3	.5	4
UDMH	24.8	.25	.25	.5	.5	.5	.5	1
UDMH	24.8	.5	.5	.5	.5	.5	.5	2
UDMH	1.7	2	2.25	3	.5	.7	2.5	3
UDMH	1.7	1.5	1.5	2	.75	1	3	4
UDMH	1	4	5	5	1	1.5	3.5	1
UDMH	1	4	4.5	6	.5	1	4	2
UDMH	3.8	1.25	1.25	3	.5	.5	1	3
UDMH	3.8	1	1	1.25	.5	.5	2	4

Table 4. Stability of the PFVDS With No Calibration

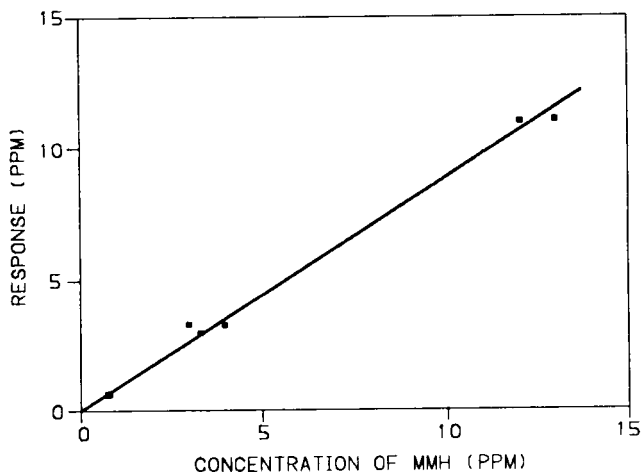
	# of Days Since Calibration	Actual Concentration (ppm)	Fuel Channel Response (ppm)	
HYDRAZINE	1	1.1	.47	
	2	1	.46	
	5	1	.32	
	6	1	.34	
	7	1.1	.32	Test gas
	0	1.1	.74	Test gas



Lag Time for First Response As a Function of Concentration for MMH



Lag Time for First Response As a Function of Concentration for UDMH



Linearity of MMH Response

Conclusion: The PFVDS is an accurate instrument for measuring the hydrazines at levels greater than 1 ppm. No interferences are known to produce a response that is similar to that of hydrazines.

On the fuel channel, the response and recovery times for hydrazine and MMH concentrations below 1 ppm are too slow for practical real-time use. The slow response of the instrument appears to be due to the hangup of the derivatized fuels in the sample lines within the instrument. The limit of detection for these vapors is near the TLV due to the large noise level. When operated in the combined mode, the vapor is diluted nine times. In this mode, the limit of detection is near 1 ppm. The scan mode should not be used for concentrations less than 5 ppm because of excessive instrument lag time.

The instrument shows much promise for UDMH detection, particularly in the amine channel where the response and recovery are rapid. The principle cause of slow response and recovery times at low ppm concentrations on the amine channel appears to be due to the sample manifold construction. Tests using the entire sampling system and only the manifold indicate the sample tubing has an insignificant effect on response times.

J. C. Travis and W. R. Helms,
867-4438

DL-ESS-31

Remote Analysis of Monomethylhydrazine Using High-Flow Sampling

Objective: To determine the performance capabilities of the MDA 7100 paper tape instrument when sampling contaminated air through tubing of differing lengths. Based on a tubing study conducted previously at the Naval Research Laboratory (NRL), the response time of an instrument is drastically reduced by long sample lines because of the adsorption of hydrazine into the tubing walls. This test was designed to determine the response times when using an auxiliary pump to deliver the contaminated air to the instrument at a faster rate.

Background: The toxicity of the hydrazine fuels and the large quantities of the fuels that both NASA and the Department of Defense use require special precautions be taken to ensure the safety of personnel. Part of the safety program involves routine air monitoring whenever hydrazines are being handled. Kennedy Space Center (KSC) requires that the hydrazine levels not exceed the American Conference of Government Industrial Hygienists (ACGIH) recommended threshold limit value (TLV). To support this requirement, KSC requested that NRL test the MDA Scientific Incorporated model 7100 hydrazine detector as a fixed-point monitor with sampling lines of various lengths.

Approach: Employing 100-, 50-, and 10-foot lengths of tubing, in addition to the 3-foot Teflon sample probe, the MDA 7100 was tested for response time to TLV concentrations using an auxiliary pump. Tests measuring the pressure drop, due to various lengths of tubing, were performed in order to find the longest length of 1/4-inch inner diameter Bev-a-line tubing that the MDA 7100 can sample at the manufacturer's suggested sampling rate of 800 milliliters per minute using an auxiliary pump pulling at 21 liters per minute.

Results: The MDA 7100 demonstrates excellent response time when an auxiliary pump is used to deliver hydrazines to the sample probe. The instrument pump can sample 800 milliliters per minute as long as the vacuum drawn by the auxiliary pump is less than 4.75 inches of mercury. Up to 115 feet of 1/4-inch inner diameter tubing can be used.

Several cautions should be observed:

1. Leaks can be a major problem with the instrument because quantification is dependent on the volume of gas sampled. Due to internal leaks or leakage around the paper tape, the sample rate should be set using a rotameter to monitor the flow rate at the inlet rather than using the rotameter that follows the paper tape internal to the instrument.

2. Considering the large volume of air sampled, contamination of the 100-foot sample line may pose a problem. A filter placed at the tubing inlet could reduce the air contaminants drawn through the tubing but could also reduce the amount of hydrazine transported.

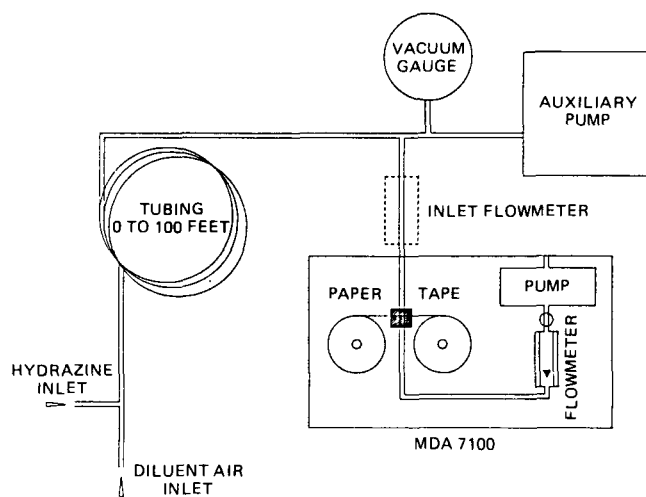
3. An indicating flow sensor compatible with monomethylhydrazine (MMH) should be placed at the inlet of the MDA 7100 to ensure that the instrument is drawing samples from the inlet of the auxiliary pump.

4. Since the instrument draws from sub-ambient pressure, a leak in the sampling line between the MDA 7100 and the main sampling line could result in a failure to detect MMH.

5. Any flow restriction of the 100-foot line would increase the partial vacuum and possibly produce a failure. This could be brought about by a clogged filter at the tubing inlet. The vacuum should be monitored to identify this possible future mode.

J. C. Travis and W. R. Helms,
867-4438

DL-ESS-31



Test Setup

***Instrument With Auxiliary Pump; Sample Set to 0.8 Liter per Minute
Using Flow Meter on Face of MDA***

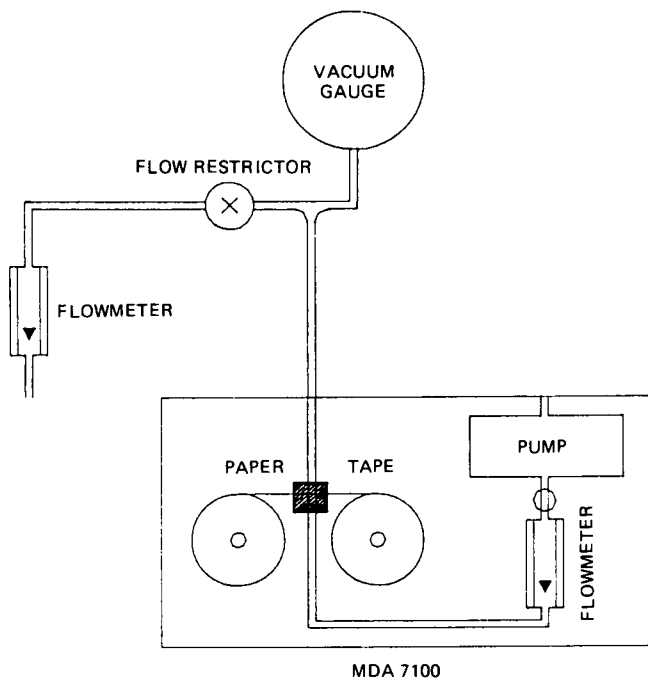
TUBING LENGTH(FT)	FLOW RATE (L/MIN)	EXPECTED RESPONSE(PPB)	ACTUAL RESPONSE(PPB)	RESPONSE TIME (MIN) 50%	RESPONSE TIME (MIN) 90%
NONE	21	288	211	2.5	10
NONE	21	288	211	1.5	6
NONE	21	288	192	.75	8
100	21	288	224	2.5	6
100	21	288	194	3	12.5

Instrument Without Auxiliary Pump

TUBING LENGTH(FT)	FLOW RATE (L/MIN)	EXPECTED RESPONSE(PPB)	ACTUAL RESPONSE(PPB)	RESPONSE TIME (MIN) 50%	RESPONSE TIME (MIN) 90%
NONE	.8	232	293	.5	2
100	.8	232	246	5.5	22

***Instrument With Auxiliary Pump; Sample Set to 0.8 Liter per Minute
Using Flow Meter at Sample Inlet***

TUBING LENGTH(FT)	FLOW RATE (L/MIN)	EXPECTED RESPONSE(PPB)	ACTUAL RESPONSE(PPB)	RESPONSE TIME (MIN) 50%	RESPONSE TIME (MIN) 90%
NONE	21	288	255	1.5	3.5
NONE	21	288	255	4	7
NONE	21	288	258	1.5	4
10	23.6	246	222	2	6
10	23.6	250	219	1.5	9
10	23.6	250	209	1	2.5
50	23	226	236	.5	6.5
50	23	246	240	1	6.5
100	21	288	302	3	8
100	21	288	302	1.5	7
100	21	246	252	2	9
100	21	246	263	1.5	7



Setup for Flow Adjustment

Evaluation of Electrochemical Hypergolic Fuel Vapor Detector Cells

Objective: To determine the most reliable replacement electrochemical sensor for the Ecolyzer 7660 hypergolic fuel vapor detectors.

Background: The Ecolyzer 7660 detects hydrazine vapor by electrochemically oxidizing the hydrazine at a fixed potential. The hydrazine diffuses through a membrane into an alkaline solution where it is oxidized. The Ecolyzer 7660 uses electrochemical cells that require replacement after about three months. The replacement cells have recently had a mean-time-to-failure of less than one month. A program was initiated to improve the sensor performance and lifetime. The cells used contain a liquid, highly caustic electrolyte solution of potassium hydroxide (KOH). The principal mode of failure is damage to the membrane because of the formation of potassium carbonate crystals in the electrolyte.

Approach: Two different vendors were selected to design and manufacture several sensor prototypes. Sensors were evaluated with a variety of laboratory tests. The cells were of three

types: (1) cells with KOH liquid electrolyte, but different membranes and construction techniques, (2) cells with cesium hydroxide (CsOH) electrolyte, and (3) cells with a gelled electrolyte.

Results: The initial batches of type 1 cells had continuing electrolyte leakage problems. The cells' sensitivity degraded with time, and they were vibration sensitive. After improving the membrane sealing techniques, the type 1 cells demonstrated acceptable performance. The cells still remained sensitive to vibration. Type 2 cells showed no improvement. Type 3 cells were vibration and position insensitive, but rapidly failed at low humidities.

J. C. Travis and W. R. Helms,
867-4438

DL-ESS-31

Table I. Premature Failure Rate

	Total No. of Cells	Failure Rate (%)
TRI KOH	14	46
TRI CSOH	3	67
ESI	8	43
DRAEGER KOH	4	0
DRAEGER GEL	4	25

Table II. Response Time and Cell Life

	Average Response Time to 90% (min)	Average Cell Life (Days)
TRI KOH	4.9 ± 2.1	29 ± 18
TRI CSOH*	4.2	57
ESI	2.4 ± 0.39	41 ± 20
DRAEGER KOH	1.8 ± 0.42	43 ± 10
DRAEGER GEL	1.9 ± 0.67	59 ± 26

Note: Premature failures were not averaged into cell life values.

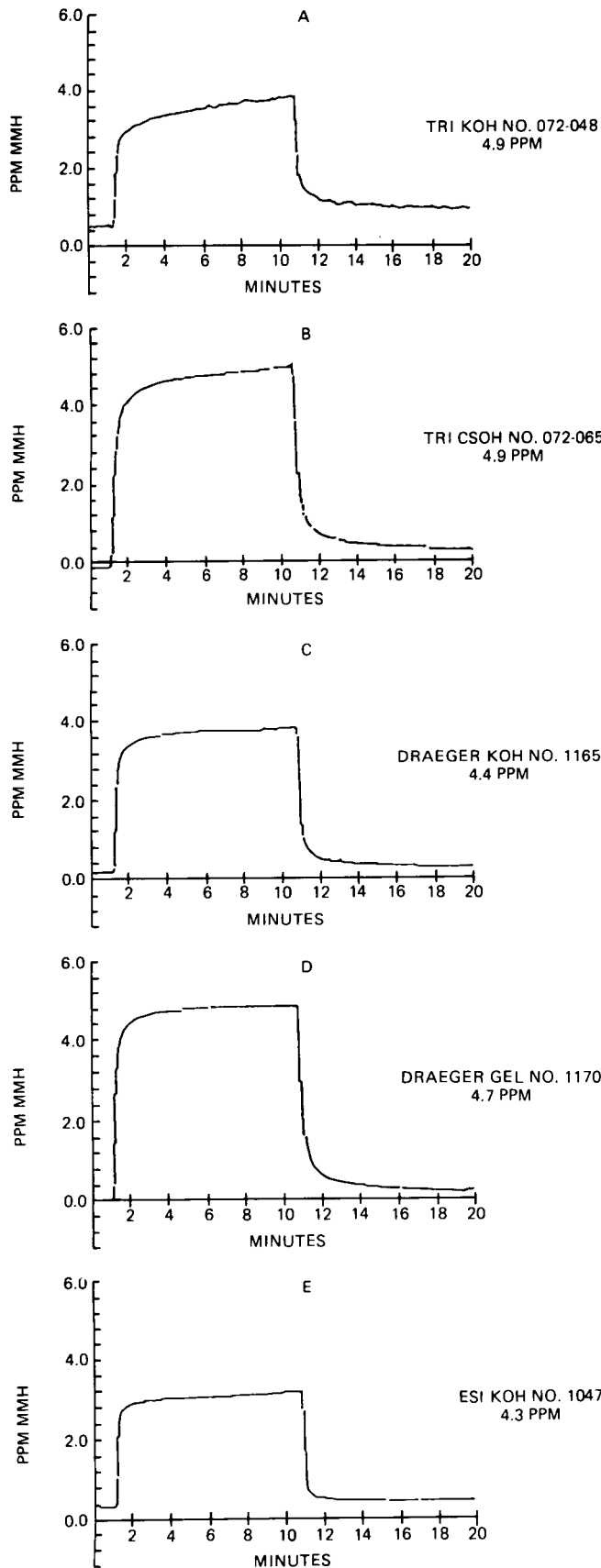
*Values are based on one cell.

Color Chemistry for Hydrazine Detection

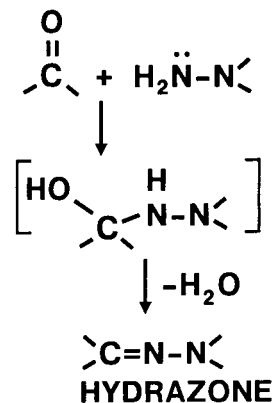
Objective: To investigate aldehyde color chemistries for hydrazine detection and find a suitable reaction that is light insensitive and quantitative. This chemistry will then be applied in the development of detector tubes, dosimeters, paper tape products, and other analytical techniques.

Background: Hydrazines are employed by NASA as hypergolic fuels for the Shuttle. The health hazards associated with these chemicals and the prospect that the levels of allowable exposures will be lowered significantly in the near future have spurred the need to investigate indicating chemistries. The current color chemistries either lack sensitivity or have interference problems that render them useless at the low part-per-billion levels.

Approach: The reaction of aldehyde with hydrazine is rapid and in some cases will produce highly colored products. Para-dimethylamino-benzaldehyde (PDAB) is known to produce an intense yellow color and is used as an indicator in an established wet chemical analysis method. This compound and a variety of aldehydes were examined for reactivity in solution. The compounds producing an observable color change were reexamined as coatings on substrate materials. The samples were exposed to controlled vapor streams of monomethylhydrazine (MMH) and hydrazine.



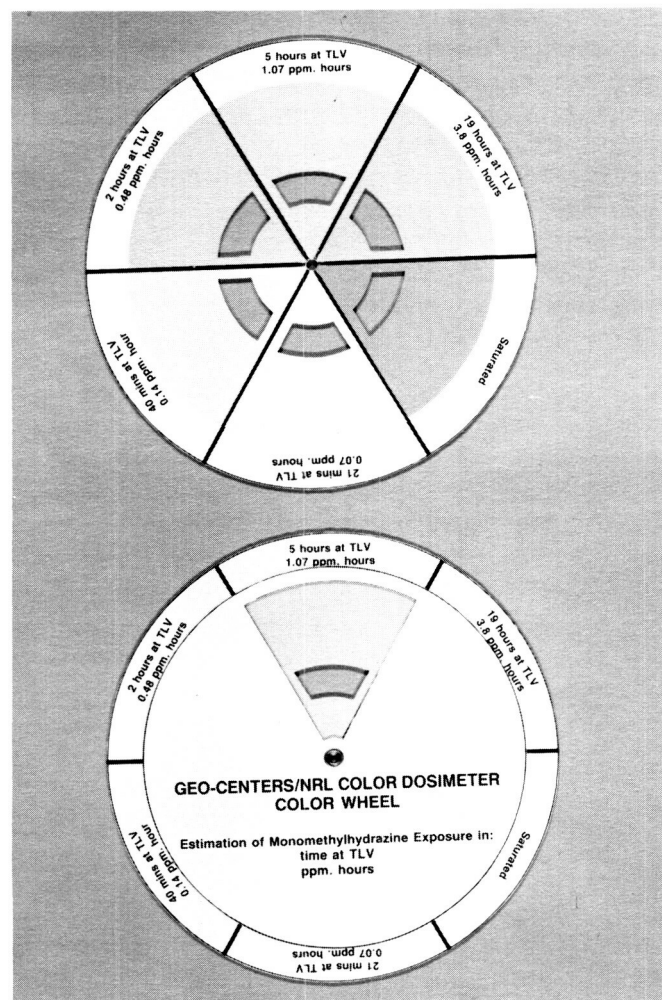
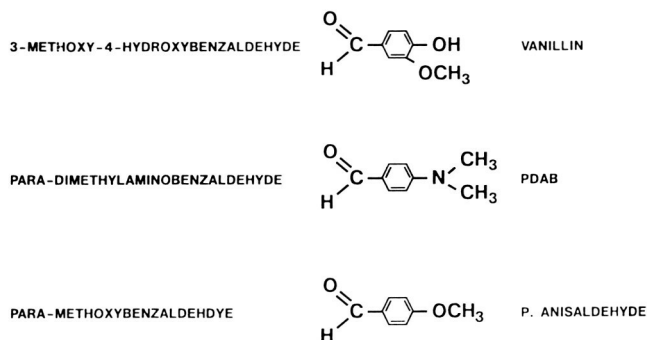
Response Curves



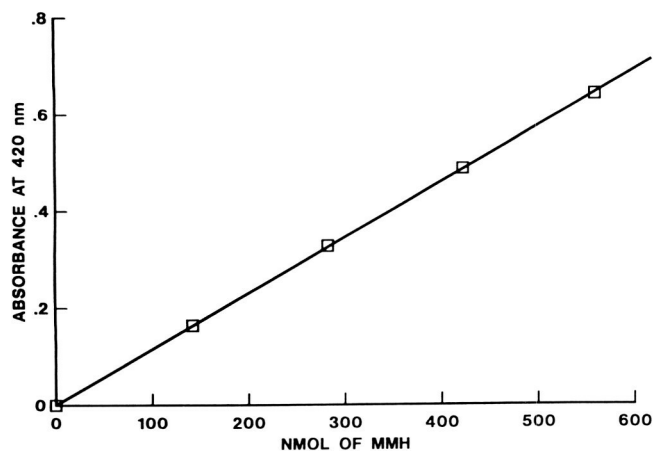
Condensation Reaction of an Aldehyde With a Hydrazine to Form a Hydrazone

Results: The sensitivity and reactivity of PDAB, vanillin, and para-anisaldehyde made them the most promising aldehyde candidates. The PDAB reaction was found to be dependent upon pH; p-anisaldehyde was found to be less sensitive to hydrazines; therefore, initial investigations focused on vanillin. The hydrazone formed from vanillin absorbs at 420 nanometers giving it a yellow color. From the absorbency readings taken on several standard solutions, it was apparent that the reaction is linear.

Several substrate materials have been considered and tested. The vanillin has been successfully coated on silica gel plates and packing, amberlite IRC-50(H) resin, and filter paper. The filter paper is a convenient substrate for laboratory testing and will be used in the evaluation of the compounds for real-time hydrazine analysis.



Aldehyde Candidates Selected for Further Investigation



Absorbance Measured at 420 Nanometers Plotted Against the Nanomoles MMH Added to Vanillin Solution

Color Wheel Developed for Estimation of MMH Exposure

Preliminary laboratory testing indicates that vanillin response to threshold limit value (TLV) levels of MMH and hydrazine is approximately 2 to 5 minutes. The stain intensity is proportional to the dose. The stain is stable for greater than or equal to 8 hours and, when acidified, is stable for weeks. Relative humidity changes had no effect on the performance of the MMH reaction; a slight effect was noticed with hydrazine.

A prototype system was developed and has been incorporated into the current passive dosimeter field evaluation being conducted at the Kennedy Space Center. This opportunity was taken to evaluate the color chemistry for interference effects. No significant problems have

been determined. The prototype consists of a vanillin-coated filter paper functioning as a passive colorimetric badge and a color wheel for dose estimation. The badge exposure can be interpolated from a comparison of the badge color with the wheel containing colors equivalent to 0.07, 0.14, 0.48, 1.1, and 3.8 parts per million hours of MMH exposure.

J. C. Travis and W. R. Helms,
867-4438

DL-ESS-31

Field Evaluation of a Quantitative Hydrazine Sampler

Objective: To evaluate, under field conditions, the passive sampling badge developed at the Naval Research Laboratory for applications in personnel and area monitoring of hydrazines present in the ambient air at the part-per-billion level.

Background: The potential carcinogenicity of hydrazines has caused concern for the health and safety of the workers that may come in contact with hydrazines. Monitoring of the employees and their work places is recommended to ensure exposure remains below the defined levels. A small, inexpensive, passive sampling badge was developed that could be distributed to a large number of personnel for monitoring quantitatively the exposure levels. Laboratory investigations were conducted to evaluate linearity, effects from relative humidity, face velocity, and storage stability. The sampling badge performed with an accuracy of ± 25 percent.

Approach: An extensive test plan was developed to evaluate the sampling badge under field conditions. Test locations were selected that would provide information about potential interferences. A double blind approach was selected involving three groups: industrial hygienists, analytical chemists, and program auditors.

The industrial hygienists performed the sampling and recorded the exposure information, which included the facility data, the activity log, and the sample data. The sampling was performed in duplicate so two different methods of analysis could be used. Random blank and spiked samples were submitted for analysis as

part of the quality control and quality assurance program. Liquid impinger samples were collected for verification of the atmosphere using National Institute of Occupational Safety and Health (NIOSH) methodology.

The analytical laboratory received the samples from the industrial hygienist. The laboratory was not informed of the samplers history; this information was known only by the auditors. A coulometric titration method and a phosphomolybdic acid colorimetric procedure were used to analyze the badges. The impinger samples were analyzed by the less sensitive NIOSH para-dimethylaminobenzaldehyde colorimetric method.

The analytical data was forwarded from the laboratory directly to the auditor where it was combined with the information provided by the industrial hygienists. Following a review of the combined data the auditors discussed the results with the industrial hygienists and the analysts.

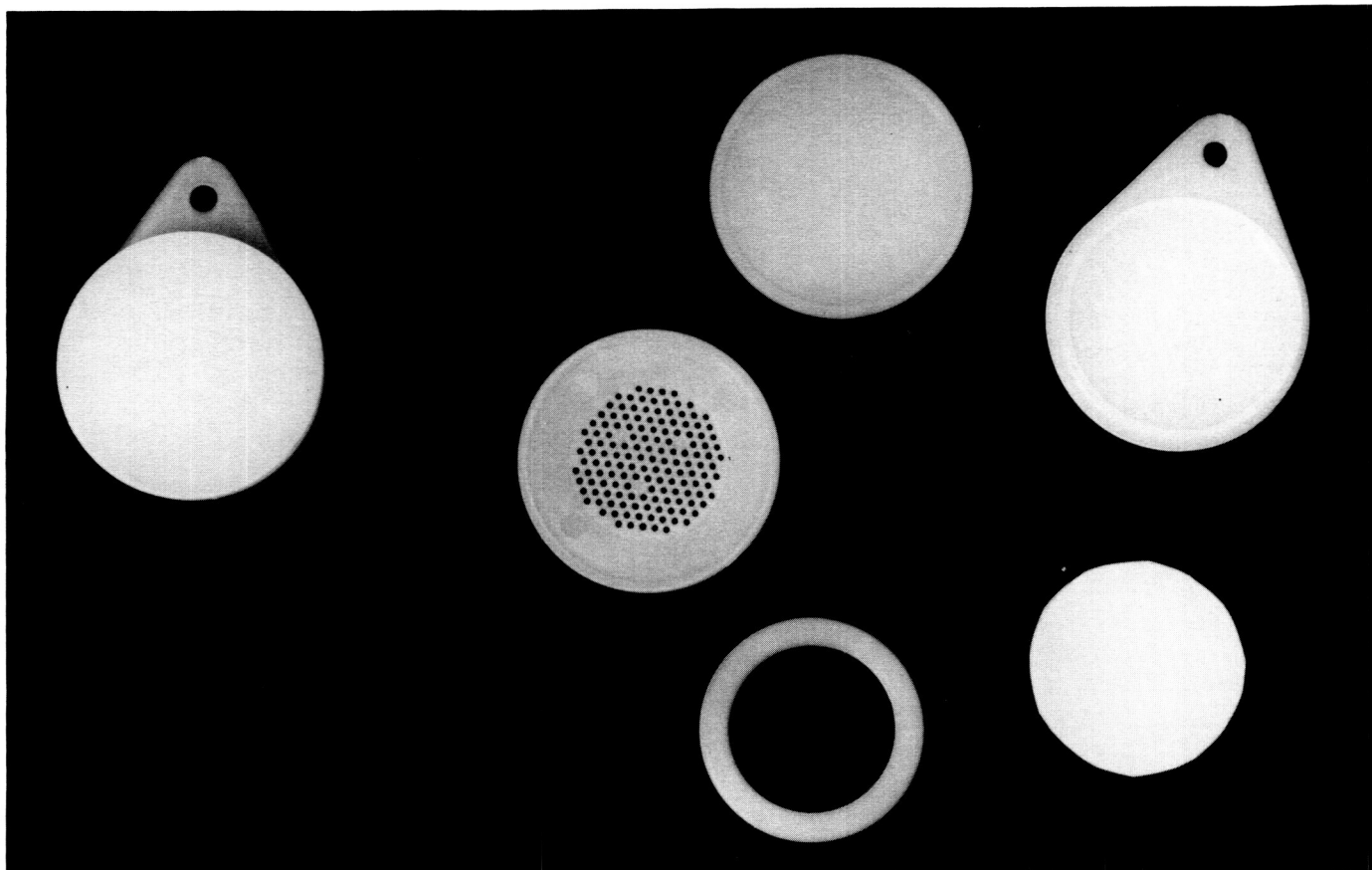
Results: The sampler has been investigated under a variety of field conditions. The location of the tests are: Wiltech, Building K7-516; Hypergol Maintenance Facility, Building M7-961; M and O Paint Shop, Building M6-486; Hanger S Life Support South Annex; Fuel Storage Area No. 1; Aft Skirt Test Facility; Rotating Service Structure (Launch Complex 39B); and Kennedy Space Center beach.

During the performance of the field test, the badge underwent two minor modifications that resulted in an improved sampler. The polyester collection disk was replaced by a paper collection disk. In laboratory tests, the paper substrate has drastically increased the storage stability of the analyte.

The second change has been to color the polyethylene badge housing. This change was made when outdoor exposures indicated an interference effect that was traced to sunlight. The phosphomolybdic acid method is not sensitive enough to be affected under normal operating conditions, but the effect on the coulometric titration data was significant. The results obtained with the colored badges are promising and testing is continuing.

J. C. Travis and W. R. Helms,
867-4438

DL-ESS-31



Dosimeter Badge

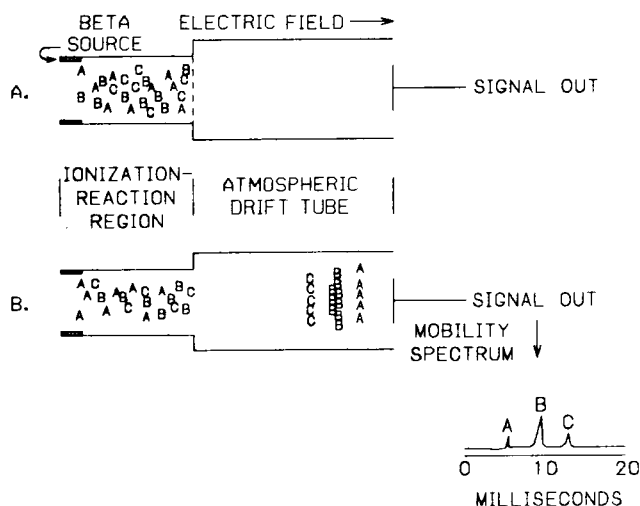
Detection of Hypergolic Vapors Using Ion Mobility and Field Domain Ion Mobility Spectrometry

Large quantities of hydrazine (HZ), monomethylhydrazine (MMH), and nitrogen tetroxide (N_2O_4) are used in both Space Shuttle and payload operations at Kennedy Space Center. Currently, both portable and fixed-point monitors for these vapors are based on technologies that use expendable chemicals, paper tapes, or high-maintenance electrochemical cells. The purpose of this project is to investigate and develop instruments based on ion mobility spectrometry (IMS) for measuring these vapors.

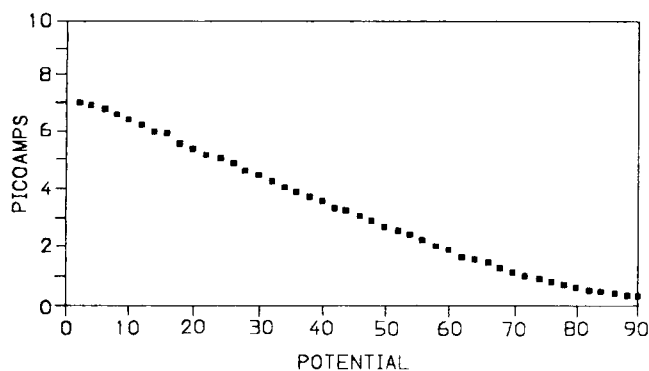
IMS offers several important advantages over conventional spectrometry. This instrument will operate at atmospheric pressure, eliminating the need for a vacuum-to-atmosphere interface and

all of the associated problems. The ion separation region of the instrument is less than 10 centimeters long. All of these advantages give IMS the potential to be a low-power, highly reliable instrument without the need for expendables such as chemicals or paper tape.

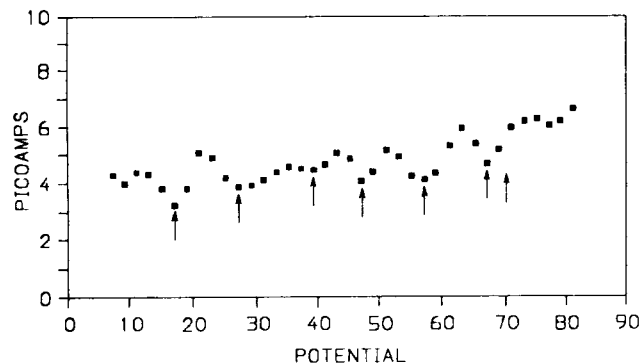
Conventional IMS devices operate by ionizing incoming samples with alpha particles from a radioactive source and then separating the ions in a drift region based on their mobilities. This separation is accomplished by applying an electric field, which exerts force on the ions and changes their drift velocity causing ions of the same mobility to cluster together. Ions separated by their mobility reach a detector in groups and, from measuring the detector current at the appropriate time, vapor concentration is determined. Modification of an IMS instrument to enhance its response to HZ, MMH, and N_2O_4 is in progress.



Generation of Ion Mobility Spectrum



Spectra of MMH in Nitrogen Carrier Using FDIMS



Derivative Plot of MMH in Nitrogen Carrier Using FDIMS

In addition to investigation of conventional IMS instruments, the technology of field domain IMS (FDIMS) has been investigated under a Phase I Small Business Innovative Research (SBIR) contract. FDIMS differs from IMS in that instead of measuring electrical current at a certain drift time, current at a certain electric field strength is measured. This method offers potential advantages in sensitivity and signal-to-noise ratio over IMS. This investigation has resulted in the development of a prototype instrument that demonstrates the concept of FDIMS. The objective of the proposed Phase II work is enhancements and production of a prototype portable field instrument.

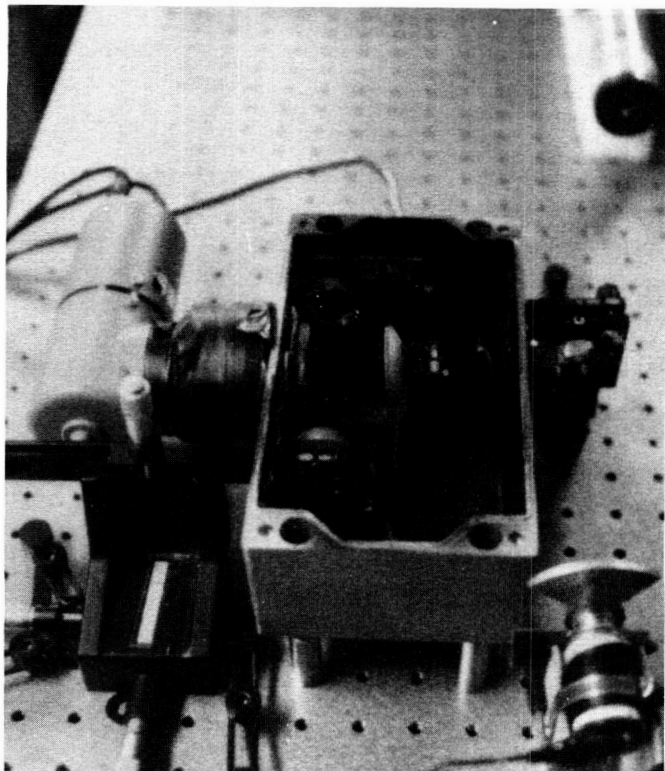
P. A. Mogan and W. R. Helms,
867-4438

DL-ESS-31

Hydrogen Laser Monitoring System (HLMS)

The checkout and launch of space vehicles involves measurement of a large number of parameters in a field operational environment. A reliable, low-maintenance hydrogen (H_2) gas monitor is needed to check for leaks in gas purge lines and to guard against flammability conditions in the launch of the Space Shuttle. The monitor must have a sensitivity of tenths-of-a-percent H_2 up to ten percent or more, and must give accurate readings in a variety of sample gases, including nitrogen (N_2), helium (He), air, or any mixture of the three.

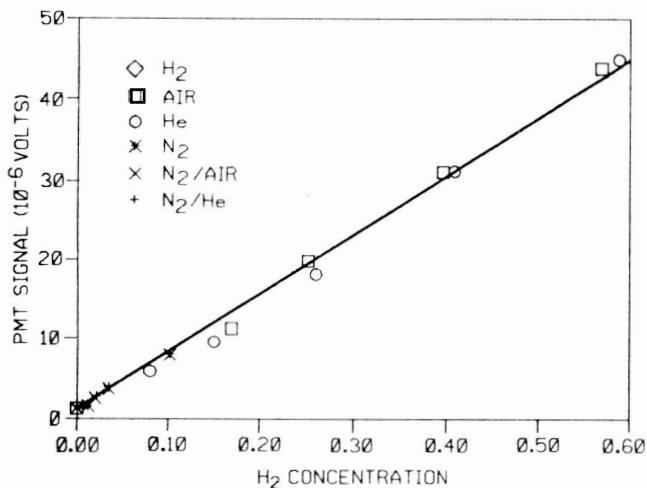
The basic concept of HLMS is the measurement of H_2 concentration by detection of its characteristic Raman scattering when illuminated by a laser. Monochromatic light from an argon ion or helium-neon laser enters a multipass optical cell where it traverses back and forth through a sample region containing the gas to be analyzed. Raman-scattered light generated by the H_2 in the sample is shifted in wavelength by a characteristic amount. This Raman light is collected and passed through a narrow bandpass filter, which blocks the nonshifted laser light and other undesired radiation, and is detected by a photomultiplier tube. Since a chopper is used to modulate the laser light, the Raman signal is modulated as well, enabling the use of lock-in detection to reject ambient light and photomultiplier noise. The output of the lock-in circuitry,



*Hydrogen Laser Monitoring System
Breadboard*

which is proportional to the H_2 concentration in the sample, is converted to the desired instrument output signal (for example, a 1- to 5-volt analog channel).

The Raman technique has unique advantages over many alternative approaches. The Raman scattering is exactly proportional to the H_2 num-



Signal Versus Hydrogen Concentration

ber density in the sample region and is independent of the nature of the background gas. These properties make calibration of the HLMS instrument simple and reliable.

As a result of the Phase I effort, the concept of using Raman scattering for sensitive and accurate detection of hydrogen concentrations in gas samples was successfully demonstrated with the laboratory breadboard instrument that was developed. The Phase II effort will comprise the development of two brassboard prototypes for laboratory characterization and field testing aboard the Mobile Launch Platform (MLP). These prototypes will be based upon the Phase I argon ion laser design and will have operating ranges of 0 to 4 percent and 0 to 100 percent with resolutions of 200 and 500 parts per million, respectively.

If the brassboards remain operational after experiencing the harsh environment of a Space Shuttle launch, a Phase III effort will be encouraged to develop this sensor commercially. Usefulness of this instrument would not be limited to hydrogen detection, as other gases could be detected by using a different series of bandpass filters.

M. A. Nurge and W. R. Helms,
867-4438

DL-ESS-31

Multispectral Imaging of Hydrogen Fires

A requirement for a camera that could display normally invisible hydrogen fires was realized during an aborted STS-14 launch. Immediately after the on-pad abort, the hydrogen flame detectors went into alarm condition. During the fire, it became apparent that visibility of the hydrogen flame was highly desirable. Fire extinguishing systems must be turned off to enable the current fire detection system to operate.

Hydrogen fires emit within the same frequency band as sunlight. While sunlight is present, a hydrogen fire is invisible to human eyes and to standard cameras. Hydrogen fires also emit in bands not visible to standard cameras (or eyes) but visible to specialized sensors. A camera that could display a hydrogen fire and be hooked directly into the standard operational television channels would be a valuable safety device.

Since hydrogen flames emit ultraviolet (UV) and infrared (IR) radiation, a UV-IR camera would allow visibility of a hydrogen flame. To properly identify the location of the fire and the extent of the action to be taken, it is necessary that a high-resolution picture of the background be displayed on the same image as the fire. It is also necessary to provide a way to easily distinguish between the frequencies of concern.

Numerous tests, using IR and UV cameras overlaid onto a black and white video background, have shown that the concept is valid. The tests have also shown several areas that need further development.

In testing performed using an image-intensified UV camera, it was apparent that the UV emissions from a hydrogen flame may be up to 1,000 times less than literature indicated. This means that either a much better UV detector or a much better image intensifier with better filtering is required to UV image a hydrogen flame. A photo spectrometer has been purchased to allow full characterization of a hydrogen flame. This will allow proper filter selection for the IR and UV cameras to help reduce sunlight noise in the area of concern.

Other problems were identified with the IR cameras. The IR cameras tested to date are too slow to allow multiple filtering, utilizing one camera. Some blooming and smearing also occurred during rapid tracking with some of the IR cameras tested.

The video processing capabilities have been improved considerably within the past year. A demonstration was performed overlaying UV and IR onto a black and white visible background at a rate of ten frames per second. UV was displayed in blue and IR in red. Thresholds are adjustable on the input signals to permit display of only high-level (fire) signals. Video resolution has been increased to 200×200 pixels.

Additional camera and video processing computers have been ordered. These will allow real-time processing and display of three video signals. It may also be necessary to use multiple IR bands instead of IR-UV if the hydrogen flame UV emissions are as low as suspected.

J. D. Collins and W. R. Helms,
867-4438

DL-ESS-31

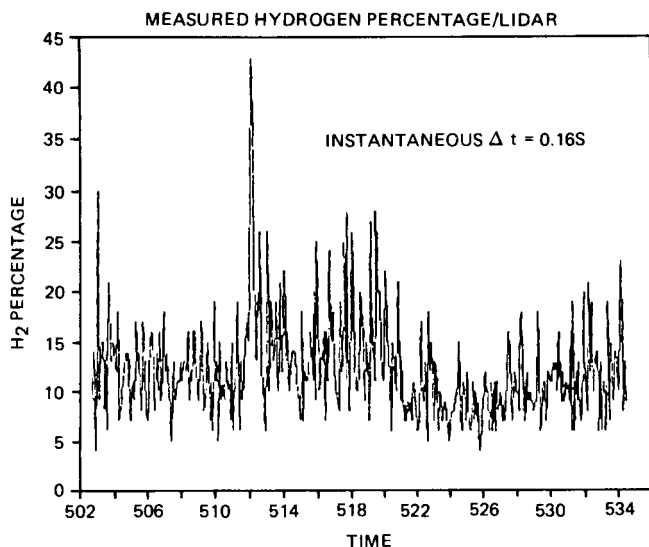
Remote Detection and Characterization of Fugitive Hydrogen by a Raman LIDAR System

The objective of this project was to develop and field test a Raman light detection and ranging (LIDAR) system that is capable of three-dimensionally mapping and characterizing fugitive hydrogen clouds associated with Space Shuttle main engine (SSME) ground firing operations.

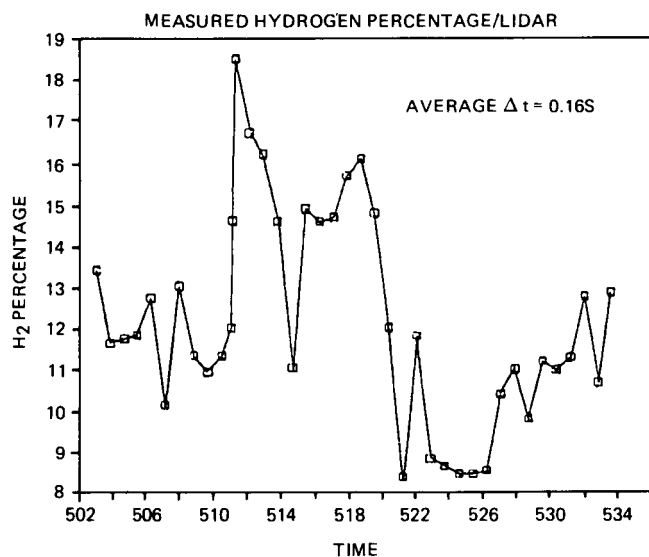
Routine launch pad preflight combustion testing of the SSME's is immediately followed by the purging of invisible, unburned hydrogen which has a finite potential to build up in open areas where traditional fixed-point detectors cannot be installed. The primary advantage of remote sensing instrumentation is its ability to scan, from one or more centrally located positions, large spatial volumes of the atmosphere in surrounding facilities, providing thousands of cubic meters of monitored area protection unobtainable with currently available instrumentation.

Operating in many respects similar to radar, the LIDAR system employs a pulsed laser as a transmitter and a photomultiplier-equipped telescope as a receiver. Pulsed laser energy propagates through the atmosphere along the telescope line of sight, radiating (exciting) all molecules along the path. Most molecules (including hydrogen, nitrogen, and oxygen) scatter electromagnetic radiation not only at the excitation wavelength (Rayleigh scattering) but also at specific shifted wavelengths (Raman scattering). The magnitude of the wavelength shift is unique to the particular scattering molecules (in this case hydrogen). The intensity of the Raman band is proportional to the scatter originally caused by the pulsed laser radiation of molecules of measurement interest received back at the LIDAR system telescope, which is "tuned" through the use of special bandpass filters to the Raman wavelength of the molecule of interest.

The initial phase of the project involved modification of an existing Raman mobile LIDAR system to detect and measure hydrogen. The system was used in field tests at Stennis Space Center (SSC) on one of the SSME test stands during engine test firings. The LIDAR van was



Instantaneous Peak Hydrogen Concentration



Average Peak Hydrogen Concentration

located approximately 1,000 feet from the test stand with a line of sight 50 to 75 feet downstream of the deflection bucket at an elevation of 50 to 60 feet above ground.

Although the unit could scan the exhaust plume, it was decided to fix the LIDAR system along a single line of sight because of the rapidly changing dynamics of the test environment. The two diagrams shown indicate the instantaneous and average peak concentrations along

the line of sight for one of the test runs. The concentration shown should not be treated as highly accurate since a number of interferences (reflection off water droplets and debris in the exhaust plume resulting in a filter punch-through and scintillation from sunlight) may have contributed to an unusually high reading. A second detection channel would need to be added to measure the reflected energy at the laser frequency to better characterize these errors; however, no further study is planned at this time.

M. A. Nurge, J. D. Collins,
and W. R. Helms, 867-4438

DL-ESS-31

Characterization of a Turbomolecular-Pumped Magnetic Sector Mass Spectrometer

Hazardous gases are used extensively in various phases of a Space Shuttle launch at Kennedy Space Center (KSC). Presence of hydrogen, even in small amounts, in unwanted areas may generate severe hazardous conditions. In order to avoid the accumulation of these gases, nitrogen is used as a purge gas in various Shuttle compartments while helium is used to purge cryogenic fuel lines. It is important to monitor the presence of hydrogen, oxygen, and other inorganic gases in the purged environments for a safe Space Shuttle launch.

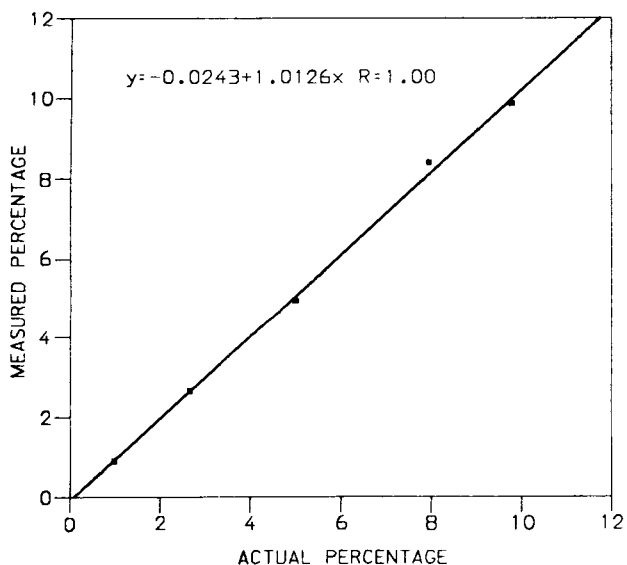
The gas detection system used at KSC for Space Shuttle launches includes the monitoring of hazardous gases in various purged environments. Mass spectrometers and other analytical instruments, located in the mobile launch platform (MLP), are used for the analysis of these purged gases. The spectrometers, in the past, had diode ion pumps for their high-vacuum systems and, over numerous Shuttle launches, have proven to be highly reliable for the detection of hydrogen, oxygen, argon, and helium in nitrogen-purged areas. Helium-purged areas could not be monitored by these systems since ion pumps are not well suited to pumping with a nearly 100-percent helium background.

Mass spectrometers with turbomolecular vacuum pumps, which are ideal for monitoring the helium-purged environments, have just recently become available. The advantage of these

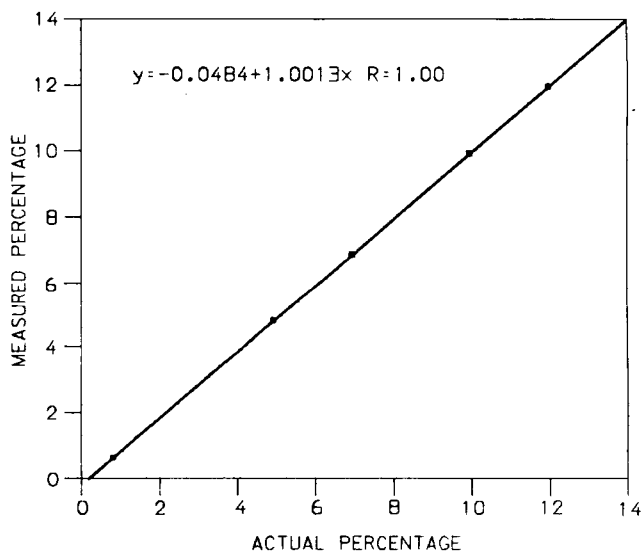
pumps is that they are not affected by the noble gases. Currently at KSC, turbomolecular-pumped mass spectrometers are being tested for use in monitoring helium- and nitrogen-purged areas; the results have been promising.

The testing under this program was performed on a Perkin-Elmer MGA 1200 mass spectrometer with a 50-torr-liter-per-second turbomolecular pump. This mass spectrometer was built for the

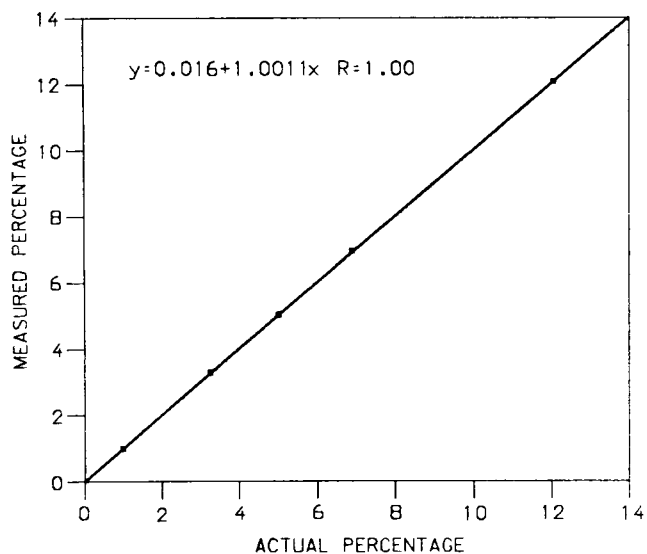
Air Force to perform measurements on the unburned hydrogen problem at Vandenberg Air Force Base. The MGA was configured to measure hydrogen, helium, water, nitrogen, oxygen, argon, and neon. The mass spectrometer was tested for linearity, precision, drift, detection limits, and overall accuracy for measurement of these gases in both a nitrogen and helium background. The linearity information is presented in the figures.



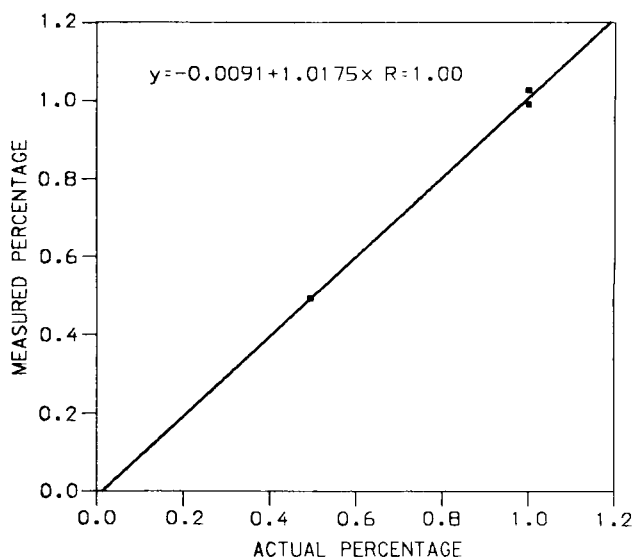
Hydrogen Linearity, 10-Percent Range, Nitrogen Background



Helium Linearity, 100-Percent Range, Nitrogen Background

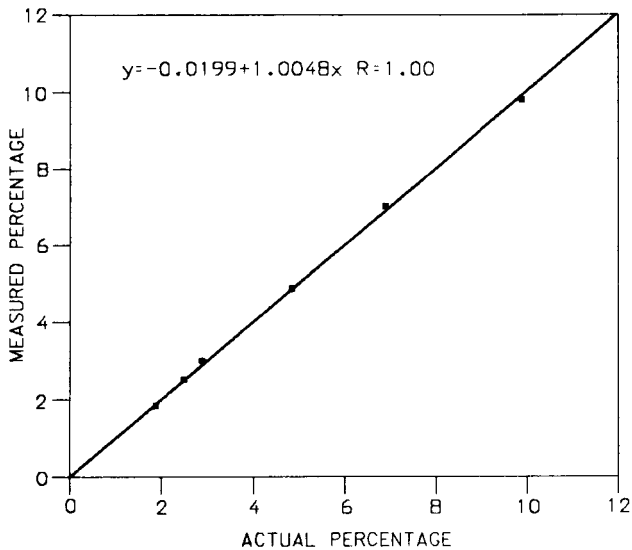


Oxygen Linearity, 25-Percent Range, Nitrogen Background

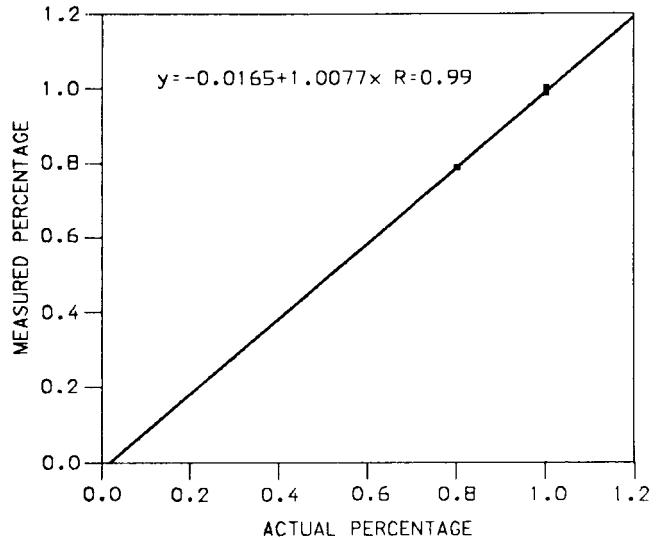


Argon Linearity, 1-Percent Range, Nitrogen Background

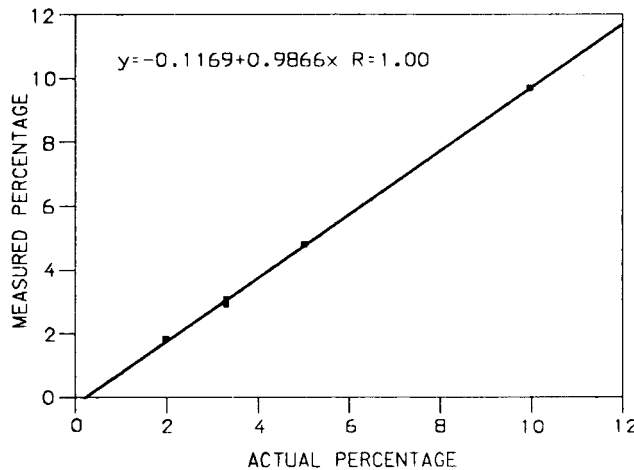
ORIGINAL PAGE IS
OF POOR QUALITY



Hydrogen Linearity, 10-Percent Range, Helium Background



Argon Linearity, 1-Percent Range, Helium Background



Oxygen Linearity, 25-Percent Range, Helium Background

All the gases had relative errors of between 0.05 and 3.05 percent except for hydrogen on two of the standard bottles. These bottles were already suspect from previous tests but are included in this report. Including all bottles, the maximum relative error was less than 10 percent.

J. D. Collins and W. R. Helms,
867-4438

DL-ESS-31

Advanced Hazardous Gas Detection System (AHGDS)

The Hazardous Gas Detection System (HGDS) monitors the Space Shuttle for potentially dangerous cryogenic leaks. The HGDS has performed well from its inception in 1979. Manufacturers' support for the HGDS will not be available by 1990 on most of the system; parts for the system are already unavailable at this time.

In order to fulfill the Space Shuttle's requirement for a highly reliable and well supported gas detection system, the AHGDS project was begun. The Navy's Central Atmospheric Monitoring System (CAMS) was chosen as a basis for the AHGDS sensor. The mass spectrometer in the CAMS is a rugged, reliable, and accurate magnetic sector instrument. It has been proven through many years of use aboard hundreds of submarines. This mass spectrometer was modified to meet NASA requirements and has undergone extensive testing. Its accuracy, linearity, and stability have been demonstrated in more than a year of testing.

In last year's Research and Technology Annual Report, it was reported that the mass spectrometer met all of NASA's requirements, except for the helium sensitivity required to perform the Space Shuttle main engine (SSME) helium signature leak test. After trying several approaches, it was decided that increasing the amount of gas introduced into the mass spectrometer would give the highest probability of increasing sensitivity. Introducing more gas into the mass spectrometer requires additional pumping in order to maintain a high-vacuum condition within the analyzer. To achieve additional pumping, a 170-torr-liter-per-second turbo pump (Balzers model TP-170) was mounted to the mass spectrometer. An extra flange, which normally supports the ion pump, was purchased. A rectangular hole was machined into the flange, and the flange was welded to a rectangular stainless steel pipe that in turn was welded to a circular pipe that mated to a standard 6-inch vacuum flange. The turbo pump was connected to the flange.

Before mounting the spectrometer, the turbo pump was vibration tested. For vibration testing, the turbo pump was mounted to a plate that was mounted to a vibration table. The plate had an O-ring groove, and an O-ring was used to make an airtight seal. The vibration table was vibrated both horizontally and vertically, and the pump was mounted with its axis of rotation both parallel and perpendicular to the table. Thus, four tests were performed. The vibration profile of the table was calculated to encompass launch conditions based upon NASA data. Table 1 presents the vibration profile. The pump successfully passed the vibrator test. No leaks occurred between the turbo pump and the rough pump, and no unusual noise from the pump was heard.

In order to measure the vacuum in the mass spectrometer when it was pumped, an ionization gauge was mounted to the pipe connected to the turbo pump. After 24 hours of operation, the background pressure was 2×10^{-8} torr. When the leak valve was opened to give a nitrogen signal of 5.8 volts, the pressure increased to about 4×10^{-8} torr. The leak valve was further opened until the pressure was 2×10^{-6} torr.

Table 1. Vibration Profile

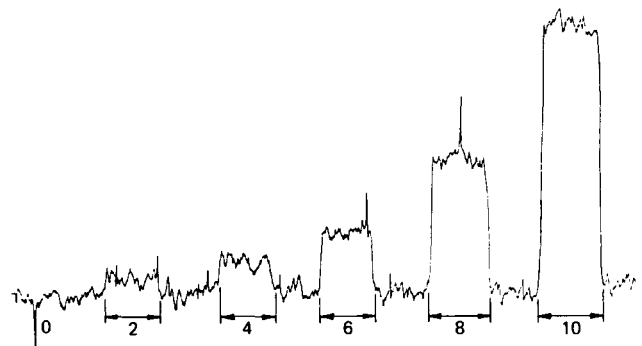
Test (table movement)	Frequency (Hz)	Acceleration (g)
Horizontal (3-minute log sweep)	2 to 3	0.10
	3 to 6	0.30
	6 to 20	0.45

Vertical (2-minute log sweep)	2 to 3	0.10
	3 to 4	0.30
	4 to 8	0.45
	8 to 10	0.20

Helium in nitrogen mixtures was added to the system, and the signal corresponding to helium was recorded. Table 2 lists the data.

Table 2. Helium Sensitivity Data

Setting	Signal (mV)	Helium (ppm)
2	12	0.7
4	20	1.3
6	38	2.8
8	78	5.9
10	152	11.7



Data for Helium Detection Using a Turbo-Pumped System

The noise level was about 15 millivolts (mV). The raw data is shown in the figure. The sensitivity to helium is 15 mV/ppm or about 30 times greater than without the turbo pump.

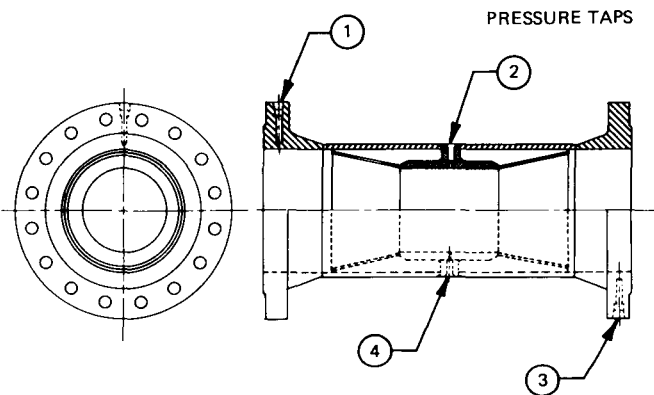
This sensitivity is adequate to meet NASA's requirements for the helium signature leak test.

J. D. Collins and W. R. Helms,
867-4438

DL-ESS-31

Bidirectional Flow Meter

When servicing the Space Shuttle, measurement of liquid oxygen flow during both the loading of the external tank and the draining back to the launch pad storage tank is necessary. A single flow meter that will provide efficient and accurate monitoring of liquid oxygen flow in both directions is therefore being developed.



Bidirectional Flow Meter

Kennedy Space Center procured a bidirectional, venturi-type flow meter from Badger Meter, Incorporated. Pressure tap 1 in the figure measures the upstream pressure, and pressure tap 2 reads the downstream pressure when the flow is from left to right. When the flow is from right to left, the upstream pressure is measured at tap 3 while the downstream pressure is measured at tap 4. The meter is rated to measure liquid oxygen flow up to 5,400 gallons per minute. The device has been under test at the component test laboratory; calibration data for flow versus pressure differential are being developed.

J. E. Fesmire, 867-3313

DM-MED-43

Chemiresistors for the Detection of Hydrazine and Nitrogen Dioxide

Objective: To develop microsensors capable of detecting hydrazine and nitrogen dioxide at sub-parts-per-million (ppm) levels.

Background: Personnel safety requires hydrazine vapor detection at sub-ppm levels. The commercially available instruments cannot reliably detect hydrazine, monomethylhydrazine, and unsymmetrical dimethylhydrazine at the National Institute of Occupational Safety and Health (NIOSH) recommended values of 30, 40, and 60 parts-per-billion (ppb), respectively.

A novel microsensor called a chemiresistor has been developed. The device is a vapor-sensitive organic semiconductor that acts like a resistor where the conductance is changed by the presence or absence of chemical vapors. A chemiresistor consists of contacting electrodes covered with a chemically sensitive semiconductor film. Several devices could sit on a dime.

Advances were previously made on this project in the areas of microsensor technology and pattern recognition methods of data analysis. An array of five different phthalocyanine-coated chemiresistors was investigated for hydrazine detection. The discrimination against hydrazine was suitable for leak detection using these coatings, although the recovery time was too slow for real-time detection.

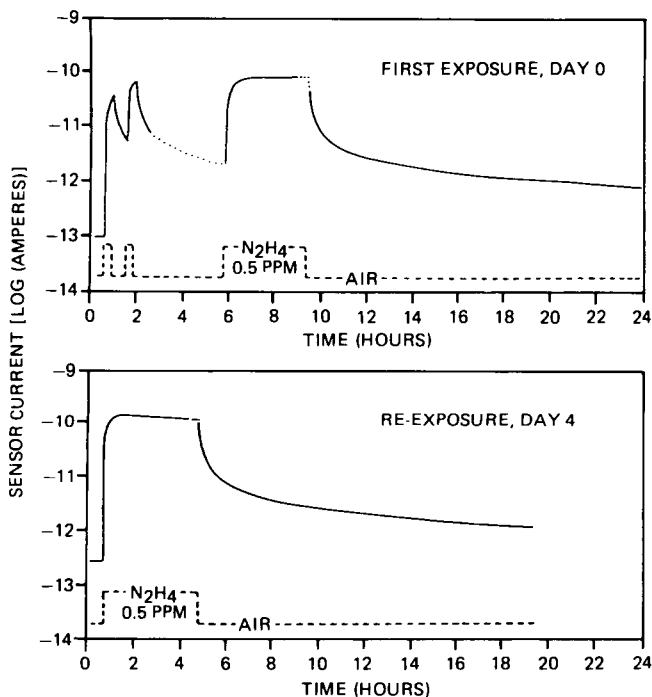
Approach: Several approaches, designed to overcome the problems observed in the previous chemiresistor study, were conducted. An improved coating for hydrazine was the first area of investigation. Dithiolene was examined as a new class of semiconductor coatings. The second investigation examined six chemiresistors of a different design, each coated with lead phthalocyanine. The devices were provided by Dr. Jones of the Health and Safety executive in the United Kingdom. The last study investigated the effect of temperature on the response and recovery time of a set of sensors using a different chemiresistor substrate.

The organic semiconductor bis(diethylamino-dithiobenzil) nickel (BDN) is a sensitive coating for hydrazine. A three-order-of-magnitude change in resistance was measured upon exposure to hydrazine at 0.5 ppm. The three-order-of-magnitude change in response was greater than

any of the phthalocyanine coatings tested to date. A positive change in conductance is an advantage for pattern recognition applications when these sensors are used in conjunction with phthalocyanine coatings. The direction of the change in conductivity for the BDN coating is opposite that of the phthalocyanine coatings for hydrazine and is the same for nitrogen dioxide.

Comparison of the Relative Sensitivity of the Sensors to Each Test Vapor

Vapor	Concentration	Change in Response
Hydrazine (N ₂ H ₄)	500 ppb	100 to 1000
Monomethylhydrazine (MMH)	500 ppb	10 to 20
Unsymmetrical dimethylhydrazine (UDMH)	500 ppb	2
Anhydrous ammonia (NH ₃)	30 ppm	3
Nitrogen dioxide (NO ₂)	10 ppm	10
Water	60-percent relative humidity	10



NOTE: THIS IS THE OVERALL HISTORY OF RESPONSE AND RECOVERY OF THE FIVE LEMUR-BLOGGETT LAYER BDN CHEMIREISTOR SENSOR FOR THE FIRST FIVE DAYS OF TESTING. THE SOLID LINES ARE ACTUAL DATA; THE DOTTED LINES ARE INTERPOLATED; AND THE DASH LINES INDICATE SAMPLE FLOW.

Five Lemur-Bloggett Layer BDN Coating on Chemiresistor

These coatings demonstrated good shelf life. Sensors aged for 19 months gave the same response as freshly coated sensors. The stability over several months is important for detection applications. These devices can be used as an alarm device without improvements.

The chemiresistor provided by Dr. Jones is easy to handle, and the heater on the chip is very convenient. The surface roughness requires

thick films that prevent equilibrium responses and fast recovery. Lead phthalocyanine presents good characteristics for detecting nitrogen dioxide. This coating, used in an array with the dithiolene coatings, could improve the discrimination capability of the array.

The responses of a set of phthalocyanine-coated sensors were determined using temperatures between 20 to 140° C. Increasing the temperature improves the recovery time of the sensors. The time is not sufficient for a real-time instrument, but the sensors do have application as alarm devices. A rise in temperature precipitated an increase in conductance and the magnitude of response for all the sensors. Before conducting the tests, an increase in temperature was expected to decrease the magnitude of response due to increased decomposition of the vapor. It is probable that the diffusion of the gas into the coating is improved at higher temperature allowing more vapor to interact with the coating, thus increasing the magnitude of the response.

J. D. Collins and W. R. Helms, 867-4438

DL-ESS-31

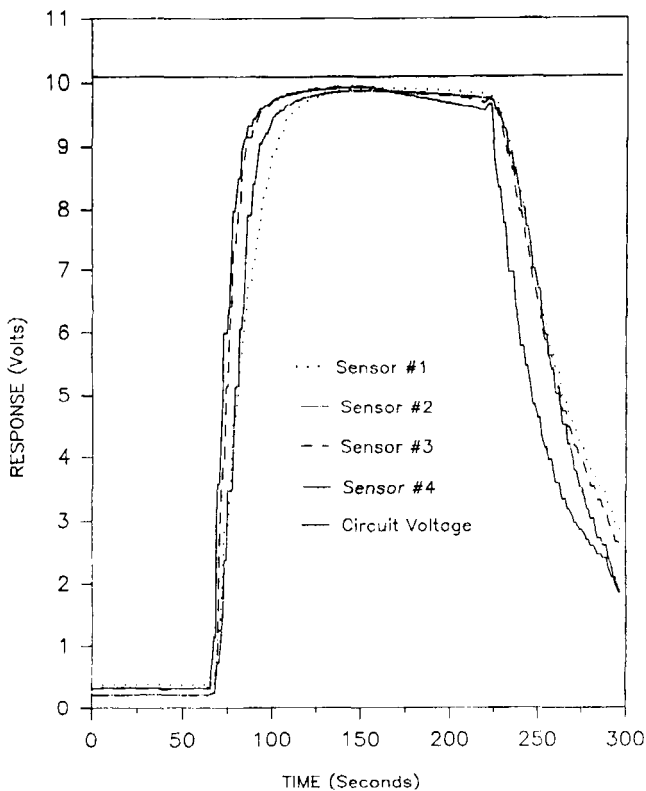
Toxic and Flammable Gas Detectors

Objective: To evaluate the Figaro TGS 813-P and TGS 821-D solid state microsensors for their response to hydrogen. The evaluation of their response to hydrazine and monomethylhydrazine was reported in the 1987 Research and Technology Report.

Background: Hydrogen, which is used in large quantities to fuel the Space Shuttle main engine, is explosive at concentrations above 4 percent. It is, therefore, important to detect hydrogen gas leaks well before they reach this level.

Approach: The Figaro 813-P and 821-D sensors were tested for their response to hydrogen gas in background gases of both air and nitrogen. These tests were conducted at various relative humidities and in the presence of potential interferants, such as alcohols, hydrazine, helium, ethylene, and general reducing agents. The lower limits of detection, response and recovery time, saturation limit, repeatability, baseline stability, and response to relative humidity were determined for the sensors.

1000 ppm H₂ : 42% RH: in GN₂



Figaro TGS 821 H₂ Sensor

Results: The TGS 813-P sensor was unusable for detection of hydrogen because of its lack of selectivity. The 821-D sensor was selective for hydrogen and was usable for concentrations up to 1,400 parts per million. The only significant interferant for this sensor was high concentrations of ammonia, but relative humidity also changed both the baseline and hydrogen response (refer to the included graph). This sensor is appropriate only as a leak detector for low levels of hydrogen in areas where there is no ammonia present.

P. A. Mogan and W. R. Helms,
867-4438

DL-ESS-31

Colorimetric Hydrazine Dosimeter Badge for Personnel Monitoring

Objective: The purpose of this research was to develop a reliable colorimetric hydrazine dosimeter badge that would be reasonably quantitative, easy to read, uncomplicated, and would respond to threshold limit value (TLV) levels of hydrazine or monomethylhydrazine (MMH) within 15 minutes of exposure.

Background: The transfer of hypergolic fuels at Kennedy Space Center (KSC) for use on the Shuttle and various payloads cannot be accomplished without human interaction, control, and servicing of the hardware. The possibility of leaks or residual contamination of components by these fuels necessitates the use of monitoring equipment to maintain the high level of personnel safety required by NASA. This is routinely accomplished by industrial hygienists and safety personnel using electrochemical hydrazine monitors; however, to provide redundancy and individual monitoring capability, it was decided that a colorimetric dosimeter badge would be the most effective method to use. Since no reliable color badge for hydrazine detection was commercially available, this research was undertaken.

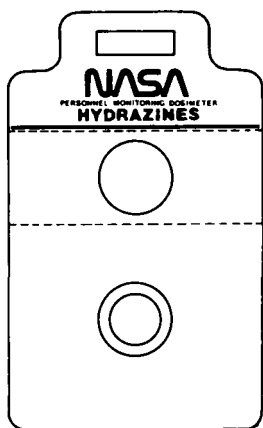
Approach: This research was conducted through a Small Business Innovative Research (SBIR) contract which is currently in its second phase. Phase I was limited to chemical research to identify the most effective chemical system

for the selective detection and quantification of hydrazine and MMH in the concentration range from 0.25 to 16 TLV-hours. This included the evaluation of various materials and other control mechanisms to determine a suitable diffusion barrier. The results of this phase indicated the feasibility for the design of a passive badge system for the detection of hydrazines.

Phase II involved the development of prototype badges for laboratory evaluation at KSC followed by the delivery of 1,000 final prototype badges for extensive laboratory and field evaluation. This phase also included the development and delivery of a colorimetric dose estimator for use with the final prototypes.

Results: Phase I resulted in the identification of two chemical systems which, with the proper control mechanisms, will meet the design goals. One system is based on paradimethylaminobenzaldehyde (p-DAB) and the other is based on 3-methoxy-4-hydroxybenzaldehyde (vanillin), a system developed at the Naval Research Laboratory. Vanillin meets the concentration range requirements without the use of control mechanisms, is insensitive to sunlight fading, and is stable; but the color change is from neutral to yellow, which does not provide great contrast. p-DAB provides greater contrast by changing from neutral to orange but is sensitive to sunlight and requires a control mechanism to meet the range requirements.

The badge housing will be a coated tag stock (a type of dense paper or cardboard). The badge will have one window that is nondiffusion-



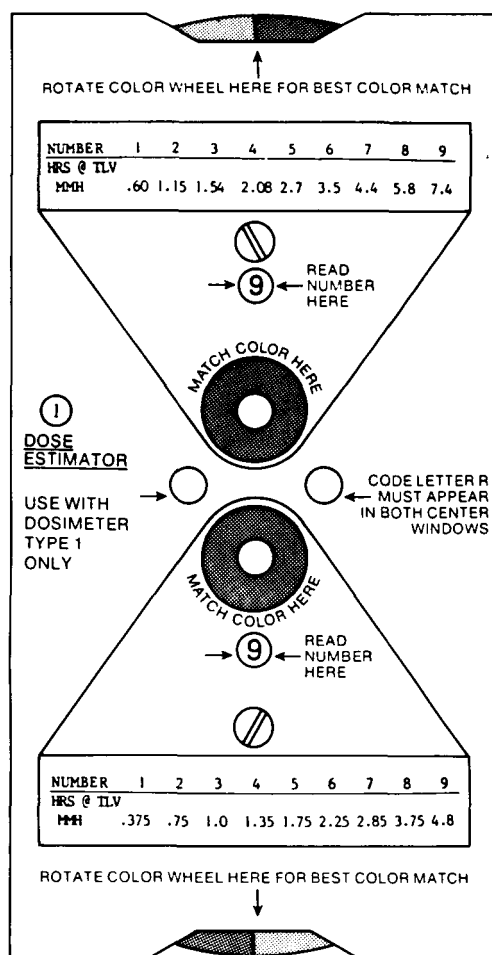
Card-Type Disposable Badge

controlled for quick response and semiquantitative measurements and a second window that is diffusion-controlled for a more accurate measurement of actual exposure levels. The colorimeter, which will be provided for measuring the level of exposure, will be designed as a color comparison wheel and will provide estimations of the actual dosage with an accuracy of plus or minus 25 percent. The badge will be small, portable, and inexpensive.

The first set of prototype badges have been received at KSC, and laboratory testing is eminent. These tests will determine which of the chemical systems will be used in the final badge design.

J. C. Travis and W. R. Helms,
867-4438

DL-ESS-31



Visual Color Comparator

Fast-Response Instrumentation Van

Some testing performed by Kennedy Space Center (KSC) involves the use of hazardous fluids such as hypergols and liquid hydrogen. It is sometimes desirable to perform these tests in remote locations for personnel safety reasons. KSC is developing an instrumentation van that can be used to support testing at remote locations. The vehicle being equipped is a 1987 Chevrolet step van.

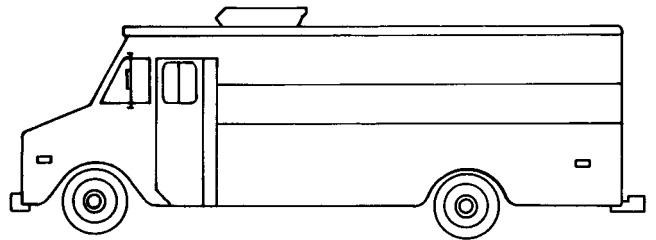
The van is being outfitted to provide measurement and data processing capability on a one-to-three week notice for support of small tests with up to 50 measurements. This capability will include installation and verification of sensors, real-time data display of selected measurements, and recording of all measurements for posttest data reduction. Strip chart recorders will be installed that will provide up to three eight-channel

direct-write recorders. A 20-channel oscillograph recorder will also be provided.

The fast-response instrumentation van will also provide support capability of fabrication and verification for advanced launch system facilities and systems.

F. N. Lin, 867-4181

DM-MED-11



Fast-Response Instrumentation Van



Protective Coating Systems for Repaired Carbon Steel Surfaces

In the past, maintenance repair of corroded carbon steel surfaces required the use of abrasive blasting to adequately clean and prepare the metal surface for application of protective coatings. Recent advances in coatings technology promises acceptable protective coating performance when surface preparations are less than perfect. The present study focuses on new products and techniques that may reduce the level of surface cleanliness required for corrosion protection in many areas at KSC.

The coatings being tested in this study include epoxy mastics, moisture-cured urethanes, chemical conversion coatings, and any other type repair coating identified during the course of the program. The study compares the performance of previously rusted panels that have been mechanically prepared using four methods and two initial conditions. The four mechanical methods used are a power wire brush, a pneumatic needle gun, a sanding disk, and a coarse wheel grinder. The two initial conditions to be used are to prepare the panels both with water washing and without water washing prior to mechanical cleaning.

The initial screening of the many products will be accomplished by exposing the prepared panels to 2000 hours in the salt fog chamber. Following the screening procedure, the material list and preparation methods will be evaluated to determine which combinations will be used in a final test exposure sequence. After preparation of all test panels using the decisive materials and methods, two different exposure conditions will be used to determine coating performance. Duplicate test panels will be exposed at the beach corrosion site and in the laboratory to search for possible correlation.

Panels exposed at the beach corrosion site and the laboratory will under-go solid rocket booster (SRB) effluent testing to simulate the

conditions at the launch site. The SRB effluent tests will be accomplished by dropping simulated effluent onto two-thirds of the panels every two or three weeks. Panels at the beach will be inspected periodically (at least at intervals of 1, 3, 6, 12, 18, 36, and 60 months) and will be rated for rusting in accordance with American Society for Testing and Materials (ASTM) D610 on a scale from 1 to 10. An expanded test plan is available under Materials Testing Branch (MTB) report number MTB-144-88.

L.G. MacDowell, 867-2906

DM-MSL-2

Study of Thermal Sprayed Metallic Coatings for Potential Application on Launch Complex 39 Structures

The objective of this study is to evaluate candidate thermal sprayed metallic coatings for potential application on the Zone 1 (high-temperature rocket motor blast) structures at Launch Complex 39. Tests are being performed to determine if the candidate coatings will protect the structure from the abrasive blast, heat, and acid-rich environment associated with the solid rocket booster (SRB) exhaust during Shuttle launches.

Launch Complexes 17 and 40 have been utilized to test the coatings. Both the Delta (Launch Complex 17) and the Titan III (Launch Complex 40) are powered by solid rocket motors (SRM's) and provide a launch environment similar to SRB exhaust.

The initial results have not been encouraging. The coatings experienced cracking and debonding from the substrate due to thermal shock. Additional test panels are being coated and improved adhesion/bonding is a primary concern. Tests are planned for Launch Complex 40.

P.J. Welch, 867-4614

DM-MSL-2

Development of New Flooring Materials for Clean Rooms and Launch Site Facilities

NASA utilizes one of two different static dissipating floor coverings in Shuttle assembly areas: flexible polyvinyl chloride (PVC) tiling or poured epoxy floor covering. Both have disadvantages associated with their use. The flexible vinyl tiling, which is currently the floor covering of choice, fails NASA's outgassing tests due to the plasticizer component within the formulation. The plasticizer can volatilize at room temperature and then recondense on sensitive optical surfaces leading to contamination problems. Although there are static dissipating vinyl tiles commercially available, none have qualified following outgassing tests. Disadvantages associated with the poured epoxy floor coverings are dusting, chalking, and repair difficulties.

A Small Business Innovative Research (SBIR) contract identified chemically resistant polymers, conductive fillers, flame retardant additives, and structural adhesives that could be used as formulation components in a specialized floor covering for installation at NASA launch site facilities, which would eliminate or minimize the current flooring inadequacies.

As a result of experimentation, a conductive fiber was determined to be the most efficient filler giving the most consistent results. Surface and volume resistivities of 10^6 to 10^8 ohms per square were achieved consistently.

At the present time, sample formulations are undergoing outgassing and hypergolic resistance tests at Kennedy Space Center. All formulations are expected to perform well since each contains no volatile component and each base resin was selected because of its proven resistance to hypergols.

C.J. Bryan, 867-4344

DM-MSL-2

Conductive Organic Polymers As Corrosion Control Coatings

The seacoast environment of the Kennedy Space Center (KSC) is extremely corrosive to

mild steel ground support equipment and structures. For over 20 years, inorganic zinc-rich coatings have afforded protection for launch structures. The launch of the Space Shuttle, however, releases high concentrations of hydrochloric acid that attack the zinc portion of the protective coating system, resulting in subsequent corrosion of the steel launch structures. This attack invokes frequent and expensive repair costs and interferes with launch-critical operations.

In the search for an acid-resistant protective coating, consideration has been given to electrically conductive polymers. Although this is a new field, research findings suggest that conductive polymers may have potential application in corrosion control. The required properties for such an organic coating are: resistance to hydrochloric acid; ease of application, maintenance, and repair; and long-term resistance to the KSC environment. The aim of this research effort is to evaluate several classes of electrically conductive polymers to assess their suitability for corrosion protective coatings in the KSC environment. The two environments presently under study are Zone 2 and Zone 3. Zone 2 environments involve exposure to 400°C for 30 minutes, hot HCl/Al₂O₃, H₂O and NaCl. Zone 3 environments encompass exposure to 66°C, HCl, H₂O, and NaCl.

One of the polymer systems in this study is polyaniline. A conjunctive effort between NASA and the University of Pennsylvania resulted in the synthesis of conductive polyaniline and application of polyaniline solutions onto iron, steel, and stainless steel by brush or dip-coating. Good protection of stainless steel in highly acidic salt solutions has been obtained with polyaniline.

In a conjunctive effort between NASA and the Los Alamos National Laboratory (LANL), several classes of high-temperature polymers were evaluated for suitability for corrosion protection in Zone 2 environments. Laboratory tests were used to evaluate the polymers' thermal resistance, acid resistance, and ability to adhere to metal substrates under harsh Zone 2 conditions. The types of materials tested were polybenzimidazole, polyphenylquinoxaline, polyimide (two structures), polyisoimide, polypyrrone (two structures), and a monomer that produces a highly crosslinked structure upon curing. Half of these materials were unavailable commercially or semi-commercially; therefore, they were synthesized at LANL.

The testing and evaluation program has identified several candidate materials that have undergone further doping and conductivity studies. Results of doping and conductivity experiments have provided information needed to judge suitability of the coatings for accelerated corrosion testing, beach exposure testing, and launch exposure testing.

Coated panels utilizing a few of the candidate materials have been prepared. These samples will undergo accelerated corrosion testing, beach exposure testing, and launch exposure testing. All of these exposure tests will be conducted at KSC.

Studies will continue at KSC and LANL on synthesis of chosen polymers, doping and conductivity evaluations, formulation of coatings, application onto metal substrates, and evaluation of suitability to the KSC environment.

K.G. Thompson, 867-4344

DM-MSL-2

Protective Coating Systems for the Space Transportation System (STS) Launch Environment

Zinc-rich coating systems exposed to the STS launch environment have suffered premature failure due to the highly acidic residue produced by the solid rocket boosters. Early attempts at top-coating these zinc-rich coatings with a thin film to increase their chemical resistance have produced only marginal results.

Currently, other topcoat systems are being tested to improve coating performance for exposure to the harsh launch environment. The present study focuses on using thicker film topcoats over the zinc-rich primers to improve the chemical resistance to both a marine atmosphere and the highly acidic residues.

In 1986, 119 materials producing 67 coating systems were exposed to atmospheric contaminants at the KSC beach corrosion site with concurrent application of an acid slurry made of hydrochloric acid and alumina (Al_2O_3). The slurry is applied to the test panels with no subsequent washdown to simulate the worst-case scenario experienced at the launch sites.

The current test will be conducted for five years to determine the suitability of the topcoat systems. The panels have been judged for performance at 6, 12, and 18 months. Further evaluations will occur at 36 and 60 months. During this five-year period, there will be approximately 130 applications of the acid slurry.

The panels are approaching the 30-month point of exposure. The results of the 18-month evaluation were published in February 1988 under Materials Testing Branch (MTB) report number 268-86B. These results indicate that the thicker film topcoats provide slightly increased protection of the zinc-rich primer, but more exposure time is required to adequately characterize the benefits.

L.G. MacDowell, 867-2906

DM-MSL-2

Ignition of Metals in High-Pressure Oxygen

During the past several years, the White Sands Test Facility (WSTF) of the Johnson Space Center has developed three methods to evaluate the flammability and ignition properties of metals in pressurized oxygen. WSTF is now evaluating the metals used in existing Kennedy Space Center oxygen systems in support of Space Shuttle operations and several other metals being considered for new systems.

The three test methods developed by WSTF are: rubbing friction, particle impact, and promoted ignition. The metals being evaluated include several stainless steels, a carbon steel typically used in vacuum storage vessels, nickel, and several nickel/copper alloys.

The particle impact tests were conducted using sand, rust, and iron particles. Ignitions were obtained only with the iron particles, which suggests that the ignition of the particles themselves plays an important role in the ignition of metals. In these tests, the particle size was kept constant and the oxygen pressure and velocity were the variables.

The promoted ignition tests have also been completed. The nickel/copper alloys were the most resistant to ignition and burning while the

iron-based alloys ignited and burned easily. Titanium ignited and burned at subambient pressures.

The rubbing and friction tests have been completed. It was found in these tests that most materials were harder to ignite at high oxygen pressures than at low oxygen pressures. This is thought to be due to the increased thermal conductivity of oxygen at higher pressures, thus conducting the frictional heat away from the test specimens.

C.J. Bryan, 867-4344

DM-MSL-2

Permeability of Polymers to Organic Liquid and Condensable Gases

Workers involved in the production, use, and transportation of hazardous chemicals may be exposed to numerous chemicals capable of causing harm to the human body. The effects of these chemicals can range from acute trauma, such as skin irritation and burns, to chronic degenerative diseases, such as cancer or emphysema. Since engineering and administrative controls may not eliminate all possible exposure, attention must be given to reducing the potential for direct contact through the use of polymeric-based protective clothing that resists permeation, penetration, and degradation.

Permeation tests are being performed by the Tuskegee Institute to evaluate the protection afforded by various materials used in the fabrication of protective clothing. This evaluation determines the breakthrough time and the steady-state permeation rate for particular chemical/clothing combinations. Materials of interest are butyl rubber, neoprene, poly (vinyl alcohol), poly (vinyl chloride), latex rubber, and chlorobutyl rubber coated Nomex fabric. Chemicals of interest include nitrogen tetroxide, hydrazine, monomethylhydrazine, hexane, toluene, and dimethylformamide.

The test matrix has now been expanded to include gloves in these evaluations. Chemicals of interest include those used routinely in the processing of Orbiters, external tanks, and solid rocket boosters in the Shuttle programs.

C.J. Bryan, 867-4344

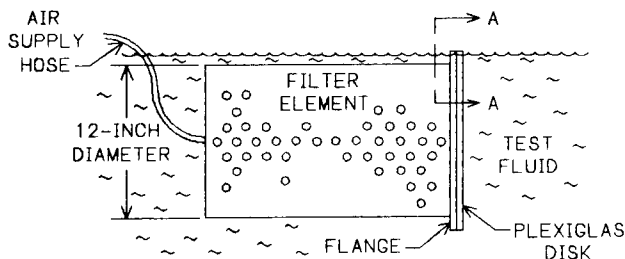
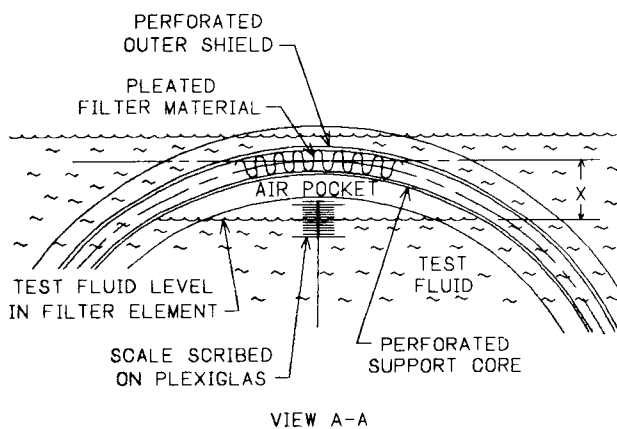
DM-MSL-2

Improved Bubble-Point Test Method

For the launch of Space Transportation System 26 (STS-26), the 12-inch-diameter liquid oxygen (LOX) filter element was bubble-point tested by a new technique devised by NASA and Wiltec, Inc., personnel. The test method previously employed produced erroneous results. The new technique produced a valid certification of the filtration rating of the LOX filter.

The bubble-point test is a method of determining the absolute filtration rating of a filter, expressed in terms of micron rating. The micron rating is the effective size of the largest pore or opening in the filter weave or mesh.

When conducting the test in accordance with ARP 901, Bubble-Point Test Method, the filter element is immersed in a tank of test fluid to thoroughly wet and saturate the porous structure. An adapter (stopper) with a sensing hose is then inserted into the filter inlet. The filter element is held just below the test fluid surface and parallel to it. The filter is gradually pressurized with air or nitrogen until the first bubble



Bubble-Point Test Configuration

appears. Then the filter is rotated beneath the fluid to find the location where bubbles appear at the lowest pressure. The pressure is read on a water manometer. This pressure, the bubble-point pressure, is correlated to the largest pore size to define the absolute micron rating of the filter element.

When conducting the test by the new method, the filter element was submerged level in the test fluid with a Plexiglas disk covering the open end. The disk was scribed to measure the size of the air pocket within the element. Air was injected into the small center hole in the opposite end of the element. The level of the air pocket was observed using an inspection mirror in the clear test fluid.

Go/no-go tests were performed. Air was injected to form an air pocket of a specific size (depth) with a specific bubble-point pressure. The element were then rotated 360°. If the element rotated without bubbling, the element could be certified as meeting the micron rating associated with the bubble-point pressure.

By visually measuring the size of the bubble within the element, the standard bubble-point pressure (P°) can be calculated. This eliminates the problem of measuring, calculating, or estimating the nominal depth of the element pleats beneath the test fluid surface. This also eliminates the problem of having test fluid in the sensing probe used to measure the pressure of the air pocket as fluid in the sensing probe causes erroneous pressure measurements.

The standard bubble-point pressure (P°) is easily calculated:

$$P^{\circ} = X \times (Sg)$$

where:

Standard bubble-point pressure is P° -in (H_2O).

Height or size of air pocket is X-inches.

Specific gravity of test fluid is Sg-dimensionless.

P.J. Welch, 867-4614

DM-MSL-2

Electrically Conductive Polymer Applications

Research in the last decade has brought to light a new class of polymeric materials known as conductive polymers. Many experts have touted this new class of materials as having the potential to combine the conductivity of a metal with the lightweight convenience of a plastic. The physical and chemical properties of polymers (such as high strength-to-weight ratios, toughness, low cost, molecular tailoring of desired properties, and ease of processing into films, filaments, and complex shapes) make polymeric materials extremely attractive for applications. Over the last several years, efforts to develop a new generation of stable and processible conducting polymers appear to be on the brink of success. At the Kennedy Space Center (KSC) a research effort has just begun to develop conductive polymeric materials for some much-needed applications.

The Kennedy Space Center has unique material requirements due to the presence of large quantities of propellants, hazardous gases, pyrotechnic devices, and other hazardous materials. Because of these extremely hazardous environments, sparks that can be built up and discharged from common materials can initiate extremely dangerous consequences. For this reason, plastic films used as spacecraft covers, clothing worn by engineers and technicians, floor tiles used in payload and checkout facilities, as well as materials for many other uses need to meet stringent requirements to avoid potential hazards. The criteria for qualification of materials for use at KSC include low out-gassing, propellant resistance, chemical resistance, flame resistance, and the ability to dissipate static charge.

Currently, numerous techniques are used on materials to invoke the ability to dissipate static charge. For example, many of the fabrics used for KSC clothing worn in hazardous areas and in clean rooms incorporate carbon filaments or metallic fibers. Other fabrics are treated with flame retardants and/or antistatic agents. Some techniques used in producing plastic films that dissipate electrostatic charges are: (1) metallization of the plastic, (2) incorporation of a conductive ink into the material, (3) incorporation of a surface layer or buried layer of conductive material, and (4) incorporation of an antistatic

agent onto the surface of the material. Two techniques used in producing floor tiles that dissipate static charges are incorporating carbon black or stainless steel in the tiles and affixing the tiles with conductive adhesive systems electrically grounded to the building structure.

There are many problems with the materials that utilize the techniques described in the preceding paragraph. For example, materials incorporating metallic fibers or carbon filaments experience mechanical loss of these materials, which is a dangerous and expensive problem around electronic components and in clean room environments. Several problems exist with antistatic agents: (1) leaching of the antistatic agent from the material, which results in contamination problems, (2) anti-static agents washing off the material and (3) nonhomogeneous dispersal of antistatic agents. Hygroscopic agents are beneficial only in humid environments (≥ 45 percent). Conductive inks incorporated into materials tend to wash off and are affected by solvents. The buried layer of conductive material found in many compounds usually employs metal doping, causing the material to lack transparency—a necessary characteristic for many applications.

The material's capacity to dissipate electrostatic charge is one of the most difficult obstacles for qualification of a material for use at KSC. Many materials that pass the electrostatic specifications do not pass all the other qualification tests. For example, floor tiles that pass the electrostatic specifications fail the outgassing qualification. In each usage area at KSC, there is room for much improvement. This is the reason a research effort is underway to develop conductive polymer systems to be used for such applications as fabrics, plastic films, and floor tiles. A prime advantage of fabricating such materials from conductive polymers is that the molecular structure of many such polymers imparts the desired characteristics; therefore, many of the present problems at KSC should be solved. Fiber-type additives would no longer be used, so the debris problem would be eliminated. Since the molecular structure of the material itself would be composed of the needed chemical groups bonded to the backbone of the polymer, there would be no problem of an additive being nonhomogeneous throughout the material or of an additive washing out. The polymer types being considered in the initial work are polypyrroles,

polythiophenes, and polyanilines. These conductive polymers may be combined with commercially available materials to form compounds with the desired properties.

K.G. Thompson, 867-4344

DM-MSL-2

Thermal Sprayed Cathodic Protection for Steel Structures

Throughout the world, hundreds of steel structures have been metalized with thermal sprayed coatings (TSC's) to provide long-term cathodic corrosion protection. Several of the structures date back to the 1930's.

Studies conducted by the thermal spray industry indicate that although the initial cost of a TSC system is more expensive than painting, the extended useful service life of the TSC makes it potentially less expensive as a long-term investment.

A study is underway to evaluate the cathodic TSC systems in the tropical marine environment of the Kennedy Space Center (KSC) and the chloride-rich environment at Launch Complex 39. The TSC's will be compared with the current protection coating system. Inorganic zinc paints are presently used to provide cathodic protection of steel structures. The test panels in this study will not be subjected to Zone 1 (high-temperature rocket motor blast) conditions.

The three cathodic-type TSC systems commonly used in industry will be evaluated. The TSC materials are aluminum (Al), zinc (Zn), and a Zn/Al alloy. All the TSC's will be applied by either combustion-spray or arc-spray systems. The three TSC materials and the inorganic zinc paint system will be applied to test panels that will be exposed to the environment at the KSC beach corrosion test site, Launch Complex 39, and the KSC Industrial Area.

P.J. Welch, 867-4614

DM-MSL-2

Corrosion of Convolute Metal Flexible Hoses

Various cryogenic supply lines and hypergol lines at the Shuttle launch site use convoluted flexible hoses and bellows constructed of 304L stainless steel. The extremely corrosive Space Transportation System (STS) launch environment, composed of sodium chloride and hydrochloric acid, has caused rapid pitting and failure of these flexible hoses. This corrosion leads to loss of vacuum, resulting in high boiloff of the cryogenics.

In 1987, a project was initiated to identify a more corrosion-resistant alloy for this service. After testing 19 corrosion-resistant alloys for pitting resistance, the study quickly focused on the nickel-based alloys such as Hastelloy and Inconel. These alloys were chosen on the basis of their reported resistance to acid/chloride environments.

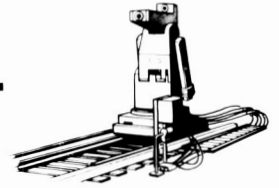
Many different corrosion tests were conducted to screen the alloys for pitting and corrosion resistance, including linear polarization, cyclic polarization, ferric chloride immersion, salt fog/acid slurry exposure, beach exposure, stress corrosion cracking tests, and galvanic corrosion behavior.

The first-year results were published under Materials Testing Branch (MTB) report number 325-87A. Several alloys, such as Inco G-3, Inconel 625, and Hastelloy C-22, C-4, and C-276, performed well. After evaluation of all mechanical data and corrosion tests, Hastelloy C-22 was determined to be the most acceptable alloy for use in the STS launch environment. Samples of all alloys continue to be exposed to salt fog/acid slurry and beach exposure testing to gain valuable long-term exposure data.

L.G. MacDowell, 867-2906

DM-MSL-2

ROBOTICS



Six-Degree-of-Freedom (6-DOF) Robot Target Tracking in KSC's Robotic Applications Development Laboratory

In the 1986 Research and Technology Annual Report under the topic "Robotics Applications for Remote Umbilicals," it was reported that NASA/KSC was working on a robotic automated umbilical system for the T-O (lift-off) umbilical that would allow a soft disconnect at several minutes before projected launch time, with the capability to reconnect promptly in case of a delay. A major step in that direction has occurred with the installation, test, and operation of the 6-DOF Robot Target Tracking Subsystem in KSC's Robotic Applications Development Laboratory (RADL).

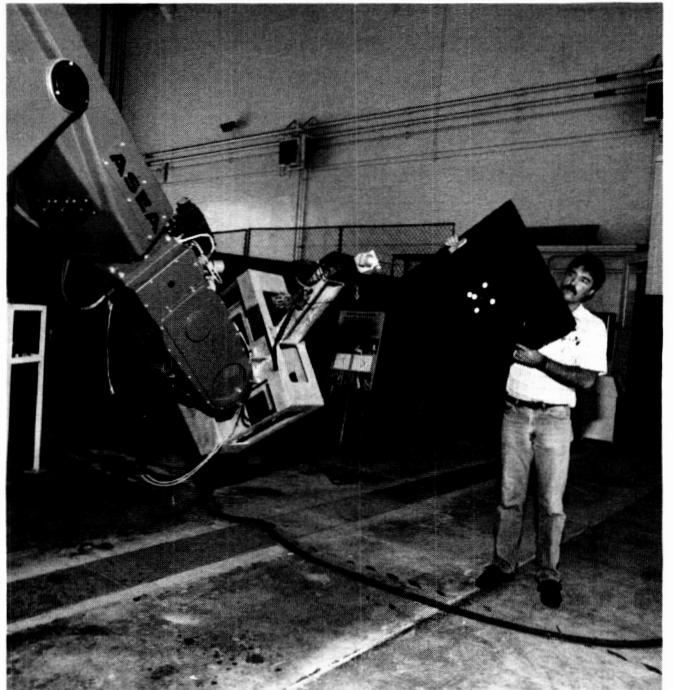
Vision-guided robotics integrated with remote umbilical lines and plates has been proposed as the methodology to allow for autonomous mating of the lines and plates with a moving flight vehicle. The 6-DOF Robot Target Tracking Subsystem in the RADL represents the eyes and the intelligence required by the robotics to track the moving vehicle.

The previous target tracking vision system (see the figure titled "NASA's RADL" in the 1986 Research and Technology Annual Report) could only track a target consisting of one blob (black dot) in 2-DOF at the frame rates of the vision system camera (thirty frames per second). The image processing hardware available at the time of delivery of the original vision system (1986) precluded the acquisition of additional positional information required to track a moving target in 6-DOF. In 1987, a new innovation in image processing hardware that allows acquisition and analysis of multiple blobs (objects) per camera frame at the above thirty-frames-per-second update rates was procured by NASA at KSC and installed in the RADL vision system in 1988.

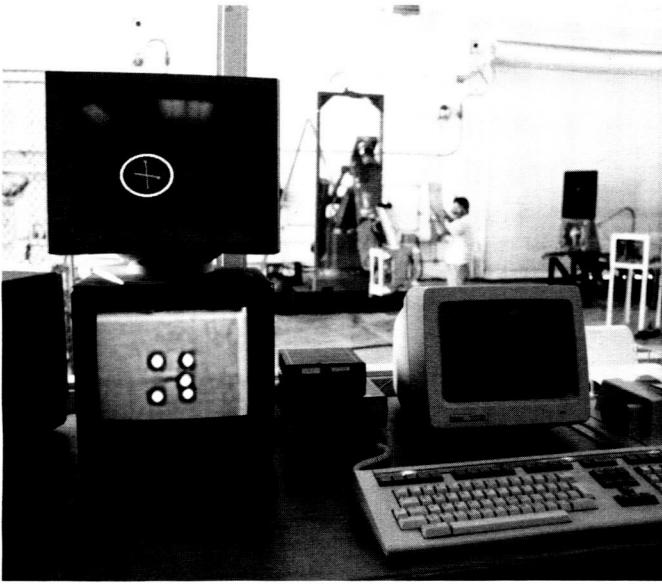
With the addition of this hardware, software was written to compute 6-DOF positional information from parameters extracted from a new

target composed of five objects (white circles). This software was incorporated in the RADL vision system computer (Motorola System 1000). In addition, control loop software was written and added to the existing laboratory supervisory computer (MicroVax II) control software in order to provide three angular coordinates of tracking to give the full 6-DOF robot tracking complement (x, y, z, pitch, roll, and yaw).

The RADL laboratory robot (an ASEA IRB-90 industrial robot) is now capable of tracking a randomly moving target composed of five white circles in real time in all six degrees of its freedom (see the figure "6-DOF Robot Target Tracking"). The laboratory robot can also be made to track in only 3-DOF with parameter changes to the control loop software (see figure "3-DOF Robot Target Tracking of RADL 3-D Simulator" in article "Robotics Applications Development Laboratory"). In addition, the vision system has been taught through software to discriminate on only the five white circles appearing in the



6-DOF Robot Target Tracking



6-DOF Target Discrimination in the RADL

camera's field of view. A series of confidence tests has been programmed into the software where "good confidence" is the ability of the vision system to perceive only the five white circles of the target during target tracking. If a particular confidence test fails, a colored circle representing the failed confidence test appears around a stylized representation of the moving target on a graphics monitor (see the figure "6-DOF Target Discrimination in the RADL"). The laboratory robot will cease target tracking after a preset time (set by a computer operator in the vision system software) if the cause of the confidence test failure does not withdraw within the preset time.

A unique aspect of the 6-DOF Robot Target Tracking Subsystem in the RADL is that any robot, not just the ASEA IRB-90 currently in use in the laboratory, can be interfaced to the subsystem and caused to track in 6-DOF.

L. Shawaga, 867-3402

DL-DSD-32

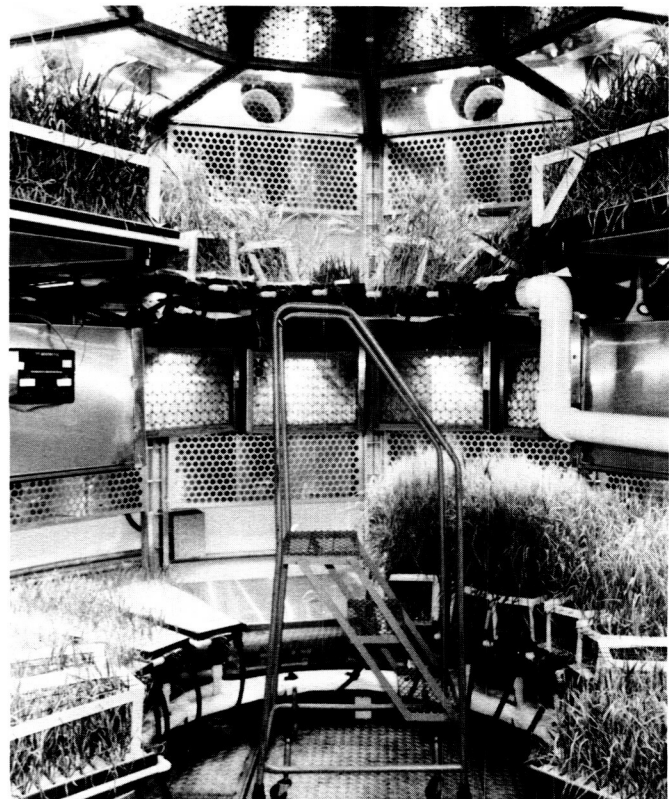
Robotic Automation in the Controlled Ecological Life Support System (CELSS)

The goal of the CELSS is to integrate elements of a biological regenerative life support system within a large (24- by 12-foot) atmospherically

sealed plant growth chamber known as the Biomass Production Chamber (BPC). The growth of food producing plants is tested by the CELSS for use in sustaining humans during long-duration space flight.

A robotic system is currently being developed to assist in the planting and care of crops within the BPC. A seed-planting end effector is being constructed that will be used to plant wheat seeds in hydroponic growing trays. The end effector uses a vacuum nozzle to pick up wheat seeds, which are then positioned over the correct location in a growing tray. Positive pressure is applied to position the seeds in the tray and to purge any growing medium from the vacuum nozzle.

The maintenance of a closed environment is of prime importance to the BPC. A robot inside the chamber which can tend to daily plant care tasks is necessary to avoid disturbing the atmosphere in the BPC. A machine vision system is being developed to give a robot the ability to move within the chamber without damage to



Biomass Production Chamber

Robotics Applications Development Laboratory (RADL)

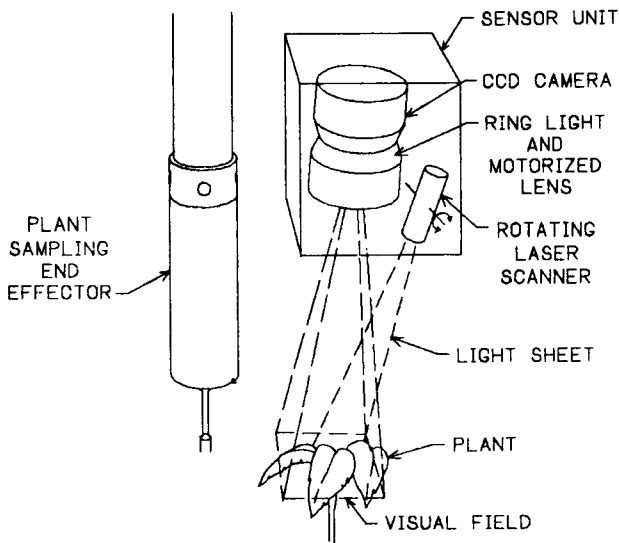
The RADL is in the high bay of the Launch Equipment Test Facility (LETF) at Kennedy Space Center. The RADL consists of an ASEA IRB90 robot mounted on a 30-foot track, various work cells, a machine vision system, and a control room. The control room contains consoles, terminals, monitors and recorders, and five computers (including a MicroVAX-II, a Motorola 1000, a controller for the robot, and an ASEA Masterpiece/Masterview; see figure "Robotics Applications Development Laboratory").

The MicroVAX-II is the heart of the RADL and monitors all test operations conducted in the laboratory. It receives data from the various sensors located on the robot, the machine vision system, and the ASEA Masterpiece/Masterview and issues commands to the robot through the robot controller. The operation itself can be observed on closed circuit television, recorders, and computer monitors.

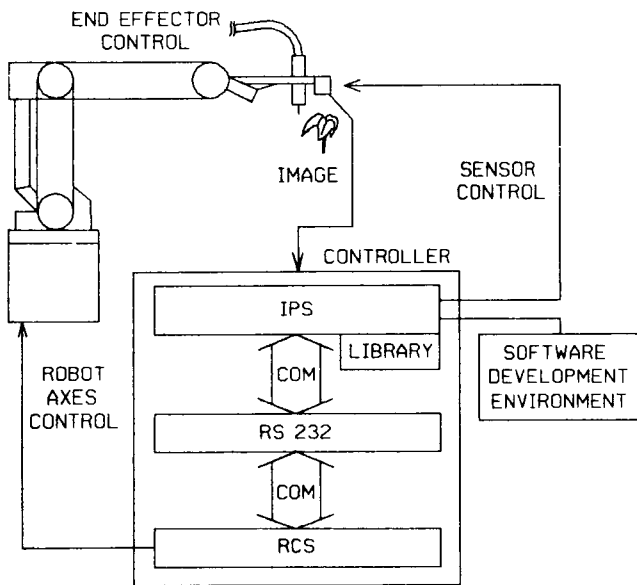
Tests utilizing the robot for hazardous servicing operations consist of opening and closing valves and activating switches on various work cells, mating a prototype umbilical plate to a simulated flight plate mounted on a random-motion mechanism, mate/demate of a quick-disconnect bayonet fluid connector, and using specialized end effectors (grippers). The purpose of these tests is to reduce hazards and to make operations more efficient.

The ASEA IRB90 robot is one of the largest industrial robots presently being manufactured. It is capable of moving a wheat seed or a 200-pound mass from one position to another with the same degree of accuracy. It can be directed manually, or automatically by a program in the controller, or by commands from the MicroVAX.

The machine vision system consists of a solid-state camera mounted on the robot, a target mounted on the random-motion simulator, special circuitry, and a Motorola 1000 computer. The system can track an object from one degree of motion up to and including six degrees of motion. The target consists of four disks mounted equal distance apart, with a fifth disk mounted off the plane and at the centroid of the other four. The vision system allows tracking of a moving target (simulating an Orbiter rocking



STRUCTURE OF SENSOR UNIT

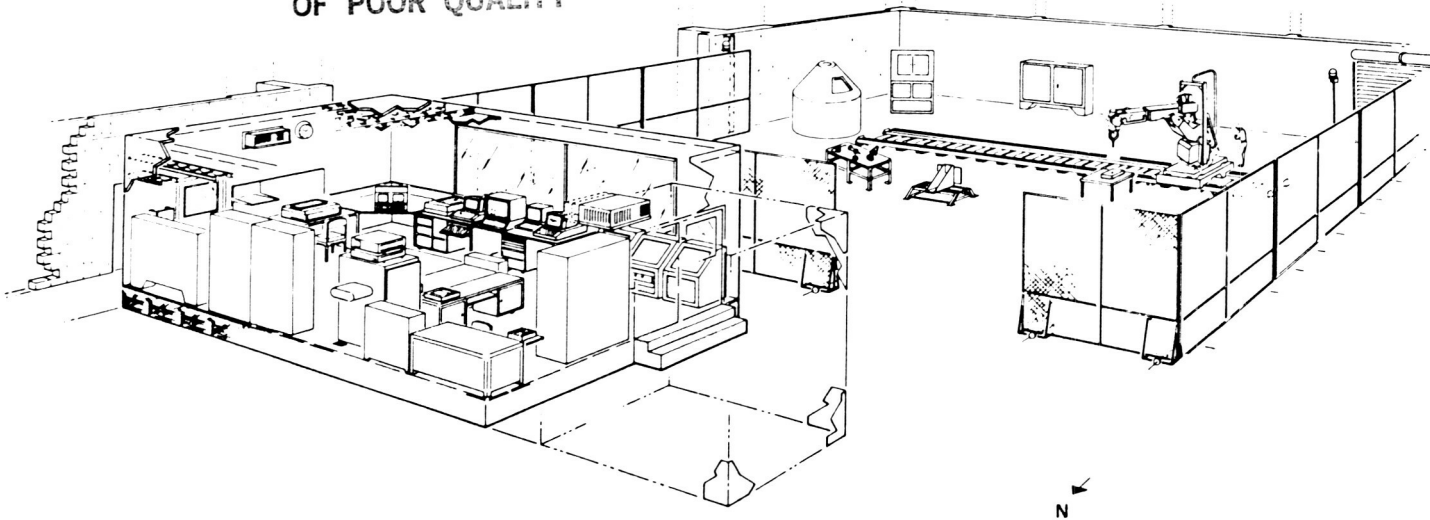


SYSTEM STRUCTURE

Plant Growth Robot Tender Vision System

the equipment or the developing plants. The vision system will also enable the robot to understand what it "sees" and identify various plants and their components. This will enable the robot to perform various cultivation tasks. While the system will initially have a man-in-the-loop setup, it is believed that with the incorporation of artificial intelligence the system may become autonomous.

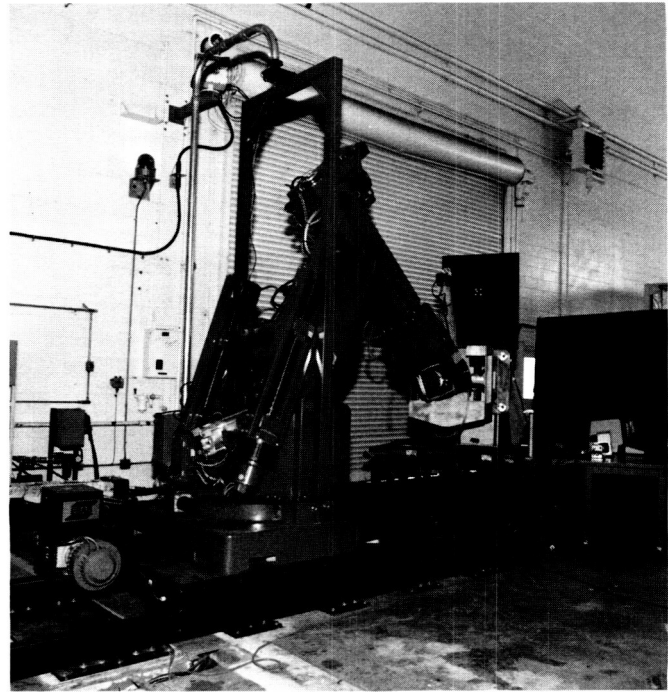
ORIGINAL PAGE IS
OF POOR QUALITY



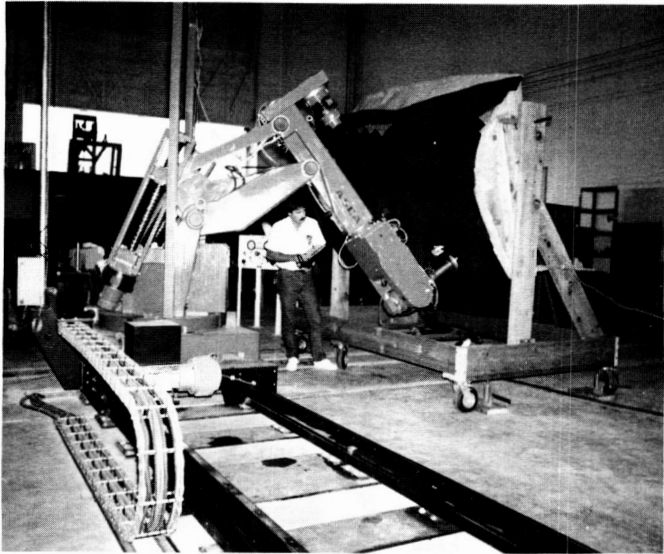
Robotics Applications Development Laboratory (RADL)

in the wind) to allow remote automatic mate/demate of fluid and power lines (see the figure "Remote Umbilical Mating With Dynamic Simulator Target"). This reduces reconnect times of 14 to 34 hours to less than 15 minutes and eliminates hazards associated with umbilicals that would otherwise have to be connected at launch. Last year this system was upgraded from a two-degree-of-freedom (2-DOF) to a 6-DOF tracking system. A state-of-the-art pipeline processor processes real-time commands at 30 hertz and sends position (X, Y, Z) and orientation (three rotations about X, Y, Z) commands to the ASEA robot (refer to the article "Six-Degree-of-Freedom Robot Target Tracking in KSC's Robotic Application Development Laboratory").

An Orbiter inspection program was also initiated this year. Simulated tiles have been fabricated and placed on a mockup (duplicating a section of the Orbiter where the wing is attached to the mainframe) in the RADL (see the figure "Robotic Orbiter Tile Inspection Mockup"). Initial tasks will be to use tools developed by Lockheed Space Operations Company to reduce labor-intensive operations and automate the



Remote Umbilical Mating With Dynamic Simulator Target



Robotic Orbiter Tile Inspection Mockup

present process to further reduce costs. Additional development will be for an intelligent sensor to combine several functions (step-gap measurements, tile contour measurements, and damage inspection of tiles and radiator sections) with CAD-CAM data bases to provide a coordinated autonomous system significantly reducing operation and maintenance costs.

These and other tasks are now in their final stages of design, including concepts of using the robot to plant seeds in hydroponic growing trays (refer to the article "Robotic Automation in the Controlled Ecological Life Support System"), measuring the "step and gap" of the heat resistant tiles mounted on the Orbiter, and further development/ refinement of the remote umbilical connect/disconnect project.

V.L. Davis, 867-4156

DM-MED-12



Thunderstorm Weather Forecasting Expert System

The Thunderstorm Weather Forecasting Expert System (TWFES) project was completed this year, resulting in a robust, real-time research prototype of a weather forecasting aid to support Shuttle operational locations at Kennedy Space Center (KSC) and Cape Canaveral Air Force Station. All the major research goals were achieved: a workable knowledge representation and a control structure were established, the knowledge acquisition was performed resulting in a dozen scenarios, the meteorological sense of the scenarios was verified, TWFES was implemented and operated in real-time, and the limits of the approach were examined. An operational implementation of the approach was considered to be too costly at this time.

The approach taken was to represent summer thunderstorm knowledge as scenarios (a variation on scripts and cases) with a control structure to process the scenarios in real-time. The research prototype has three major modes: real-time, simulation, and knowledge acquisition. The simulation mode was derived from the real-time mode by explicit control of the clock and the use of archived data. The knowledge acquisition mode utilizes a graphic and text editor "smart" about scenarios. The logical, temporal, and spatial relationships of the events in the scenario are explicit in a graph; this is an outstanding feature. It allowed domain experts (with modest training) to directly enter scenarios into TWFES without the assistance of a knowledge engineer. A knowledge engineer was, however, required to interpret event descriptions into LISP for the machine.

Shuttle operational forecasting is difficult because of KSC's coastal location on the Florida peninsula. Shuttle operational forecasting is compounded, rather than simplified, by the wealth of information available from conventional weather data sources and from a multi-

tude of specialized instrumentation systems. In the process of making a short-term forecast, it is difficult for a duty forecaster to always know which data sources are appropriate at any particular moment, much less to assimilate, interpret, and integrate the data from the sources.

Shuttle operational weather forecasting is provided by the U.S. Air Force from the Cape Canaveral Forecast Facility. The expertise developed by duty forecasters was oftentimes lost when they completed their tours-of-duty (typically from two to four years) and left. In this context, the TWFES project developed a research prototype of a real-time weather forecasting aid that captured the corporate and individual expertise developed by the forecasters. This enabled the forecasters to concentrate on data appropriate to the current events and conditions and to use their expertise to evaluate possibilities, not to select information.

A perceived limitation of the scenario approach is the need for strong interaction with a user in recognizing many of the events. This derives from the orientation of the domain and the experts in utilizing visual observations and imagery from radar and satellite displays in their descriptions of events. Recognition of these visually oriented events required the visual processing capabilities of a trained person. The visual processing problems were outside the scope of the TWFES project, but it did identify those areas in which further research would increase autonomy of the scenario approach.

A perceived benefit of the scenario approach is its ability to fuse disparate data sources (data fusion) into a common data structure about which a machine can reason in real-time. Furthermore, expert interpretation of a data source is implicit by the inclusion in a scenario of one or more events dependent upon it.

A brief history of the project begins with the selection of Arthur D. Little, Inc. (ADL), in 1985 to perform a feasibility study to apply expert

systems technology to Shuttle operational weather-related problems. ADL recommended summer thunderstorm forecasting as the best choice in terms of benefits (severe weather associated with thunderstorms affects many Shuttle operations) and in terms of appropriateness to expert systems technology. Follow-on contracts resulted in a demonstration prototype in 1986 and the first leg of a research prototype in 1987. The second leg of the research prototype was completed in-house in 1988 with civil service and contractor personnel at KSC. The demonstration prototype was developed using an expert system shell, the Automated Reasoning Tool, and ZetaLISP on a Symbolics 3640. The research prototype has been written entirely in ZetaLISP.

A.E. Beller, 867-3224

DL-DSD-22

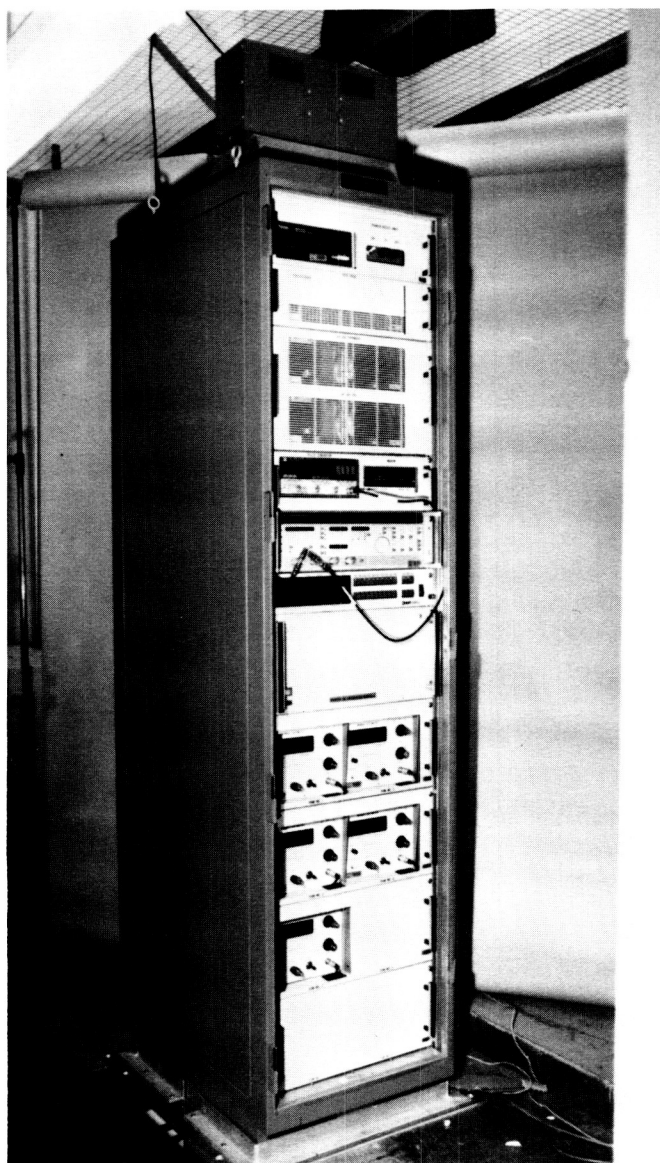
Atmospheric Science Instrumentation Laboratory (ASIL)

The ASIL provides the facilities, equipment, and technical personnel required to develop and demonstrate prototypes of atmospheric science instrumentation at Kennedy Space Center. Laboratory capabilities include microprocessor development, high-voltage testing, data acquisition and processing, sensor testing and evaluation, circuit design and fabrication, and applications software development.

During the past year, projects that have made use of the ASIL facilities include the Lightning and Transients Monitoring System (LATMOS), an instrumentation system developed for Vandenberg Air Force Base (VAFB), the Launch Pad Lightning Warning System (LPLWS) or field mill system upgrade, and the Clear Air Doppler Radar (CADR). The ASIL also provides instrumentation support for visiting scientists working at the Atmospheric Science Field Laboratory.

R.P. Wesenberg, 867-4438

DL-ESS-31



The LATMOS Data Acquisition Rack for VAFB

Clear-Air Wind-Sensing Doppler Radar

A reliable, 90-minute thunderstorm forecasting capability is essential if the Space Shuttle is to land at Kennedy Space Center (KSC). Advanced warning of thunderstorms is also necessary so weather-sensitive Shuttle components are not damaged when they are being moved out into the open. Discussions at KSC meteorology workshops with many weather research people suggest that clear-air wind sensing using a doppler radar may provide such a capability. This project has been planned to move the

Clear-Air Doppler Radar (CADR) from the forefront of research to an operational system at KSC as quickly as possible to meet KSC's requirements.

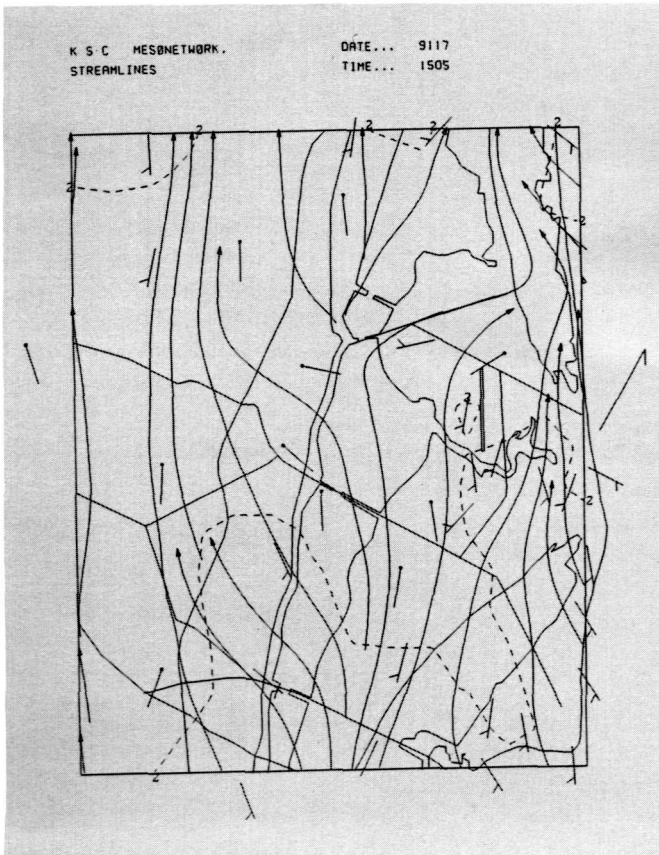
The first step of the plan was to develop a CADR modification to a KSC C-band tracking radar so that it could sense clear-air wind velocities. So that qualified investigators can work with the data, software was then developed for formatting the data in the Universal Doppler Radar Data Format, and developed to de-alias, display, infer meteorological parameters, and transform the data to the meteorological coordinate system. This set of software constitutes the CADR analysis work station. The work station software is a specialized research environment, in Ada language, that provides utilities and tools for the research software developer. Software developed on the work station can be easily written to meet minimum software quality standards. Analysis software that meets these stan-

dards can be quickly ported to a prototype real-time CADR system at KSC for test and evaluation.

The CADR modification to a KSC C-band tracking radar was accomplished in 1987. During the summer, KSC and the Air Force Geophysical Laboratory (AFGL) jointly tested the clear-air wind-sensing radar at KSC. The radar was operated simultaneously with the KSC data acquisition system and the AFGL data acquisition system. About 100 hours of data were collected. The two systems were compared to make sure the CADR and KSC data acquisition system performed correctly. Calibration procedures were also developed.

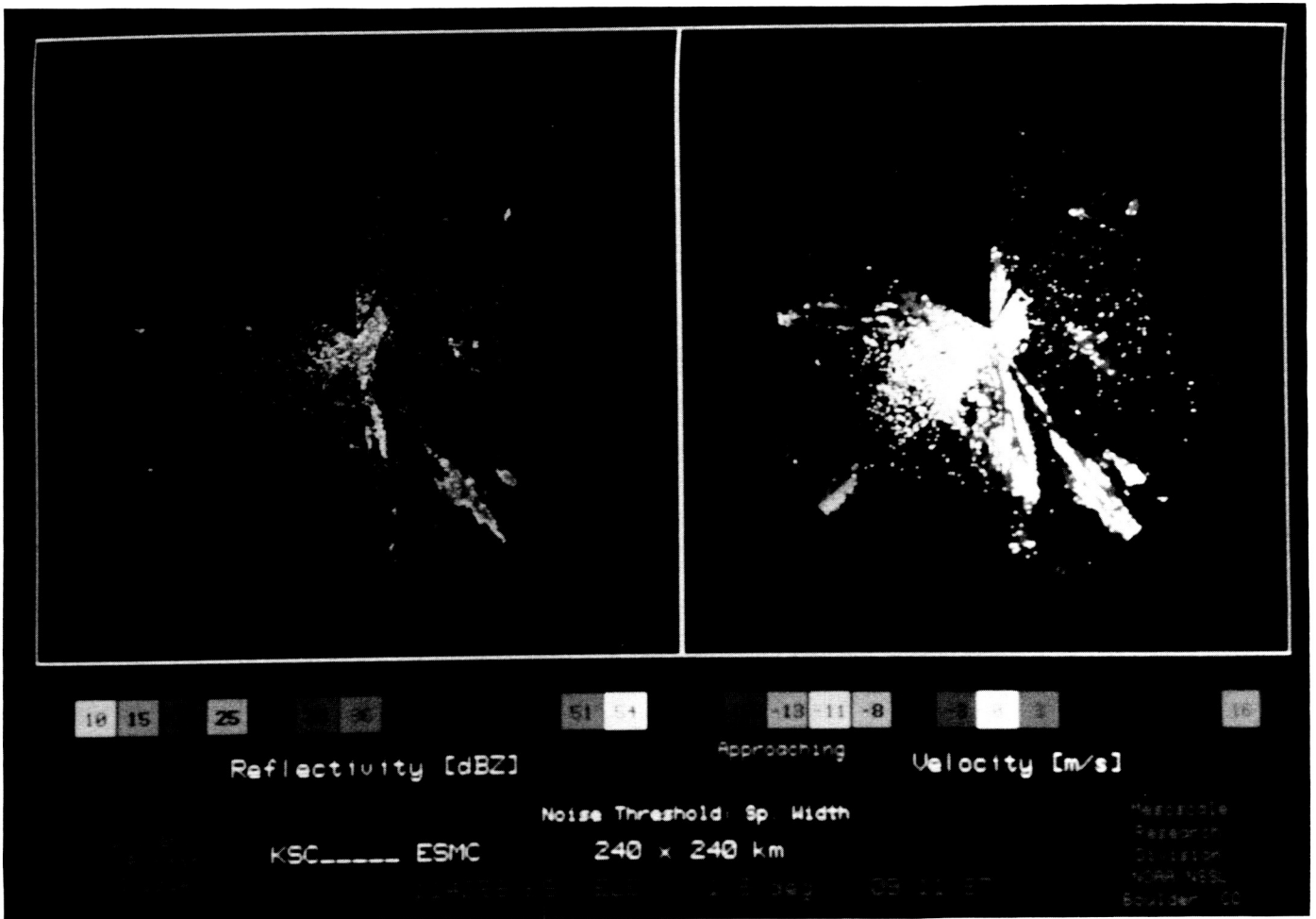
The second step of the plan was to develop software to process the nine-track data tapes from the KSC data acquisition system to the Universal Doppler Radar Data Format. This format was chosen because it is accepted as a standard throughout the research community. The first working version of this formatter was on-line in March 1988. One day's data, September 19, 1987, was converted to Universal Format and edited. The formatter was written entirely in Ada language.

The third step was to develop a CADR analysis work station. This effort was performed in parallel with the development of the C-band tracking radar modifications and the Universal formatter. The concept was to develop an integrated CADR work station software package that allows technique development on small, inexpensive microcomputers of the 80386 or 680X0 class. Ada language was employed throughout, and software standards were used to provide portability. Object-Oriented Design (OOD) was used to stress the scientific correctness of the software implementation of the analysis techniques. The resulting system provides data displays, data conversion, de-aliasing, and three basic, single-doppler, clean-air, wind-sensing analysis techniques [Volume Velocity Processing (VVP); Box Velocity Processing (BVP); and Convergence Line Velocity Processing (CLVP), a new technique developed at KSC]. These techniques must be modified to work with the sparse CADR data. With this accomplished, these three analysis techniques will optimally estimate the values of basic meteorological parameters from the raw radar data, so sophisticated modeling and pattern recognition techniques developed elsewhere can be applied to the data.



Mesonet Winds

ORIGINAL PAGE IS
OF POOR QUALITY



Reflectivity and Velocity PPI's

To complete this development, the work station software must be integrated under UNIX, documented, and released for use by scientific investigators. The CADR radar data acquisition system needs to be upgraded to support the real-time test and evaluation of the forecast analysis techniques developed by the scientists. The CADR system will then be ready to support the test and evaluation of analysis techniques developed by the research community.

R.P. Wesenberg, 867-4438

DL-ESS-31



Compaq 386 Workstation

***** VVP ANALYSIS *****

Z	COUNT	U	V	DIV	SPEED	DIREC	W
100.0	24331	-3.5	13.1	-0.00005	13.5	165.1	0.00
300.0	26903	-5.2	17.8	-0.00019	18.5	163.6	0.03
500.0	19101	-6.3	21.1	-0.00023	22.0	163.2	0.07
700.0	15824	-5.6	23.7	-0.00042	24.3	166.8	0.14
900.0	12751	-2.3	24.2	-0.00040	24.3	174.6	0.22
1100.0	9731	1.6	23.0	-0.00020	23.1	184.0	0.29
1300.0	8415	4.3	21.7	-0.00006	22.1	191.3	0.32
1500.0	6176	6.2	20.0	-0.00000	20.9	197.3	0.34
1700.0	5697	6.3	18.9	0.00018	19.9	198.4	0.33
1900.0	5476	7.5	18.3	0.00018	19.8	202.2	0.30
2100.0	5634	9.0	17.7	0.00011	19.8	206.9	0.28
2300.0	5320	10.1	17.4	0.00005	20.1	210.2	0.27
2500.0	5396	10.7	16.9	0.00004	20.0	212.2	0.27
2700.0	5713	10.2	17.1	0.00004	19.9	210.9	0.27
2900.0	4181	9.8	17.3	0.00000	19.9	209.5	0.27
3100.0	3804	8.9	17.9	-0.00002	20.0	206.5	0.28
3300.0	3772	8.7	18.9	-0.00003	20.9	204.8	0.29
3500.0	3231	8.5	19.6	-0.00001	21.4	203.6	0.30
3700.0	2326	7.8	20.4	0.00010	21.9	200.9	0.25
3900.0	2189	8.0	20.4	0.00017	21.9	201.6	0.27

***** BVP ANALYSIS *****

Z	V [m/s]						
	X	250.0	750.0	1250.0	1750.0	2250.0	2750.0
-19000.0	*****	14.2655	21.3965	*****	20.8020	18.7071	
-17000.0	*****	6.4990	18.2566	23.4290	19.8129	18.9341	
-15000.0	-0.3466	4.2997	24.1244	26.6347	23.4842	18.7697	
-13000.0	7.3670	17.4795	26.5019	27.0883	24.8878	21.6470	
-11000.0	17.0259	23.1520	24.6690	22.2770	22.4013	21.8392	
-9000.0	19.5204	22.7070	22.3435	20.5098	21.0224	21.7057	
-7000.0	18.9081	23.5855	22.0953	19.9898	21.0598	21.1853	
-5000.0	17.3735	23.4716	22.8453	19.4530	20.0186	19.2991	

***** BVP ANALYSIS *****

Z	WIND SPEED [m/s]						
	X	250.0	750.0	1250.0	1750.0	2250.0	2750.0
-19000.0	*****	14.3084	21.4487	*****	20.8299	18.8182	
-17000.0	*****	6.5368	18.6852	23.8858	19.8980	18.9555	
-15000.0	0.5424	5.5072	24.1720	26.9325	23.5011	19.0757	
-13000.0	9.3253	18.7100	26.5386	27.1999	25.3899	22.5080	
-11000.0	19.3342	24.4371	24.7061	23.4079	23.6233	22.9634	
-9000.0	22.4819	23.7247	22.4365	21.4677	22.4009	23.6252	
-7000.0	21.7892	24.8190	22.2536	20.8620	23.1295	24.9223	
-5000.0	19.8730	24.8564	22.9431	20.6735	23.5556	24.5740	

***** BVP ANALYSIS *****

Z	WIND DIRECTION [m/s]						
	X	250.0	750.0	1250.0	1750.0	2250.0	2750.0
-19000.0	*****	175.5630	176.0022	*****	182.9648	186.2304	
-17000.0	*****	173.8339	167.7043	168.7775	174.7017	182.7195	
-15000.0	50.2735	141.3284	176.4036	171.4722	182.1711	190.2757	
-13000.0	142.1850	159.1047	176.9881	185.1934	191.4140	195.8996	
-11000.0	151.7161	161.3359	183.1418	197.8030	198.5096	198.0025	
-9000.0	150.2583	163.1570	185.2190	197.1810	200.2055	203.2557	
-7000.0	150.2007	161.8604	186.8385	196.6262	204.4230	211.7823	
-5000.0	150.9532	160.7844	185.2912	199.7859	211.8055	218.2474	

***** CLVVP ANALYSIS *****

HORIZONTAL DIVERGENCE

Z	Y					
	X	40000.0	20000.0	0.0	-20000.0	-40000.0
50000.0	*****	*****	0.00042	*****	*****	
45000.0	*****	0.00091	0.00021	0.00051	*****	
40000.0	*****	0.00078	0.00021	0.00022	*****	
35000.0	-0.00176	0.00016	-0.00014	0.00009	0.00111	
30000.0	0.00106	0.00005	-0.00014	-0.00001	-0.00245	
25000.0	-0.00091	-0.00011	-0.00037	-0.00065	0.00041	
20000.0	0.00021	0.00012	-0.00008	-0.00020	-0.00066	
15000.0	0.00016	0.00005	0.00001	0.00052	0.00105	
10000.0	-0.00064	0.00042	0.00004	0.00053	*****	
5000.0	0.00101	0.00008	-0.00011	-0.00014	*****	
0.0	-0.00015	-0.00011	-0.00047	0.00002	*****	
-5000.0	-0.00161	0.00071	0.00050	0.00022	-0.00055	
-10000.0	0.00057	-0.00078	-0.00063	-0.00013	-0.00121	
-15000.0	0.00237	-0.00240	-0.00152	-0.00084	*****	
-20000.0	-0.00308	0.00058	0.00042	*****	*****	
-25000.0	-0.00171	0.00016	-0.00015	0.00003	0.00106	
-30000.0	-0.00325	0.00002	-0.00108	-0.00087	-0.00039	
-35000.0	0.00081	0.00000	-0.00050	-0.00066	0.00033	
-40000.0	0.00031	-0.00028	-0.00017	-0.00016	*****	
-45000.0	*****	-0.00029	0.00002	0.00030	*****	
-50000.0	*****	*****	0.00005	*****	*****	

Kinematic Analysis Sample Outputs (cont)

Lightning Tower Measurements System

A lightning characteristics climatology is needed to specify lightning protection design requirements at Kennedy Space Center (KSC). The concept is to develop and instrument a tower to measure the current waveforms, the near-field electromagnetic field, and the far-field electromagnetic field. This data can be used to characterize lightning strike effects upon ground facilities, power, communications, and electronic equipment. The data will be collected over an extended period of time (a decade) and will be used to improve and validate KSC lightning protection design specifications.

The design is complete, the equipment is procured, and the software is being developed. This software will be written in Ada language, and includes an Ada binding to an IEEE-488 interface on a 80386-based computer under an MS Disk Operating System (MSDOS). The system will be tested at the Atmospheric Science Field Laboratory (ASFL) next summer, with installation to follow in the winter of 1989.

***** BVP ANALYSIS *****

Z	DEFORMATION [1/s]						
	X	250.0	750.0	1250.0	1750.0	2250.0	2750.0
-19000.0	*****	0.0022	-0.0009	*****	0.0004	0.0009	
-17000.0	*****	-0.0011	-0.0020	-0.0014	0.0002	-0.0000	
-15000.0	-0.0040	-0.0024	0.0008	0.0025	0.0023	0.0008	
-13000.0	0.0025	0.0023	0.0020	0.0013	-0.0004	0.0010	
-11000.0	0.0019	0.0009	-0.0018	-0.0014	-0.0015	-0.0004	
-9000.0	0.0012	-0.0003	-0.0004	-0.0002	-0.0004	0.0004	
-7000.0	-0.0010	0.0002	0.0003	-0.0004	-0.0003	-0.0006	
-5000.0	0.0000	-0.0003	0.0001	0.0003	-0.0005	-0.0009	

***** BVP ANALYSIS *****

Z	DIVERGENCE [1/s]						
	X	250.0	750.0	1250.0	1750.0	2250.0	2750.0
-19000.0	*****	0.0025	-0.0007	*****	0.0000	-0.0007	
-17000.0	*****	-0.0002	-0.0026	-0.0011	-0.0001	0.0006	
-15000.0	-0.0016	-0.0010	0.0010	0.0009	0.0008	0.0006	
-13000.0	-0.0029	-0.0022	0.0016	0.0045	0.0024	0.0011	
-11000.0	-0.0011	-0.0003	0.0000	0.0005	-0.0001	0.0003	
-9000.0	-0.0010	-0.0004	0.0005	0.0004	0.0001	0.0020	
-7000.0	0.0006	-0.0007	0.0003	-0.0000	0.0008	0.0021	
-5000.0	0.0001	-0.0004	0.0001	0.0020	0.0015	0.0014	

***** BVP ANALYSIS *****

Z	W [m/s]						
	X	250.0	750.0	1250.0	1750.0	2250.0	2750.0
-19000.0	*****	-0.9279	-1.4630	*****	-1.2601	-1.1824	
-17000.0	*****	0.0586	0.7658	1.7991	2.2352	2.2616	
-15000.0	0.1967	0.8660	0.9317	0.5038	0.0820	-0.2815	
-13000.0	0.3656	1.7166	2.0021	0.5632	-1.2103	-2.2077	
-11000.0	0.1408	0.5284	0.6380	0.5462	0.4687	0.4429	
-9000.0	0.1281	0.4963	0.4910	0.2783	0.1542	-0.3725	
-7000.0	-0.0756	-0.0731	0.0310	-0.0315	-0.2312	-0.9797	
-5000.0	-0.0170	0.0464	0.1286	-0.3933	-1.3135	-2.1363	

***** BVP ANALYSIS *****

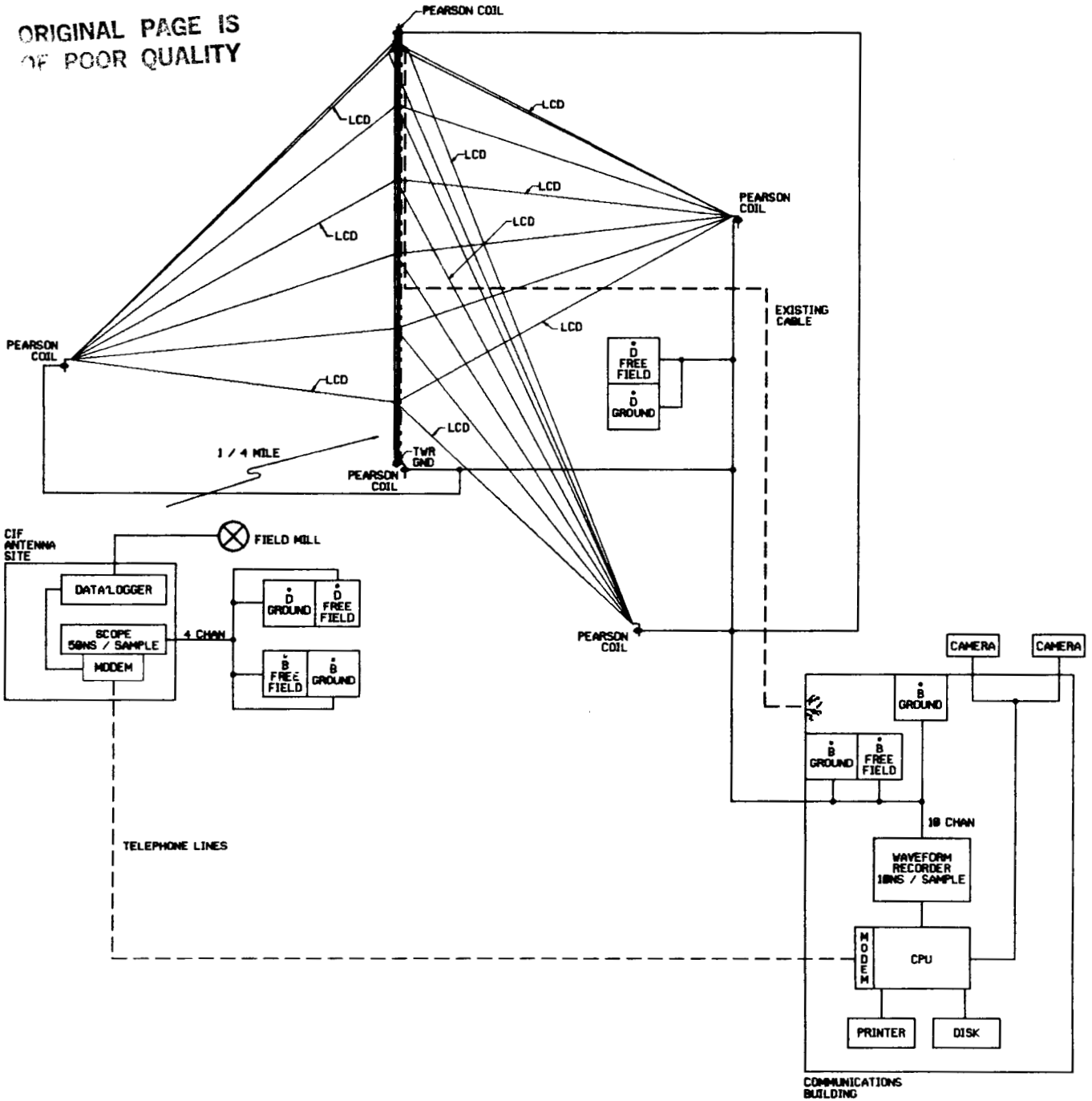
Z	U [m/s]						
	X	250.0	750.0	1250.0	1750.0	2250.0	2750.0
-19000.0	*****	-1.1069	-1.4953	*****	1.0774	2.0423	
-17000.0	*****	-0.7021	-3.9792	-4.6486	-1.8374	0.8994	
-15000.0	-0.4171	-3.4412	-1.5162	-3.9938	0.8903	3.4028	
-13000.0	-5.7175	-6.6731	-1.3944	2.4621	5.0246	6.1661	
-11000.0	-9.1613	-7.8203	1.3541	7.1880	7.4995	7.0970	
-9000.0	-11.1531	-6.8742	2.0409	6.3414	7.7370	9.3281	
-7000.0	-10.8285	-7.7270	2.6498	5.9692	9.5633	13.1264	
-5000.0	-9.6488	-8.1808	2.1158	6.9981	12.4147	15.2127	

Kinematic Analysis Sample Outputs

R.P. Wesenberg, 867-4438

DL-ESS-31

ORIGINAL PAGE IS
OF POOR QUALITY



Lightning Tower Measurements System

Lightning Hazard Detection and Warning

Lightning can make the handling of propellant and ordnance materials at Kennedy Space Center (KSC) a hazardous occupation. A system that detects the potential for lightning is in operation at KSC; however, the system cannot predict whether the lightning hazard is increasing

or decreasing during thunderstorms. To do that, the state of the thunderstorm generator itself must be determined.

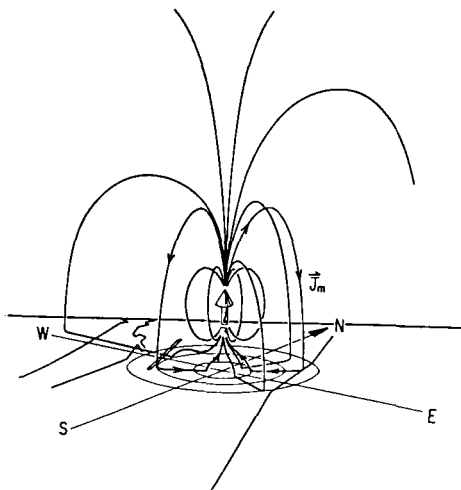
The Institute of Atmospheric Physics at the University of Arizona has been conducting research into this problem for KSC for about five years. They have discovered that an electric current sensor network may be able to track the

state of a thunderstorm generator which produces electricity that results in lightning. In the figure below, the large arrow in the center represents the thunderstorm generator, while the contours represent the current density streamlines. Since charge is conserved, the streamlines make closed loops. This suggests that the state of a thunderstorm generator might be determined at the ground from a ground-based array of current sensors. Field experiments have been conducted to determine how this can best be done. To evaluate this research and chart a course for future investigations, an independent review by a panel of experts in atmospheric electricity was held this year.

The independent review committee included scientists from government and academic institutions. A three-day extensive research review was held at the University of Arizona, and a list of recommendations was developed. The committee did not recommend further development of the so-called Maxwell current sensor, because it is unsuitable for operational application. The committee did recommend application of the field-mill-based thunderstorm current-sensing algorithm on KSC's field mill system, the development of a slow-antenna-like displacement current sensor, and further research into thunderstorm electricity using thunderstorm current sensors. It is unclear whether thunderstorm current sensing will ultimately improve operational support to the Shuttle, but it does show promise and has significant research applications.

R.P. Wesenberg, 867-4438

DL-ESS-31



Theoretical Description of Typical Thunderstorm Generator's Structure in Terms of Current Density (J_m)

Rocket-Triggered Lightning

Background: The Kennedy Space Center (KSC) is located in an area of the highest frequency of thunderstorms and lightning activity in the United States. This unique characteristic allows KSC and industry to perform extensive studies of lightning and thunderstorm phenomena. The rocket-triggered lightning launch site, located in a remote area approximately 10 miles north of the Vehicle Assembly Building, is used to launch rockets and to monitor the effects of rocket-triggered lightning. The launcher consists of two banks of six 10-inch diameter tubes mounted on a 13-foot wooden platform and surrounded by a large copper wire Faraday cage grid system. The 3-inch-diameter by 3-foot-long plastic rockets are designed to carry a spool of conducting wire into the atmosphere when launched into a thunderstorm having adequately high electric fields. The rockets, with the conducting wires, simulate a rapidly rising corona distortion in the electric field and upward streamer. A breakdown in the potential between cloud and ground is initiated, which vaporizes the grounded conducting wire and establishes a lightning channel.

Approach: The 1988 lightning experiments included launching rockets from a lightning strike object attached to one of the tethers of a helium-filled balloon, 25 inches in diameter by 85 feet in length. Also attached to a tether was an airborne field mill sensor. The data from this sensor was compared with data from ground-based field mills and aircraft flyover tests. The balloon was flown at 1,500 feet. In addition, rockets were launched from a land-based launcher and a water-based launcher.

Results: Rockets were successfully launched from the balloon; however, weather and opportunity precluded triggering lightning. One particular lightning flash was triggered on October 3, 1988, at the land base. The initial strike was followed by 12 restrikes. This is the most restrikes from a single flash recorded during the program. The waveform recordings are shown below. The initial strike, which could be classed as artificial, showed a slow rate of rise ($\sim 14 \text{ kA}/\mu\text{s}$) and was a bit unstable while establishing the channel. The restrikes on the other hand, occurred at much higher rates of rise (as high as $-57.3 \text{ kA}/\mu\text{s}$). Table 1 is a summary of both the 1988 and the 1987 triggered-lightning programs.

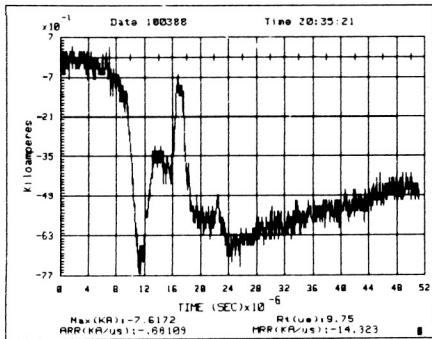
W. Jafferis, 867-4438

DL-ESS-31

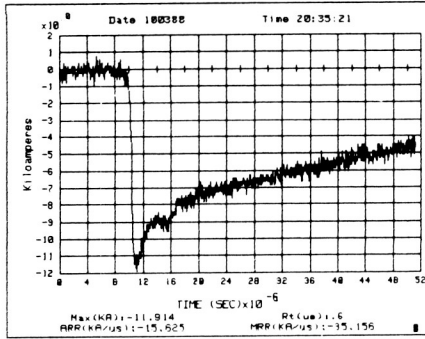
Waveform Characteristics

Date : 100388 Time : 20:35:21
Flash number : 8

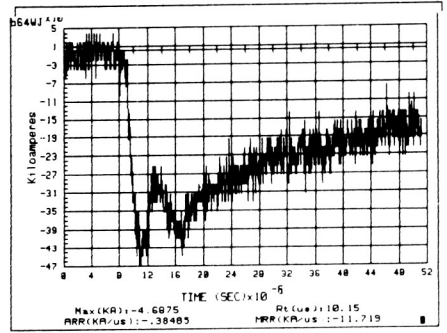
Initial strike Record # 212



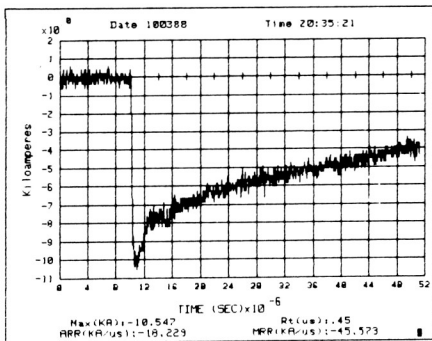
Re-strike # 1 Record # 213



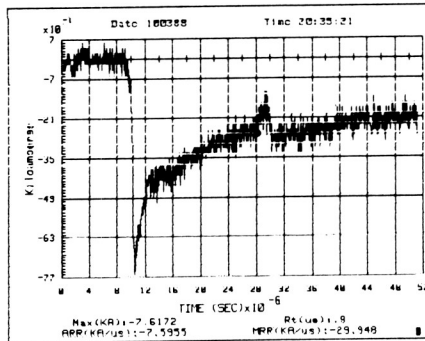
Re-strike # 2 Record # 214



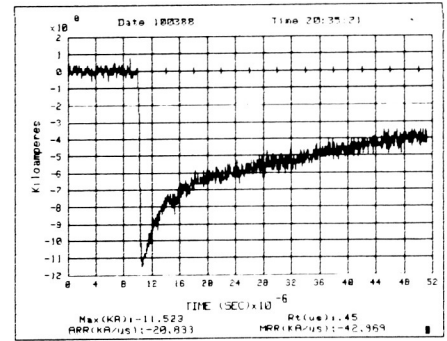
Re-strike # 3 Record # 215



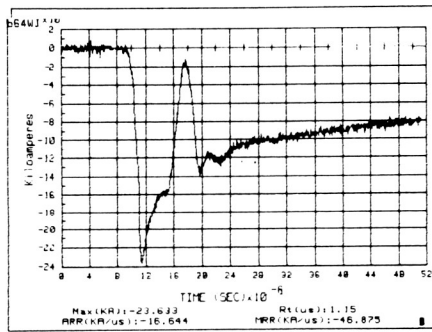
Re-strike # 4 Record # 216



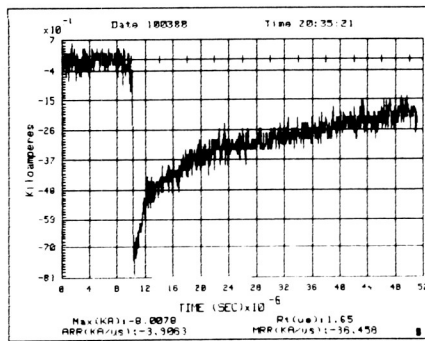
Re-strike # 5 Record # 217



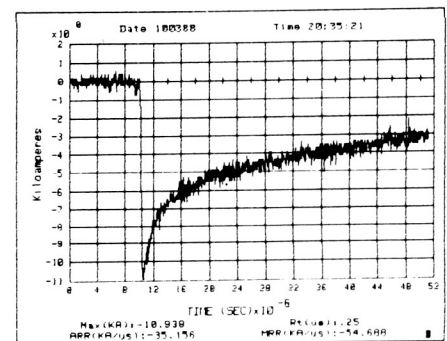
Re-strike # 6 Record # 218



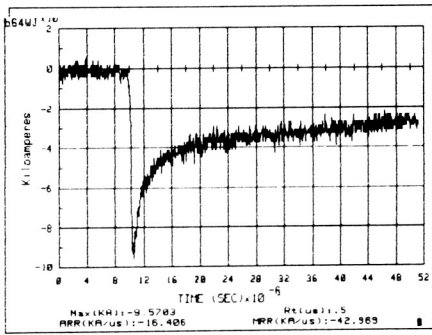
Re-strike # 7 Record # 219



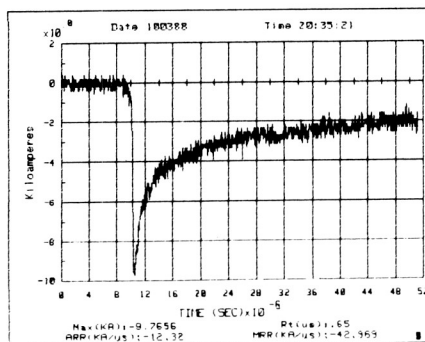
Re-strike # 8 Record # 220



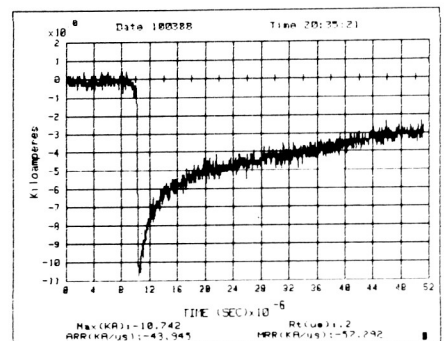
Re-strike # 9 Record # 221



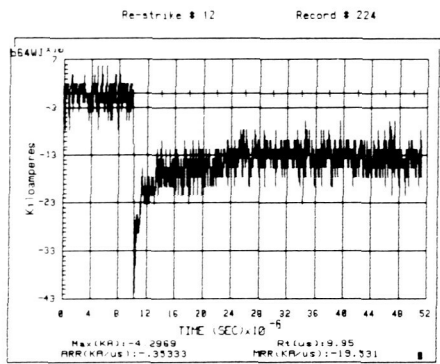
Re-strike # 10 Record # 222



Re-strike # 11 Record # 223



Lightning Current Waveforms



Instrument Settings

Range (volts) -----> 1.00E00
 Offset (volts) -----> 000.E-03
 Trigger position -----> -20%
 Hysteresis (volts) -----> 40.00E-03
 Timebase mode -----> MAIN
 Main timebase -----> 050.00E-09
 Delay timebase -----> 050.00E-09
 Record length -----> 1024
 Conversion Factor (kA/V) ----> 100

Lightning Current Waveforms (cont)

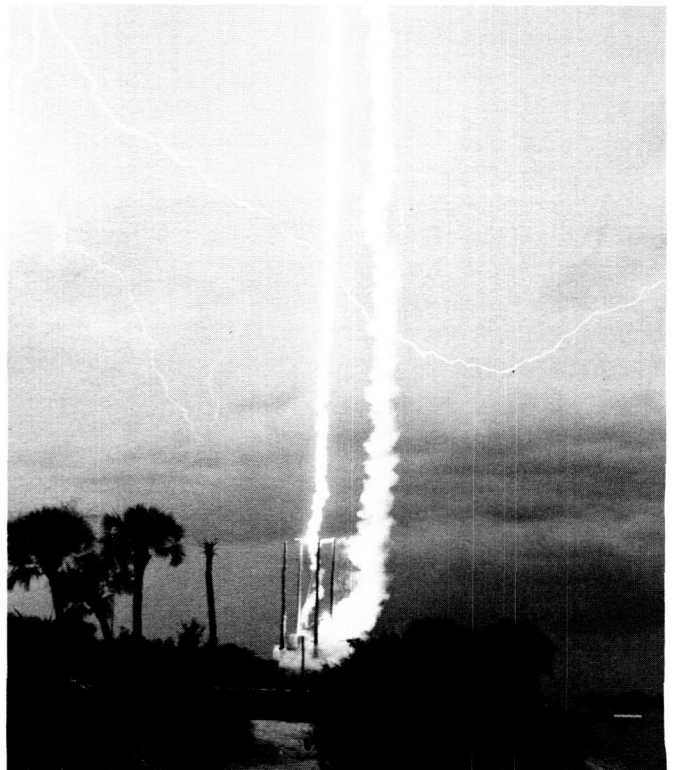
Table 1. Triggered-Lightning Summary

Year	Total Strikes	Maximum I (kA)	Minimum I (kA)	Rise Rate (Max. kA/μs)	Rise Rate (Min. kA/μs)	Rise Time (Min. μs)	Rise Time (Max. μs)
1988*	27	-33.9	-4.3	-132.0	-11.7	0.1	10.2
1987*	24	-32.0	-4.5	-134.1	- 7.8	0.2	26.4
1987**	13	-38.5	-9.8	-411.0	-36.0		

Lightning-Induced Effects

Background: Rapidly changing magnetic fields from lightning currents may induce voltages in computer and equipment circuits that can cause damage or upsets in the case of computers. Voltages can also be induced in ordnance and ignition circuits associated with propellant systems. When lightning strikes a building housing sensitive operations, the path through the building conductors (electric wiring, conducting water pipes, air conditioning ducts, steel reinforcing rods in concrete, and others) may be unknown. Even with a lightning protection system on the building, the current may flow through the building as well as the protection system since they are usually not well isolated.

The Spacecraft Assembly Building at ESA-60A is a building where important computer and spacecraft operations are scheduled to be conducted and where it is desirable to continue operations during thunderstorm warning periods. To prevent lightning current flow through the building, it was proposed to provide an external network of lightning conductors, well isolated

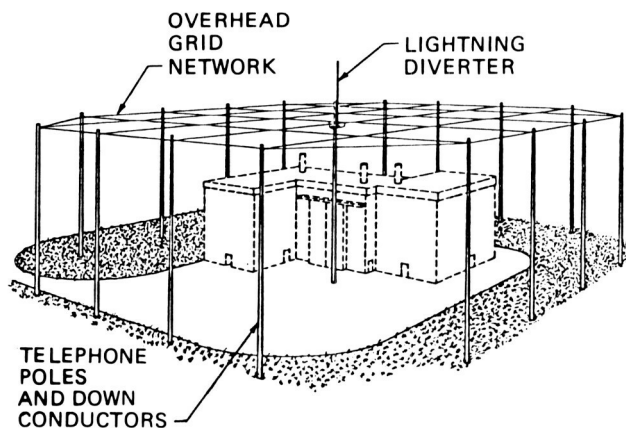


Rocket-Triggered Lightning

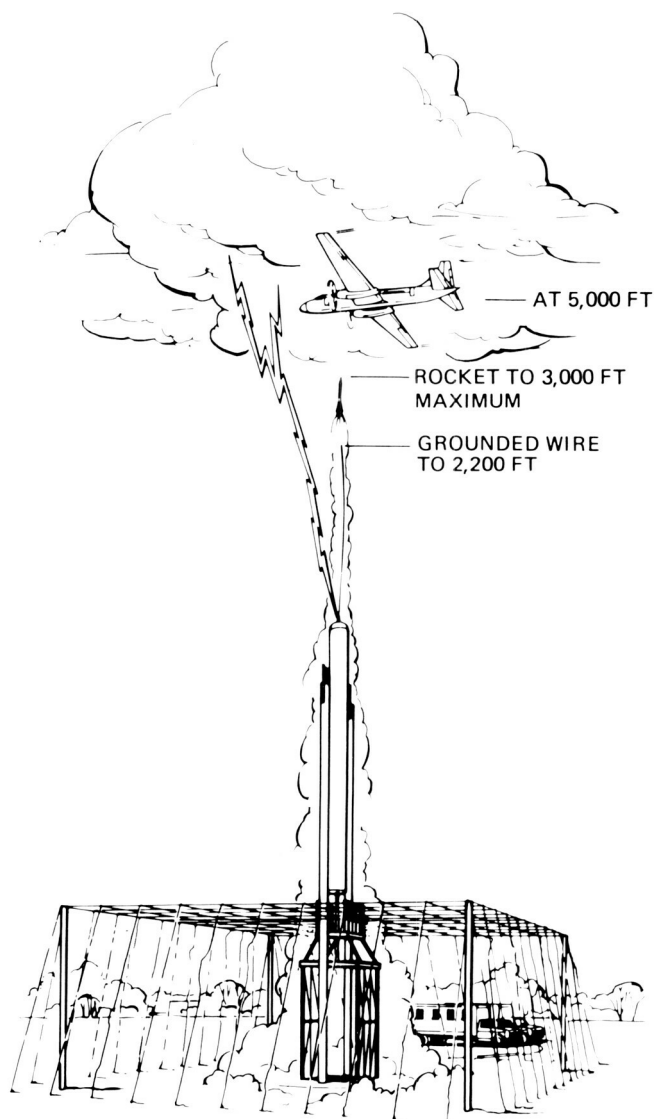
from the building (see the figure of the overhead grid wire system). A diverter was placed at the center top of the network to equalize the currents to ground in the down conductors, located on 100-foot telephone poles. The top of the network was about 30 feet above the roof of the building. The use of the 16 poles reduced the current in each down conductor to one-sixteenth of the total current. Since the magnetic field vectors inside the network, due to the network, generally are oriented so they cancel near the center of the network, the magnetic fields are minimized both by current reduction and magnetic field cancellation. The magnetic fields due to the lightning channel above the network are reduced by the height of the network, which is also high enough to prevent flash-over to the building. For experimental purposes, a one-fifth scale model of the ESA-60A network was constructed at the rocket-triggered lightning (RTL) Site. A lightning flash triggered to the RTL site is shown in one of the figures.

Objective: The objective of this program was to trigger lightning to a Faraday Cage network similar to that proposed for ESA-60A and to measure the effectiveness of this technique for protection against lightning-induced effects. As a start, it was decided to construct a one-fifth scale model of the ESA-60A protection network. The rate of change of the magnetic and electric fields was measured inside the network near its center and also, for reference, outside the network.

Results: The sensor measuring the rate of change of the magnetic field ($B \cdot \dot{\text{sensor}}$) inside the network was located about one meter from the center of the network and about one meter above its floor. A similar sensor was located outside the network at an arbitrary distance of 25 meters from the center of the network. The boundary of the network was approximately 8 meters from its center. Measurements showed that the fields outside the network exceeded those inside by factors of 2.5 to 10. The magnitude of the field rates of change were roughly proportional to the rate of rise of the lightning current, which varied from 30 to 100 kiloamperes per microsecond. The shape of the lightning channel above the network also contributes to the field magnitude. The field changes inside the network varied from 60 to 400 Teslas per second. A Tesla per second is equivalent to one volt per square meter of induction. The fields measured outside the network ranged from 300 to 1,000 Teslas per second. Assuming a linear



Overhead Grid Wire System at the ESA-60A Spacecraft Assembly Building



One-Fifth Scale Model of ESA-60A Protection System at RTL

BLACK AND WHITE PHOTOGRAPH

field relationship with distance, which is valid near the lightning strike, the field at the center of the network is the same as fields 25 meters x (2.5 to 10) or 62.5 to 250 meters from the stroke. As an illustrative example of the shielding effectiveness of the network, assume that a computer is located in the corner of a building one meter from a lightning down conductor. If lightning hits that corner of the building, at least 50 percent of the total current could flow in that down conductor. The induced voltages in the computer circuits without the network would then be 31 to 125 times greater than they would be with the network in place. Further, since the lightning is full scale, the measurements inside

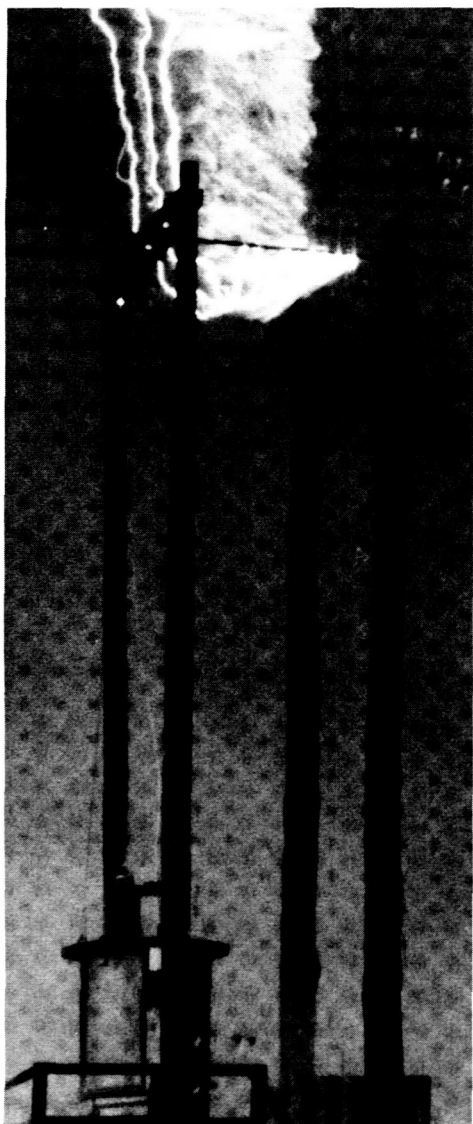
the one-fifth scale model are five times closer to the lightning as compared to a full-scale network. The external measurements would not be affected. The fields inside a full-scale network would then be expected to be reduced by another factor of about five, which could result in greater field reduction factors maximizing at about 150 to 600.

Electric field displacement (D dot) currents were also measured inside and outside the network. These measurements were proportional to the rate of change of the electric field. It was expected that the network would not be an effective shield against electric field changes. At current rates of rise of about 50 kiloamperes per microsecond, the displacement currents, measured inside the network, varied from 1.25 to 3 amperes per square meter while those outside, 25 meters from the center of the network, ranged from 0.69 to 1 ampere per square meter. At higher rates of rise of lightning current of about 100 kiloamperes per microsecond, the shielding effectiveness increased and displacement currents inside and outside the network were about the same at 2 amperes per square meter. Electric field shielding was not the main purpose of the network since it is normally easier to provide electric field shielding for equipment with the usual metal cabinets and other shielding than it is to provide good lightning magnetic field change protection.

In future experiments, the configuration of wires could be changed to optimize the field reduction factors. For example, a cylindrical grid of wires would provide more effective field cancellation at the center. The number of wires could be varied to determine the effect, a closer mesh could be used on top, and the affect of the presence or absence of a ground mesh counterpoise could be studied.

W. Jafferis, 867-4438

DL-ESS-31



Lightning Flash at RTL Sight With Multiple Strikes

Electric Field Measurements Aloft

Background: As a thunderstorm approaches, the electric field gradient on the ground, which is initially positive due to a negative charge on the earth, reverses polarity and begins to climb in a negative direction due to the generally negative charge located in the lower portion of the

thunderstorm cloud. When the field gradient is sufficiently negative, space charge is produced near the ground due to the high field gradient which results in corona current from vegetation and structures. A positive charge accumulates above the ground. Some of the thunderstorm field then terminates on this charge and only part of the field reaches the earth and the field measuring equipment located on the ground.

Objective: The objective of measuring electric field gradients aloft and comparing the measurements with similar measurements on the ground is to determine the magnitude and variations of space charge effects on ground-based field mills in relation to various phases of the thunderstorm. The work was sponsored by the New Mexico Institute of Mines and Technology (Bill Winn) and the University of Mississippi

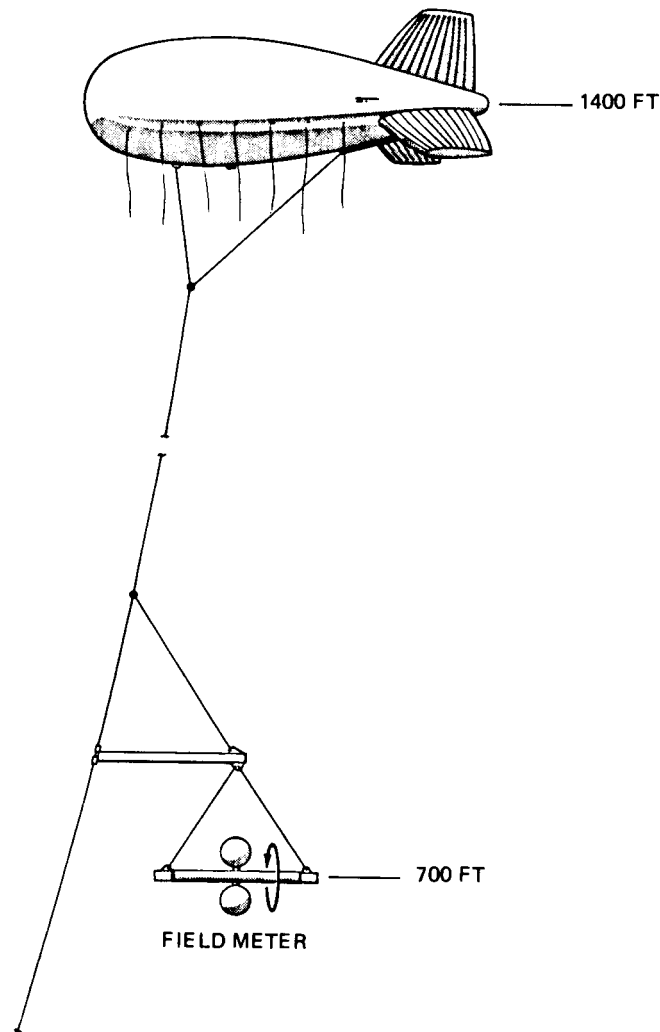
(Tom Marshall). The measurements were made by Christopher Phelps of Embry-Riddle Aeronautical University during the 1988 KSC Rocket-Triggered Lightning Program (RTLTP).

Results: In order to measure the electric field gradient above the space charge, a field meter, provided by the New Mexico Institute of Mines and Technology, was suspended from a balloon at an altitude of about 700 feet. The measurements data were sent by telemetry to the control caboose at the NASA Rocket-Triggered Lightning site where it was recorded on chart recorders along with other ground-based field mill data. During initial phases of the storm, the ground and airborne meters read about the same. For the more active phases of the storm, the readings aloft were as high as 50 kilovolts per meter, about ten times the readings on the ground.

During this program, fields aloft were also measured by the New Mexico Institute of Mines and Technology Schweizer 845A aircraft which was flown over the site.

W. Jafferis, 867-4438

DL-ESS-31



Balloon-Supported Field Meter

Numerical Weather Modeling

Reliable thunderstorm forecasting is required for many different operations at Kennedy Space Center (KSC); primary of these is the launching of the Shuttle and landings of the Orbiter. Summertime thunderstorms at KSC, however, are difficult to predict because they are usually caused by seabreeze circulations. These circulations occur because of the difference in temperature between land and sea. Since Florida is a peninsula, there are two seabreeze circulations: one develops on the west side and moves east and one develops on the east side and moves west. Seabreeze circulations alone or where they collide (seabreeze convergence zone) can trigger thunderstorms. After a seabreeze convergence zone develops, it often moves east. Whether thunderstorms develop or not is not a certainty. It depends upon the moisture available in the atmosphere, upper-air winds, and many other factors. Reliable summer thunderstorm forecasting presents a significant technical challenge. A computer numerical weather

model that could predict if the seabreeze will occur, where the seabreeze convergence zone will form, and when the seabreeze convergence zone would move into the vicinity of KSC, would be helpful for predicting thunderstorms at KSC.

Such a model has been developed by R*SCAN Corporation and ASTER Corporation under contract to NASA. The computer model, called the P2DM/P3DM, can be applied only when seabreeze conditions dominate the weather at KSC (about 20 percent of the days in a year). A field test using the P2DM model has been in progress three years. Eighty-five case days of data have been collected, and the model outputs have been provided to forecasters for evaluation. In addition, R*SCAN conducted a blind test of the computer model to determine whether a forecaster using the model will really do a better job. The forecaster made predictions of thunderstorms at the Shuttle Landing Facility (SLF) weather observing station and also a forecast

for thunderstorms anywhere within a 25 mile radius of the SLF, first without using the outputs of the P2DM model and then with the outputs of the P2DM model. The tests suggest the model can significantly improve the capability of forecasters to predict thunderstorms at KSC.

The next step is to independently evaluate the P2DM model to determine whether the model has significant value for KSC. The independent testing will be performed by a cooperative effort between KSC and Goddard Space Flight Center. A positive outcome would indicate that meteorological meso-models have come of age and may be applied to operational problems. Meso-models that are more sophisticated than the P2DM/P3DM exist, and could be applied at KSC. Based on the experience gained with this project, a specification could be developed so that meso-model support for KSC operations could be procured.

R. P. Wesenberg, 867-4438

DL-ESS-31

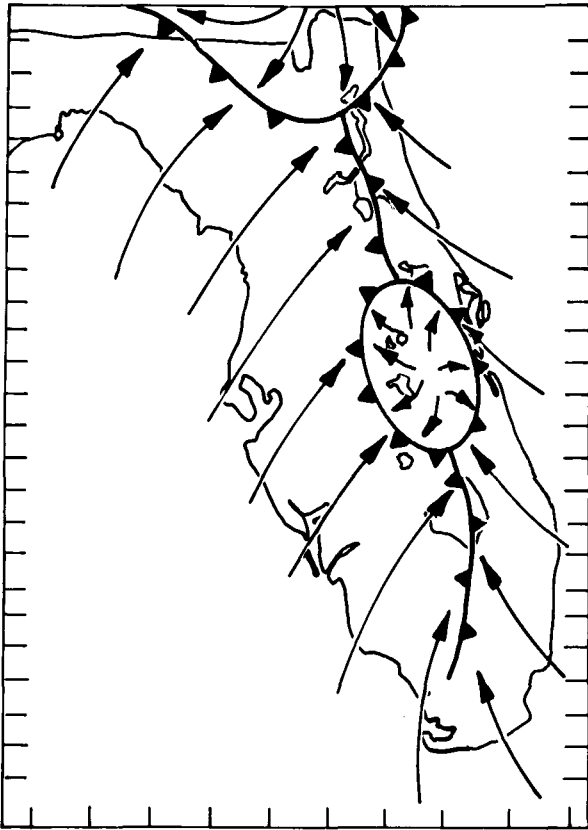
*1986 KSC Blind Test Forecasts
Calculation of Hit Rate or Probability of Detection (POD), False Alarm Rate (FAR),
and Critical Success Index (CSI) for Thunderstorm Probability Forecasts*

	POD = $d/(b+d)$		FAR = $c/(a+c)$		CSI = $d/(b+c+d)$	
	W/O Model	W/Model	W/O Model	W/Model	W/O Model	W/Model
AT X 68	0.400	0.933	0.357	0.571	0.300	0.609
25 miles of X 68	0.722	0.944	0.364	0.727	0.591	0.654

Blind Test Forecast Results

	POD = Probability of Detection		FAR = False Alarm Rate		CSI = Critical Success Index	
	W/O Model	W/Model	W/O Model	W/Model	W/O Model	W/Model
AT X 68	0.478	0.913	0.100	0.233	0.423	0.700
25 miles of X 68	0.543	0.833	0.167	0.176	0.500	0.769

Note: The signal detection theory false alarm rate (FAR) is defined as the ratio of false alarms to the total number of observed nonoccurrences of the event. This is different from the National Weather Service false alarm rate, which does not incorporate the correct forecasts of nonoccurrence and therefore does not credit the forecaster with any skill in forecasting the nonoccurrence of an event. A perfect set of forecasts is shown by $POD = CSI = 1.0$ and a $FAR = 0$.



NOTE: At least two large thunderstorm mesohighs were in evidence over the Florida Peninsula along with the confluence line of the southwesterly and southeasterly sea breezes meeting over mid-peninsula.

Mesoanalysis of Surface Winds, 2300Z, 5 May 1984

Measurement of Electromagnetic Enhancement Due to Site Nonuniformities

Kennedy Space Center (KSC) has been making electric field measurements to monitor the lightning activity since 1964. An array of electric field sensors, installed by NASA and operated by the Air Force, are used to issue warnings regarding the potential for lightning activity. The warnings enable the safe evacuation of people from exposed areas and the cessation of hazardous operations, and provide the means to avoid triggered lightning. A joint effort between KSC and Cape Canaveral Air Force Station (CCAFS) has been undertaken to modernize the electric field measurement system. The sensor electronics, the communication system, and the data processing system are being redesigned to reduce system errors and improve reliability. The

current system consists of 31 sensors covering approximately 150 square kilometers. The system provides real-time contours of the electric field variations over the KSC/CCAFS area and a location of the charge transfer center for each incident of lightning that occurs over the array. There is no similar system in the world that is as large or produces the complex electric field data products in real-time.

Errors can be introduced in several areas. The sensors are subject to loss of sensitivity if they are not maintained properly. Secondly, the models, used to locate lightning charge centers, are simple by necessity, but the absolute accuracy is hard to determine. Lastly, differences in sensor mounting and site characteristics can cause relative enhancement or reduction of electromagnetic signals between sites. Although maintenance, analysis, mounting, and site errors may individually be relatively small, the cumulative effect can be unacceptable. For this reason NASA is in the process of performing a thorough error analysis. In the future, the absolute system error will be known and understood by the user.

This report focuses on the measurement of the errors due to nonuniformities between sites. The electromagnetic signal can be enhanced or reduced at a site depending on (1) the slope of the local terrain, (2) the coverage and height of the local vegetation, and (3) the proximity and geometry of nearby man-made structures. NASA's approach to quantifying and enhancement factors is discussed below.

For years researchers studying lightning and atmospheric electricity have made electric field measurements to document and ultimately to understand the properties of lightning and cloud electrification. Frequently, the electric field measurements were made with a flat-plate antenna. When flush-mounted with the earth's surface, the gain of the antenna is simply proportional to the area of the sensing surface. To improve sensitivity, the antenna can be elevated similarly to the electric field sensors but, unfortunately, elevating the antenna makes quantitative measurements more difficult. In other words, the gain factor for the elevated antenna is not simply related to the antenna's area. An antenna flush-mounted with the ground and located several hundred feet away from an elevated antenna has been used to obtain an absolute calibration for the elevated antenna. The

gain factor for the elevated antenna is the ratio of the signal detected between the elevated and the flush-mounted systems due to a distant electromagnetic source. For an accurate measure of gain, the signal must be produced from a source whose distance is much farther than the distance between the two antennas.

NASA is adapting this technique to measure the differences due to site nonuniformities by comparing the signals between the two flush-mounted antenna systems at two different locations.

Previously, this technique has been used to determine gain relative to a "good" site. Primarily, this technique has been used to calculate gain factors due to variations in antenna configurations and not to evaluate the effects of the local environment.

In large networks of electric field sensors, the site form factors have been ignored or assumed to be uniform. NASA has set strict guidelines to define a good electric field sensor site, but to get adequate coverage the sites may not always be optimal. As part of the effort to perform a complete system analysis, NASA will temporarily place portable flat-plate antenna systems at each of the sites and compare the relative enhancement factors between sites using the electromagnetic signal generated by distant lightning.

The accuracy of this measurement is dependent on the assumption that the comparative electromagnetic signal is much farther away than the distance between the sites being compared. To determine the distance to the lightning, one of two techniques can be used. First, if the lightning is a cloud-to-ground stroke, it is detected by the CCAFS lightning location system. If the lightning was not detected by the lightning location system, any clouds as observed by satellite and radar that are capable of producing lightning must be sufficiently far away so signals emanating from their vicinity would be uniform across the measuring sites. If there is any question that lightning occurred within a cloud mass too close to obtain reliable measurements, then that lightning will not be used in the site factor analysis.

This is the first time this type of calibration has been attempted with this network at NASA/KSC and the first time the calibration has been

attempted on a network this large. A followup test will be performed a year later to detect any significant changes in the enhancement factors. If the errors are greater than 5 percent between sites, software corrections will be applied to the processed data.

This calibration test procedure was documented and accepted in June of this year. Testing is scheduled to begin before the end of the year. This is a major breakthrough that will better educate NASA and the Air Force on the capabilities and limitations of the electric field system.

The number of sensors and the area of coverage is large. In order to accomplish this task economically, it is necessary to restrict the portable measurement system to a few of the sites at any one time. Six portable units are being constructed to accomplish this task. Out of the six measurement sites, one site will always be used as a reference, so that the relationships between sites can be derived as accurately as possible.

Each portable measurement unit consists of a flat-plate antenna, the electronics to measure the remote lightning signatures, and a data recorder. Data from each of the recorders will be compared to derive the site factors.

This task is unique because of the size of the sensing network. Such a complete error analysis has never been performed before. Consequently, the possible errors as a result of site nonuniformities are not known.

L. M. Maier, 867-4993

TE-CID-3

Atmospheric Science Field Laboratory (ASFL)

The ASFL provides the facilities, equipment, and technical personnel required for field support in atmospheric research at Kennedy Space Center. This laboratory, which has an international reputation, has facilities that include a rocket-triggered lightning test site at Mosquito Lagoon, a full-threat portable lightning simulator, shielded vans for lightning test instrumentation, remote observation sites, and data acquisition instrumentation.



The ASFL at Mosquito Lagoon

During the past year, projects that have made use of the ASFL facilities include the Launch Pad Lightning Warning System (LPLWS) or field mill upgrade project, the rocket-triggered lightning project, and the thunderstorm currents project. The ASFL field research invites participation from state and Federal government agencies, universities, industry, and foreign governments.

R. P. Wesenberg, 867-4438

DL-ESS-31

Solid State Instrumentation for Electric Field Detection of Lightning Potential

The hazard of lightning is assessed by measurements of electric fields at the ground. The value of electric fields infers the electrified condition of the clouds. The measured field at the ground is also influenced by charges on atmospheric particles (ions) that originate and circulate

late near the earth's surface. These charges originate from needle-like points on objects such as trees, grass, and poles when the surface fields are greater than some threshold value (approximately 2 kilovolts per meter) that occurs when thunderstorms are present. This corona space charge, induced by higher electric fields, is of a polarity that tends to reduce the surface electric field. The measured surface electric field then becomes a weaker representation of the electrical charge of clouds.

Over water, an opposite effect occurs during thunderstorms. Ions of opposite polarity to the earth's charge migrate toward the earth's surface; this is called the electrode effect. An intense layer of space charge is produced below a height of 100 meters which is of the same polarity as the cloud charges and thus the surface electric field intensity is increased. This charge can be blown by the wind over adjacent land areas where it would affect electric field intensity; thus, both the corona and electrode effect space charge will influence electric field mea-

measurements made to determine cloud electrification and lightning potential.

At prestorm conditions and early into a developing thunderstorm, little space charge exists. After the storm develops and the threshold value of electric field is exceeded, space charge is created by point discharge (corona) and the electrode effect. The extent that the space charge is created and distributed during and after a storm is being studied.

Calibration flights have been flown by instrumented aircraft at Kennedy Space Center, and variations of fields aloft compared to those measured on the ground were found to range from 1 to 1 through 7 to 1 by Dr. Kasemir, Final Report, Contract No. 59753, June 1976.

To determine what effects space charge has on the measured electric field at the surface, Dr. R. Markson of Weather Corporation has been investigating the development and behavior of space charge with the intent of providing a compensating algorithm for its effect. The program involves measuring electric fields at the ground, at 20 meters from towers and poles, and aloft from balloons and aircraft.

This project involves developing corona current sensors for measurement of cloud level electric fields for several reasons:

1. They are simpler, cheaper, have no moving parts and are more robust than field mills, which have generally been used in the past.
2. They work best at elevated locations where they can be mounted relatively easily; thus, they are above much of the space charge that affects surface measurements.
3. They can be mounted at remote locations where little power is available with minimal site preparation or maintenance.
4. They are unaffected by rain or snow.

While the corona principle is well known, it has not been suitable for quantitative measurements of electric field intensity in the past because of wind dependence arising from space charge generated by the corona point shielding and reducing the field on the point. A second limitation has been the corona threshold that

prevented corona instruments from working in weak fair weather fields. Both of these problems have been overcome through innovative features of the new system, which provides the first corona current instrument capable of supplying quantitative electric field measurements under most conditions.

Work continues on these effects of space charge on measuring cloud electric fields. The objective of the continuing study is to provide instruments and an algorithm to improve the determination of lightning threat potential and the ability to determine the lightning threat to facilities and flight vehicles.

Dr. Markson has identified various effects of space charge on ground-based electric field measurements.

1. Corona: Ions, liberated from sharp points of opposite charge to the inducing electric field, reduce measured fields over land.
2. Electrode Effect: Ions of the same polarity as the electric field migrate toward the earth's electrode (surface) and increase the measured fields over water.
3. Depth of earth surface space charge is variable: While it can extend above 200 meters it frequently is concentrated near the surface.
4. Space charge ions migrate with the wind and under the influence of electric fields.
5. Life of space charge, on the order of minutes, may reduce, increase, or reverse the field at the earth's surface.
6. An electrode positioned at a height of 20 meters on a pole may be above the preponderance of space charge and, thus, provide a more representative measure of the probability of lightning.
7. The corona instrument developed measures electrical potential at the point rather than potential gradient (electric field), which is measured by field mills. This can be converted to the potential gradient by dividing the potential by the height of the point; but there is no reason to make such a conversion since the potential at 20 meters can

represent the intensity of cloud electrification as well as potential gradient at ground level.

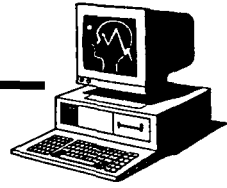
pliment or possibly be used in place of field mills in the future.

8. The new corona instrumentation can com-

R. J. Wojtasinski, 867-4993

TE-CID-3

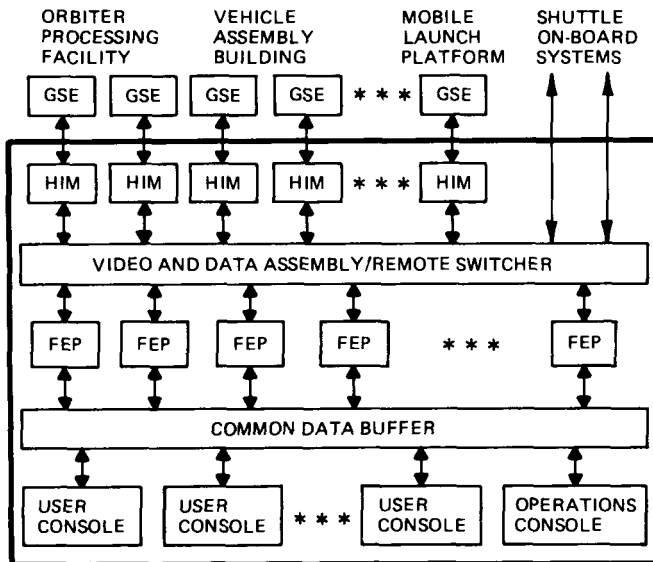
ARTIFICIAL INTELLIGENCE



Checkout, Control, and Monitor Subsystem (CCMS) Operations Analyst (OPERA) Expert System

The CCMS is one of three subsystems that comprise the Shuttle Launch Processing System. The CCMS network (see the figure "CCMS Network") integrates computers, data links, displays, controls, hardware interface devices, software and microcode. This network provides the only real-time interface between Shuttle engineers, the Orbiter vehicle, and its associated ground support subsystems (e.g., fuels and environmental controls). Four independent CCMS sets, called Firing Rooms, are used to process and launch Shuttle vehicles, to train launch teams, and to develop new CCMS software. The CCMS Operations charter is to provide and maintain error-free CCMS configurations to support all user testing requirements, such as launch countdown or Orbiter power-up sequences.

OPERA assists Operations personnel in performing CCMS support tasks, including Firing Room configuration and management and the detection, isolation, and correction of CCMS set faults. The goal of the OPERA project is to improve existing Operations capabilities by increasing automation and standardizing task performance. Each expert system in OPERA will act as a consultant, assisting the operations staff assigned to particular functional task sets (see the figure "OPERA Expert Systems, Operations Staff and Tasks"). The specialized information and skills required to perform these tasks range from expertise concerning the design and behavior of CCMS hardware and software subsystems [central processing units (CPU's) and Operating System components] to knowledge of CCMS operating procedures and configuration



FEP = FRONT-END PROCESSOR
 HIM = HARDWARE INTERFACE MODULE
 GSE = GROUND SUPPORT EQUIPMENT

OPS STAFF ROLE \ OPS TASK	TEST CONFIG ROOMTS	ERROR DETECT	ERROR EVAL	CPU STATUS/HISTORY	ACTION XQTD	ERROR LOG/TRACK
SET MANAGER	PIA CRA		RTSEM	PIA DBIF	PIA CM	PIA
TEST CONDUCTOR	PIA CRA	RTSEM	RTSEM	PIA DBIF	PIA CM	PIA
ANALYST	CRA	RTSEM				
SYSTEMS ENGINEER			RTSEM MBFI	PIA DBIF	PIA	PIA
HW ENGINEER (TECHNICAL)			RTSEM	PIA DBIF	PIA	PIA

OPERA Expert Systems, Operations Staff and Tasks

requirements. OPERA will eventually encompass six expert systems:

- Real-time System Error Management (RTSEM)
- Problem Impact Analysis (PIA)
- Model-Based Fault Isolation (MBFI)
- Database Interface (DBIF)

The CCMS Network

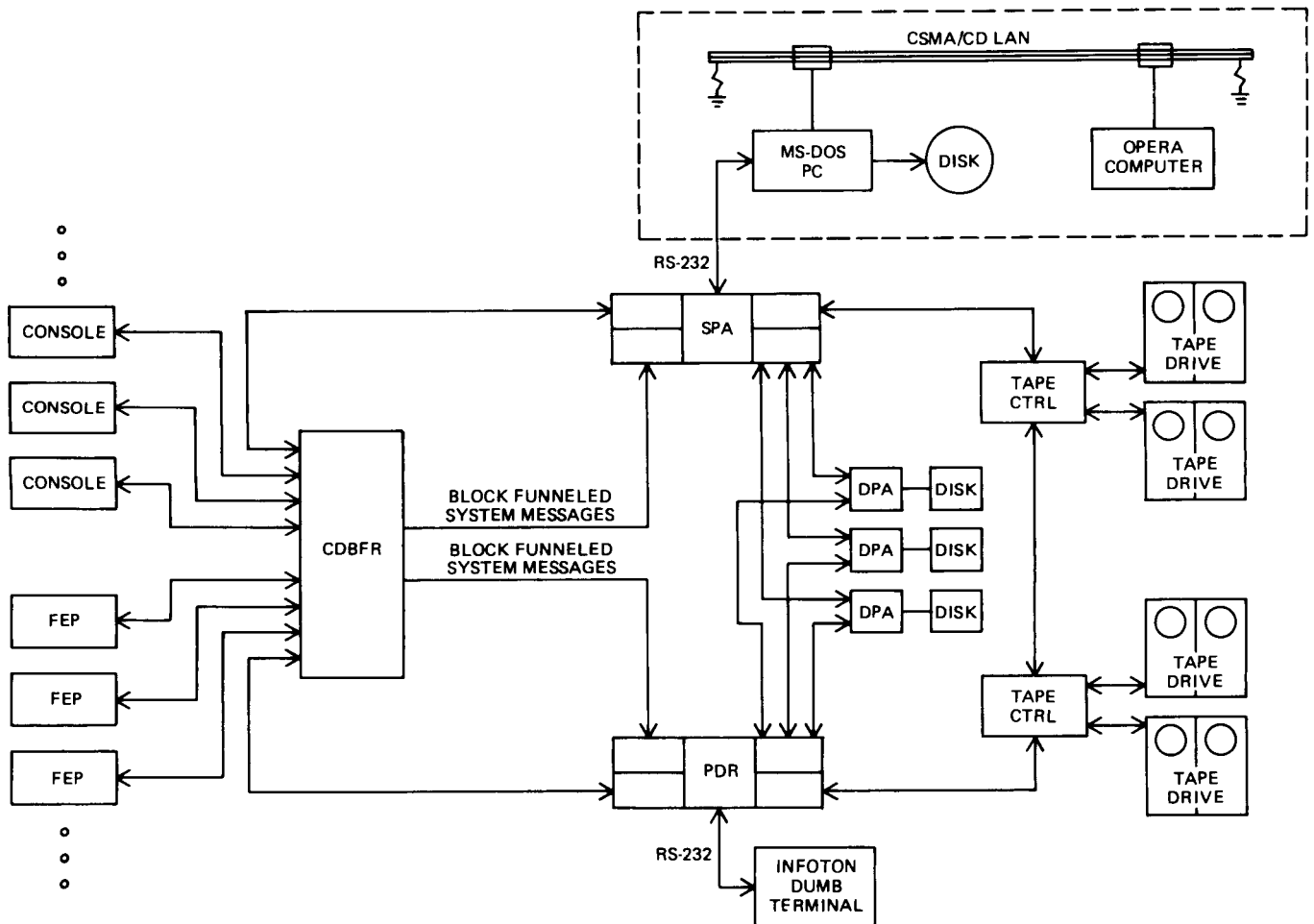
Configuration Requirements Analysis (CRA)

Configuration Management (CM)

The initial OPERA prototype incorporates two expert systems, RTSEM and PIA. When problems occur in Firing Rooms, rapid fault isolation and correction are essential in minimizing impacts on user tests and in retaining data integrity. RTSEM and PIA will help the Operations staff to troubleshoot CCMS faults, to restore Firing Room functionality, and to identify existing related problem conditions. Two extension expert systems, DBIF and MBFI, will supply additional data resources and model-based reasoning to enhance OPERA's initial troubleshooting capabilities. The CRA and CM expert systems will extend OPERA to assist users in planning network configurations that satisfy test and launch requirements and in managing network utilization.

The primary CCMS fault detection and isolation tools are Operating System error messages. These messages are currently manually monitored and interpreted, as generated by interrupt handlers embedded in CCMS Operating System components. OPERA's RTSEM Expert System operates by reading CCMS-generated system messages, interpreting them, and then evaluating any CCMS problems that may have occurred as identified by the messages. The off-line OPERA prototype simulates Firing Room configurations. The user can enter specific message occurrences for analysis or can retrieve the message streams from a Processed Data Recording (PDR) tape.

CCMS system messages which come from front end processors, consoles, the Processed Data Recording (PDR) Subsystem, and the Shared Peripheral Area (SPA) Subsystem are funneled in data blocks through the CCMS com-



PDR/SPA Versus OPERA Configuration

mon data buffer, and recorded at the CCMS PDR or SPA (see the figure "PDR/SPA vs. OPERA Configuration"). Near real-time data is stored on disk while historical data is stored on tape. A link between the OPERA computer and the PDR/SPA hardware was necessary to further automate OPERA's capability to process system messages.

For user input, each PDR/SPA CPU has an Infoton "dumb" terminal without disk storage capability. The terminal communicates over an RS-232 cable. While at the terminal, the user can retrieve and view system messages that have been recorded on tape or disk. It is a simple task to replace the Infoton dumb terminal with a MS-DOS PC having a hard disk drive, and a terminal emulator communications software package.

The retrieval program, which displays recorded system messages at the PDR/SPA terminal, is called SPBLOK. While acting as a terminal, the MS-DOS PC records all SPBLOK output on its hard disk. The format of an SPBLOK output is shown in the figure below.

A program written in the 'C' programming language was developed that reduces the raw SPBLOK output into an OPERA-formatted file. This program runs on the MS-DOS PC and creates the OPERA-formatted file on its hard disk drive. The file's format is as follows:

```
200:2128/45.061 FEP 136 (GS4 ) NO RESPONSE
TO THREE SUCCESSIVE DATA BUS TRANS-
MISSIONS, OLDEST ADRS (033400) REMOVED
FROM EXPECTED LIST,
```

```

SPBLOK04 INPUT COMPLETE.  DATA PROCESSING STARTING.

SPBLOK                                WTS14                                F815-1.1.0.0 PAGE
1
BLOCK FUNNEL LOG DATA RETRIEVAL PROGRAM
USER ID:  CCS TCID WTS14 S814

SPCOMM01 (SPBLOK) START TIME FOUND.  TIME OF 1ST RECORD=  200:
2127/59.999

   CDT= +08:1728/45   GMT= 200:2128/45.061   CPU= MSTR   LOG ID=
SM
0000  0000 4645 5020 3133 3620 2847 5334 2029  ..FEP 136 (GS4 )
0008  204E 4F20 5245 5350 4F4E 5345 2054 4F20  NO RESPONSE TO
0010  5448 5245 4520 5355 4343 4553 5349 5645  THREE SUCCESSIVE
0018  2044 4154 4120 4255 5320 0A0D 5452 414E  DATA BUS ..TRAN
0020  534D 4953 5349 4F4E 532C 204F 4C44 4553  SMISMISSIONS, OLDES
0028  5420 4144 5253 2028 3033 3334 3030 2920  T ADRS (033400)
0030  5245 4D4F 5645 4420 4652 4F4D 2045 5850  REMOVED FROM EXP
0038  4543 5445 4420 4C49 5354 2C20 908E  EXPECTED LIST, ..

   CDT= +08:1728/45   GMT= 200:2128/45.113   CPU= MSTR   LOG ID=
SM
0000  0000 4645 5020 3133 3620 2847 5334 2029  ..FEP 136 (GS4 )
0008  204E 4F20 5245 5350 4F4E 5345 2054 4F20  NO RESPONSE TO
0010  5448 5245 4520 5355 4343 4553 5349 5645  THREE SUCCESSIVE
0018  2044 4154 4120 4255 5320 0A0D 5452 414E  DATA BUS ..TRAN
0020  534D 4953 5349 4F4E 532C 204F 4C44 4553  SMISMISSIONS, OLDES
0028  5420 4144 5253 2028 3033 3334 3035 2920  T ADRS (033405)
1 SPCOMM08 (SPBLOK) ENTER 'C' FOR NEXT PAGE

```

Format of an SPBLOK Output

200:2128/45.113 FEP 136 (GS4) NO RESPONSE TO THREE SUCCESSIVE DATA BUS TRANSMISSIONS, OLDEST ADRS (033405) REMOVED FROM EXPECTED LIST,

200:2128/45.220 FEP 136 (GS4) NO RESPONSE TO THREE SUCCESSIVE DATA BUS TRANSMISSIONS, OLDEST ADRS (033414) REMOVED FROM EXPECTED LIST,

200:2128/45.325 FEP 136 (GS4) NO RESPONSE TO THREE SUCCESSIVE DATA BUS TRANSMISSIONS, OLDEST ADRS (033420) REMOVED FROM EXPECTED LIST,

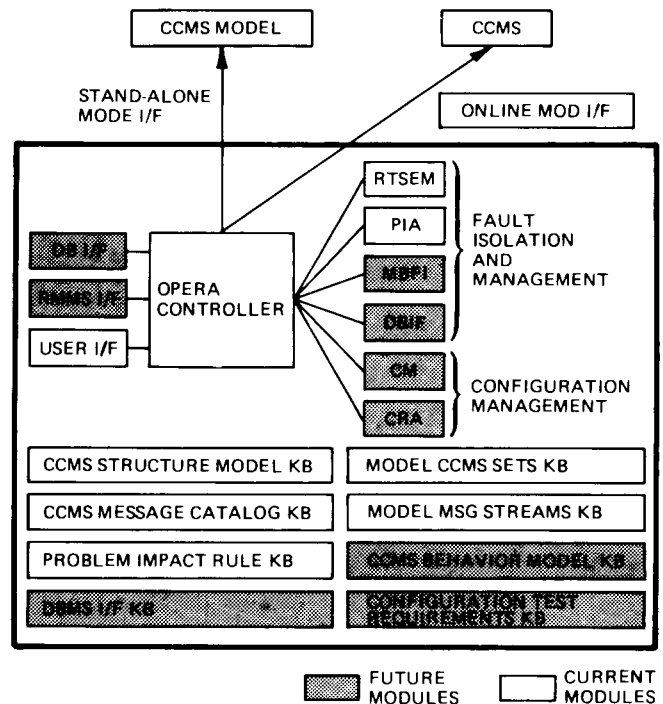
200:2128/45.425 FEP 136 (GS4) NO RESPONSE TO THREE SUCCESSIVE DATA BUS TRANSMISSIONS, OLDEST ADRS (033424) REMOVED FROM EXPECTED LIST,

The OPERA computer makes a physical link to the MS-DOS PC through a CSMA/CD LAN, running the higher level TCP/IP protocol. Once the MS-DOS PC has finished creating an OPERA-formatted file, the PC is set to run as a dedicated server. This allows the OPERA computer, via File Transfer Protocol, to access the OPERA-formatted file on the PC's hard disk. The OPERA computer is then free to read the formatted file, interpret the messages contained in the file, and then evaluate any CCMS problems that may have occurred.

In the planned, on-line real-time system, OPERA will receive the system messages directly from the CCMS Common Data Buffer (CDBFR) as they are logged to the Processed Data Recording (PDR) bulk disk and tape. Using the developed reformatting process, the messages will be stored for OPERA analysis.

The expert systems, RTSEM and PIA, are currently hosted on a Texas Instruments Explorer II LISP machine using Intellicorp's Knowledge Engineering Environment (KEE). The systems are integrated by a blackboard architecture that uses an OPERA controller to coordinate the information request and transfer between the expert systems. This same blackboard architecture will be extended as additional expert systems are added to the OPERA system (see the figure "Planned OPERA System Architecture"). In addition, work will begin in 1989 in the area of code optimization for porting the OPERA application to a hardware host which has reduced

disk storage and performance capabilities and possibly a non-LISP-based operating system. This would make deployment of the systems in each Firing Room much less costly.



Planned OPERA System Architecture

By applying artificial intelligence technology to CCMS in the form of OPERA's expert systems, both current and future, it is hoped to capture some of the volatile corporate knowledge of CCMS Operations before it is lost to job mobility or employee attrition. The automation of standard tasks and the constant availability of expert consultant capabilities will improve the efficiency and effectivity of CCMS operations. Thus, we can continue to improve our operations without losing the visibility of passed lessons learned.

A. E. Heard and P. P. Pinkowski,
867-3926

TE-LPS-11

Remote Maintenance Monitoring System

In its current configuration, the Launch Processing System (LPS) at the Kennedy Space Cen-

ter (KSC) relies on over 200 ModComp computers to perform launch-critical monitor and control functions between the Space Shuttle and ground support equipment (GSE). While hard failures seldom present troubleshooting challenges, operational ModComp computer history shows that 17.4 percent of the intermittent failures are never found and cannot be duplicated in a troubleshooting environment. Due to the system's nature, maintenance of these 200 computers is performed in an off-line environment, thus making the task of troubleshooting and repairing the system both manpower and time intensive. When fully integrated into the LPS, the Remote Maintenance Monitor System (RMMS) will function as an automatic maintenance diagnostics system capable of anticipating approaching failures, and troubleshooting both hard and intermittent failures down to the line replaceable unit (LRU) level while expending minimum time and manpower.

Spanning a five year development life cycle, the program schedule included the development of the RMMS Phase I prototype, RMMS Phase II design and specification work, and RMMS Phase III demonstration and concept validation.

The Phase I prototype focused on the development of a proof-of-concept evaluation unit that demonstrated the ability to implant data acquisition hardware into the ModComp computer, monitor various operating parameters and error conditions, and automatically diagnose the cause of the failure using the artificial intelligence facilities built into a knowledge-based maintenance Diagnostics Expert System.

Following the successful completion of Phase I, the start of Phase II represented the beginning of full-scale design and development toward the goal of producing a deliverable maintenance monitor. In its final configuration, the maintenance monitor will be able to capture ModComp data in real-time and subsequently use this information to anticipate failures, diagnose irregular or spurious system conditions, automatically analyze central processing unit (CPU) dump information to determine the source or sources of failure, and provide system maintenance engineers with an interface for performing on-line background testing of ModComp parameters and processes. Design and development efforts required during Phase II include the specification of a dedicated LISP processor to host the RMMS Expert System, an Expert System Shell

to assist in the development of expert system software, and a stand-alone workstation to provide communication and control between the various blocks within the entire system.

The RMMS system architecture in Phase II consists of a Data Manager, Data Analyst, Logged Data Monitor (LDM), ModComp CPU Implant, Common Data Buffer Implant, and a Communication Network. The Data Manager serves as the interface between the implants and the Expert Diagnostic System. In addition, the Data Manager serves as the system archiver. The Data Analyst controls the implants and serves as a workstation for diagnosing ModComp failures. The Logged Data Monitor captures ModComp system messages and data dumps from the Common Data Buffer. The ModComp CPU Implant monitors and evaluates ModComp memory and registers accesses, CPU/Option Plane Handshaking operations, Option Plane microcode execution and all regulated voltages. The Implant also provides failure mode information through images and traces. The Common Data Buffer Implant detects and captures Common Data Buffer errors. The Ethernet Communication Network links the CPU implants and the Data Manager.

In 1988, RMMS engineers finalized the system software architecture for the Data Manager and initialized software development on a SUN 3/160 workstation. Major software tasks include LAN interfacing, file handling, user interface, and LDM simulation. System architecture and hardware design for the Logged Data Monitor has also been completed. The LDM is designed around the host SUN 3/160 Data Manager and includes an 11-MIPS, 32-bit microcoded CPU, a 96-bit Control Store, and a standalone I/O card for high-speed communication.

The preliminary version of the expert system tool has been implemented with Intellicorp's Knowledge Engineering Environment (KEE). Functioning as an information analyst, this tool provides system engineers access to ModComp data information recorded by the Data Manager through the Logged Data Monitor, and subsequently performs automated diagnostic analysis on the retrieved information.

Additionally, RMMS engineers have accomplished the downloading of information to the Data Analyst, as well as testing the user interface. The user interface is being functionally en-

hanced as a result of suggestions generated by KSC system engineers.

The design specifications and implant system architecture have been finalized for the CPU Implant. Conceived as a large-scale data acquisition system, the implant monitors the execution of various ModComp processes to detect impending failures. Subsequently, this enables the implant to create a "snapshot" look at the state of the machine prior to ModComp-detected errors and subsystem Autodumps. The implant will consist of a Zilog Z8002 microprocessor, a bit slice memory Image Processor with 4K writable control store, a CPU Memory Trace Processor, a bit slice Register Evaluation Processor design with 4K writable control store, a Microcode Address Trace, Microword Comparison Logic, a Communications Interface, 5- and 12-volt voltage monitors, isolation logic, and a local monitor interface.

Capable of providing enhanced support to the LPS through 1995 with advanced designs, the RMMS concept efficiently incorporates continuous realtime monitoring of the Checkout, Control, and Monitor Subsystem (CCMS) hardware, the central integration of various diagnostic data acquisition processes, and the automation of the diagnostic process through expert system technology.

M. Lougheed and T. Ross,
867-4946

TE-LPS-13A

Expert Mission Planning and Replanning Scheduling System

The Expert Mission Planning and Replanning Scheduling System (EMPRESS) is an expert system created to assist payload mission planners at the Kennedy Space Center (KSC) in the long-range planning and scheduling of horizontal payloads for Space Shuttle flights. Using the current flight manifest, these planners develop mission and payload schedules detailing all processing to be performed in the Operations and Checkout Building at KSC. The EMPRESS system generates these schedules using standard flows that represent generic carrier processing timelines. Resources are tracked, and resource conflicts are determined and resolved inter-

actively. Constraint relationships between tasks are also maintained and can be enforced when a task is moved or rescheduled. The EMPRESS prototype, developed jointly by NASA and the MITRE Corporation of Bedford, Massachusetts, became operational in March 1986. A new version of EMPRESS, currently under development, will correct many of the limitations of the original prototype and enable EMPRESS to work with the ARTEMIS scheduling system.

As the primary launch site of the Space Transportation System (STS), KSC is responsible for the final checkout, preparation, and installation of payloads into the Space Shuttle Orbiter. Processing of a horizontal payload occurs, primarily, at the Operations and Checkout Building in the KSC industrial area. The processing includes the tasks needed to assemble and install experiments onto a Spacelab carrier as well as the steps needed to perform experiment and subsystem functional verifications prior to installation into the Orbiter.

To monitor and control this processing activity, NASA generates and maintains a hierarchy of schedules. At the top of the NASA schedule hierarchy is the flight manifest, which assigns launch dates, Orbiter vehicles, and payloads to STS missions. KSC uses the manifest to generate long-range plans and schedules that detail support for the launch date milestones.

One such long-range plan is the Multiflow Assessment (MFA). This document contains Gantt charts that illustrate the major processing activities needed for each payload listed in the manifest. The MFA also contains information on the critical resource needs of these payloads. This enables early recognition of potential conflicts between limited resources. Because of the dynamic nature of Shuttle operations, payload mission planners are often called upon to develop new MFA's quickly when the manifest is changed, or to produce "what-if" schedules when examining unusual mission scenarios. EMPRESS is an effort to automate the process of producing the MFA and to respond quickly to changes in the launch manifest.

In a hypothetical EMPRESS session, the operator would first load a new flight manifest into the system. EMPRESS would then create a schedule for each horizontal payload on each mission. When creating a mission schedule, EMPRESS first determines if a schedule already

exists. If not, EMPRESS creates a default schedule using a standard flow, which is a list of the tasks, task constraints, and resources required to process a horizontal carrier. When the default schedule is generated, the planner can modify the tasks and resources as required. EMPRESS gives the planner the ability to verify that resource conflicts have not occurred between parallel operations and to revise resources and tasks automatically if conflicts exist. Constraint relationships between tasks are maintained and can be enforced when tasks are moved or rescheduled. The user interface is robust and gives the planner a graphical representation of the schedule and detailed histograms of resource utilization. The operator can then save the schedule.

The domain knowledge base for EMPRESS is divided into three major areas: tasks, resources, and system heuristics. Task data include the various activities required to process a payload and the parent-child or predecessor-successor relationships between these tasks. Resource knowledge encompasses the people, hardware, and facilities required to process a payload. Resources are stored in a 1-to-n hierarchy. The heuristics in EMPRESS control the planning and scheduling. In addition, EMPRESS has a small forward chaining rule set used to resolve resource conflicts. These rules allow the operator to substitute an alternative resource, to increase the workload of the resource (e.g., add more shifts), or to reschedule the task that caused the problem. The operator may choose to let EMPRESS resolve all resource conflicts automatically without operator input.

EMPRESS development during fiscal year 1988 concentrated on converting the prototype into an operational system. A new user interface and a standard command structure have been implemented and new functions for creating calendars and producing graphical output have been developed. In addition, an interface between the ARTEMIS and EMPRESS scheduling systems has been established and work continues on extending EMPRESS to support ARTEMIS in the production of the MFA.

R. L. Pierce, 867-3526

CS-ISO

Automatic Test Expert Aid System Environment (AT-EASE)

The Launch Processing System (LPS) at Kennedy Space Center (KSC) is made up of over 3,000 individual line replaceable units (LRU's). It is the responsibility of the Intermediate Level Maintenance Facility (ILMF) to test, repair, and verify these components. A large percentage of these components lend themselves to be tested and verified at the ILMF, using automatic test equipment (ATE). Presently, the ILMF uses two major ATE systems to test and verify those components within the LPS that are suited for automated testing. Specifically, these systems are the GenRad 1796 functional printed circuit board test system and a NASA enhanced Tektronix 3270 system that performs as a functional high-speed printed circuit board test system. The task of developing the test program sets (TPS's) that these systems use to perform these tests and verifications is both manpower and time intensive. The AT-EASE project has developed a product to facilitate the development of these TPS's for the GenRad ATE. This product is designed to be useful to the seasoned as well as the novice ATE engineer. The fruits of this project will be a substantial reduction in the TPS development time and more comprehensive, standardized automatic test packages.

AT-EASE will reside on line with the GenRad software development station as a "smart" front end. The hardware will consist of PC-AT workstations that will communicate with the GenRad PDP-8 through an interface that was designed at KSC. The utilities of this system include: an automated on-line transferable data base of reusable GenRad code, a context sensitive full-screen editor, an on-line knowledge base of GenRad automatic test processes, an on-line automated PDP-8 error code translator, a bidirectional file and data transfer system, and a GenRad TPS development fact and rule base. These data and knowledge bases are accessed and manipulated by three major sets of software. The data bases are controlled by a modern, high-speed, high-capacity relational data base management system called DataFlex. The knowledge bases utilize an object-oriented inference engine

called Goldworks. Goldworks also provides for both forward and backward chaining within the knowledge base. The link to the user is a voice-recognizing menu-driven, windowing package embedded within the editor. The fact base is nearing completion and the first workstation has been delivered to the ATE Test Engineering Group for evaluation and testing.

Further enhancements to this system will be realized by the continuous growth of the reus-

able code bank and rule base. In addition, this expert system approach to TPS development will be applied to the other Automatic Test Systems at the ILMF. These expert systems will continuously improve test and verification of LPS components at KSC.

M. Lougheed, 867-4946

TE-LPS-13A

BIOMEDICAL



Biological Flight Research Program: Chromosomes and Plant Cell Division in Space

An experiment currently being developed at Kennedy Space Center (KSC) entitled Chromosomes and Plant Cell Division in Space (CHROMEX) is presently undergoing final certification and testing in preparation for a February 1989 launch. The CHROMEX experiment is designed to observe the patterning of cell division with specific attention to chromosomal material in plant roots after exposure to microgravity. The primary experiment carrier is the Plant Growth Unit (PGU), which replaces a standard locker in the Orbiter middeck. In previous flights of the PGU, the Plant Growth Chambers (PGC's), which house the plant specimens, have been sealed. An enhancement to the PGU, the Atmosphere Exchange System (AES), was developed at KSC to provide filtered, fresh air to the plant specimens contained within the PGC's.

The AES replaces one of the six PGC's that the PGU can carry. The AES consists of a small instrument pump, a replaceable battery pack, a filter cartridge, and a passive dosimeter. The instrument pump is adjustable over a range of 1 to 20 liters per hour. The battery pack consists of ten zinc/air button cells that have a capacity of 6.5 Ahr each at 1.4 volts. The battery pack can be easily replaced while in orbit. The dosimeter is an assembly of special photographic emulsions and plastics that will provide information on the radiation exposure level of the experiment. The filter cartridge was developed to remove organic contaminants and to regulate carbon dioxide of the incoming cabin air to an acceptable level for plant growth. The filter cartridge consists of a lithium hydroxide bed to remove carbon dioxide, potassium permanganate to remove ethylene, zeolite to remove low molecular weight organics, and a mixture of activated carbon and platinum to remove larger molecular weight organics and carbon monoxide, respectively.

Test results have shown that the filter cartridge can perform for 20 days at one-liter-per-hour

flow rate under Orbiter environment conditions, and the entire AES can operate for six days before battery exchange is required.

Dr. W. M. Knott, 853-5142

MD-RES-L

Muscle Exercise Machine for Concentric Only Exercise

A research study on muscle training is in progress at Kennedy Space Center. The basic intent of the study is to investigate a countermeasure for muscle atrophy experienced by the astronauts during space flights of long duration. Three groups are involved in the study: one, the control group, has no exercise program; the second performs both concentric and eccentric exercises; and the third does only concentric exercises. The latter group receives leg muscle conditioning during the concentric contraction only, thereby relieving the muscles of the work done during the eccentric phase; i.e., unloading the muscle fiber while it is extending.

A commercially available exercise machine was obtained and modified, through the use of a hydraulic cylinder, to eliminate the weight from the individual when the maximum limit of muscle contraction was reached. The modified system allows hydraulic fluid to freely drain through check valves during extension. During return, flow is regulated through a valve that is adjusted to accommodate the weight and frequency of the exercise regimen.

Premodification testing of the exercise machine showed serious frictional losses. Extension and flexion forces were not only different for a selected weight but significantly different from each other. The substitution of lowfriction bearings has brought these forces to within 5 percent of each other, and calibration and

proper labeling of the weight stack has made the selection of force more accurate.

D. F. Doerr, 867-3152
A. B. Maples, 867-4742
C. M. Campbell, 867-4742

MD-ENG
MD-ENG-A
MD-ENG-A

Human Physiology Research Projects: Blood Pressure Control

It is well documented that following spaceflight some astronauts experience low blood pressure (hypotension) while standing. This condition has been termed orthostatic hypotension and can lead to fainting. Because of the potential consequences to the health, safety, and performance of crews during and immediately following reentry and landing, scientists of the Life Sciences Research Office at Kennedy Space Center undertook several research projects to examine physiological characteristics associated with orthostatic hypotension and factors that affect them.

Some researchers have reported that endurance-trained athletes with high aerobic capacity develop orthostatic hypotension and tendency to faint more readily than sedentary individuals. This evidence has been used to recommend that astronauts should not participate in exercise activities that increase aerobic capacity such as jogging, cycling, etc. This past year, a study was conducted in which 16 men underwent 10 weeks of exercise training on a cycle ergometer. The training program caused a 20-percent increase in aerobic capacity. Contrary to the belief that this training regimen should have caused greater orthostatic hypotension and tendency to faint, these subjects showed a 28-percent increase in their tolerance to lower body negative pressure (which causes hypotension and fainting). The results of the study suggest that aerobic exercise training using cycling may provide a beneficial preflight training program for astronauts.

In 1987, a bed-rest study was conducted by scientists of the Biomedical Operations and Research Office in collaboration with Ames Research Center. During this study, it was determined that orthostatic hypotension and fainting

following exposure of 30 days to simulated microgravity (bed rest) were associated with the impairment of the carotid baroreflex. The carotid baroreflex is responsible for causing heart rate to increase so that blood pressure can be maintained during standing. During the past year, a number of experiments have been conducted in an effort to gain more knowledge and understanding of this reflex. Through a collaborative study with Humana Hospital-Lucerne in Orlando, the response of the baroreflex has been examined in wheelchairdependent people (e.g., quadriplegics) to determine if the long-term loss of exposure to 1-G posture might produce changes in the reflex response similar to those observed in bed rest subjects. These comparisons might provide a model to study the long-term effects of microgravity on reflexes that are important in control of blood pressure in astronauts. The study to determine the effects of various forms of acute and chronic exercise and hydration states on the baroreflex response is also continuing. These results from present and future experiments should provide critical information about the human cardiovascular adaptations to long-term spaceflight and development of countermeasures against adverse effects.

Dr. V. A. Convertino, 867-4237 MD-RES-P

Controlled Ecological Life Support System (CELSS) Breadboard Project

A preliminary growout and systems check was conducted with a wheat crop in the Biomass Production Chamber (BPC). Both levels of the upper chamber were planted with "Yecora rojo" cultivar, and the chamber was operated at 20 °C with continuous light (i.e., 24-hour photoperiod) and 1,000-parts-per-million carbon dioxide (CO₂). Plants were sequentially harvested at 68, 74, 80, and 86 days of age to determine the optimum harvest stage. The highest productivity of over 20 g m⁻² day⁻¹ of seed dry weight occurred at 74 days of age. This yield is equivalent to 1,500 gm/m² of dry seed which is five times the yield of the average U.S. field. The variability in yield data suggests a significant position effect on plant growth. This seemed to correlate best with the gradient in levels of photosynthetically active radiation. The followup study scheduled

with wheat in the BPC will provide a statistical analysis of position effects.

Support studies for the biomass production effort included tests with lettuce, potatoes, and soybeans. The studies have focused on the use of a nutrient film technique (NFT), high-pressure sodium (HPS) lighting, and CO₂-enriched atmospheres, all conditions that will be encountered in the BPC. Specific experiments have entailed a growout of potatoes using the NFT approach, a comparison of fluorescent and HPS lighting for lettuce and soybean growth, a comparison of photoperiod effects on soybean growth and flowering, and a continuing study of CO₂ level and soybean growth and yield with NFT usage. Sterile cultures of nodal cuttings for sweet potatoes and potatoes were maintained throughout the year to supply planting stock for experiments.

Bench-top studies (i.e., not conducted in growth chambers) using high-pressure sodium lamps were conducted to assess storage root development of sweet potatoes, germination and growth of rice and cowpeas, and growth of wheat on nutrient solutions supplemented with minerals leached from wheat straw. During the summer, two visiting scientists, Dr. Dennis Dubay and Dr. Don Wetherell, conducted research on hydrocarbon emission from potatoes, lettuce, and wheat and control of root growth in wheat.

Tests with the tubular membrane system (TMS) continued through the year to assess the ability of different porous materials and pressures to sustain plant growth. Studies comparing the effects of solution delivery pressure showed that the growth of wheat and lettuce appears to be a direct function of system pressure and water potential at the root-membrane interface. Studies comparing effects of membrane pore size on wheat showed that production increases with an increase in pore size under constant pressure. Monitoring and control of nutrient solution pH, electrical conductivity, and delivery pressure have recently been automated and converted to computer control. Mock-ups of the individual plant growth chambers (PGC's) for the flight plant growth units (PGU's) were fitted with porous tubes for providing nutrient solutions. Preliminary germination and growth studies with wheat showed that the TMS should work well within the constraints of the

PGU. An initial draft of a potential flight study using the TMS in a PGU was written.

The biomass processing activities continued toward the goal to maximize the conversion of inedible CELSS-grown crop residues (i.e., cellulose and hemicelluloses) into edible products. Studies continued on optimization of the production of the cellulase enzyme complex by *Trichoderma reesei* with supplemental addition of beta-glucosidase enzyme from *Aspergillus phoenicis*. Both organisms were grown in small batch cultures on purified substrates (alpha cellulose and starch) to determine base-line enzyme production rates and then on CELSS wheat residue to determine rates from authentic CELSS substrates. Studies to optimize the production of xylanase enzyme complex (a hemicellulase) were initiated this year. *Aureobasidium pullulans*, a yeast-like organism, was selected to produce the enzyme from CELSS wheat residue. Studies of crop residue pretreatments were initiated and focused on removal of soluble organic and inorganic compounds from wheat residues through cold water leaching. Utilization of these soluble compounds was examined. Studies of the replacement of hydroponic solution nutrients by the leached soluble inorganics and production of microbial and fungal biomass from the leached organics were both initiated. Pretreatment to remove lignin and hemicellulose from crop residues has continued, with major emphasis on a chemical removal method and on combining cellulase and xylanase in the enzymatic hydrolysis phase to eliminate the need for this pretreatment. Plans have been developed for studies leading to product recovery and enzyme recycling by ultrafiltration and studies for conversion of the product sugars to protein, for feeding of conversion process residues to tilapia, for computer monitoring and control of all conversion processes, and for process scale-up to handle crop residues as produced by the BPC.

Development of Aquaculture systems continued in 1988. The objective was to produce plant crop biomass and fish biomass in a combined aquaculture/hydroponics system. Wheat, cowpeas, and lettuce have been carried from germination through harvest, and fish biomass has been produced successfully on the combined system. Other studies have included feeding trials to determine the utility of wheat inedible biomass as a fish food source. Direct use of wheat and use of fungal mycelial products from

the biomass conversion activities have been tested. A computer monitoring and control system is being developed and tested.

Dr. W. M. Knott, 853-5142

MD-RES-L

Environmental Monitoring Program

The environmental monitoring activities at Kennedy Space Center (KSC) are categorized into three broad areas that are linked by the exchange of information generated by individual tasks. The three areas of activity include operations and construction monitoring, long-term ambient monitoring, and ecological research. The program plan (MD-LTP1) was updated and republished (MD-LTP2) during the past year; it provides a summary of all activities.

Operations and construction monitoring focuses on the environmental impacts produced by new facilities development or the effects of existing operations such as the launch of the Space Shuttle.

Long-term ambient monitoring is used to baseline existing conditions at KSC and to monitor the range of natural variability that exists in the environment, allowing managers to separate man-made impacts from natural changes. Data bases are maintained for air quality, rainfall volume and chemistry, water and sediment chemistry, soil chemistry, vegetation communities, and select threatened and endangered species.

Ecological research activities are used to develop an understanding of ecological processes and controlling factors that operate in the unique environment at KSC. The information derived through these various activities is incorporated into computerized data bases including a Geographic Information System (GIS) for analyses and interpretation. The goal of this research is to develop models for the purpose of predicting impacts before they occur.

During 1988, the GIS system was expanded to include two work stations and additional software, greatly enhancing its utility and capabilities. Mapping support was provided to the U.S. Air Force at Vandenberg Air Force Base and at

Cape Canaveral Air Force Station. Comprehensive land-use maps, similar to the ones previously developed for KSC and the Canaveral National Seashore, were developed for both facilities using LANDSAT data, aerial imagery, and groundtruthing. In addition to the maps, a set of technical reports covering a variety of subjects, including soil erosion, fire history, vegetation communities, and species of special concern, were developed for Vandenberg Air Force Base as part of a multidisciplinary baseline inventory.

The major activity undertaken at KSC in the area of operations and construction monitoring during the past year involved the return to launch with the successful STS-26 mission. Monitoring activities focused on Launch Pad 39B and the unique environment in that area. Vegetation transects were resampled and soil and sediment samples were collected for chemical analyses to update the baseline data base. A set of water quality experiments was initiated to determine if projected impacts, based on results from previous studies at Launch Pad 39A, would occur. Results are pending completion of chemical analyses. A master's thesis, covering fish bioaccumulation of metals in the vicinity of Launch Pad 39A, was completed and is currently being developed into a NASA technical memorandum.

In prediction of construction impacts, several investigations continued during the year. A master's thesis was developed that defined some of the habitat characteristics that are unique to areas used by gopher tortoises, an important, protected species at KSC. Specimens were equipped with radio transmitters allowing the staff to develop information on territory size, home range, and habitat preferences. The listing of the Florida scrub jay as an endangered species by the U.S. Fish and Wildlife Service brought the large population at KSC into the program during 1988. A project was initiated that will define habitat preferences and territory sizes. This information will be used to develop a set of maps for KSC that defines important breeding areas and critical habitat. This information can then be used for site selection of new facilities and the development of environmental assessment documentation and impact minimization strategies.

Long-term ambient environmental monitoring activities proceeded as planned. Ambient air quality monitoring of the Environmental Protec-

tion Agency priority pollutants (SO_2 , NO_x , CO , O_3 , and particulates) and recording of local meteorological conditions continued at the permanent air monitoring station (PAMS A). Several pieces of new equipment including meteorological sensors, a meteorological tower, and a high-volume air sampler were installed. The process of obtaining Florida state certification of PAMS A was initiated. Monitoring of atmospheric deposition at the KSC National Atmospheric Deposition Program site continued. The pH of rain at KSC generally ranges between 4.5 and 4.9 units. Water quality monitoring proceeded as scheduled, and a study was initiated that will provide synoptic water temperature and conductivity data for the Indian River, Banana River, and Mosquito Lagoon. The resampling of permanent vegetation plots located across KSC was initiated, and it was determined that beach erosion had significantly altered the vegetation distribution on the coastal dunes.

Ecological research activities at KSC covered a variety of topics. As part of the NASA Biospherics program, researchers from KSC and Langley Research Center joined forces with members of the local U.S. Fish and Wildlife Service to study the effects of fire on global atmospheric chemistry. The third year of a study evaluating the role of beach nest temperatures on the sex ratios of sea turtle hatchlings was completed in conjunction with the University of Toronto and the U.S. Fish and Wildlife Service Endangered Species Office. Research continued concerning the factors that control the distribution and abundance of manatees in KSC waters and concerning the evaluation of water bird use of impoundments. Three students assisted with field and laboratory activities during their summer internship at KSC. A graduate student is using the KSC area to assess the role that water levels and fluctuations of food resource abundance have on the distribution of select species of water birds. These data may be directly used in future environmental assessments and mitigation activities. A new graduate student project was initiated in 1988. A student from the University of Florida is evaluating stormwater runoff and ground water interactions in the vicinity of the KSC industrial area with the ultimate goal of providing managers with better alternatives for the management of nonpoint sources of runoff pollution.

Dr. A. M. Koller, 867-3165
Dr. W. M. Knott, 853-5142

MD-PLN
MD-RES-L

Controlled Animal Nutrients Delivery System (CANDS)

The objective of the CANDS project is to provide investigators with a system capable of supplying research rodents with a sterile, nutritionally complete, and balanced diet (including water) in a manner that facilitates intake monitoring and maintains biocontainment capabilities while in microgravity. CANDS has approached the problem of nutrient delivery and monitoring by developing an integrated, two-component system that combines hardware and diet to achieve desired results. The hardware incorporates a passive delivery system that interfaces with existing flight hardware (the Animal Enclosure Module, shown in the figure "Diet Delivery Concept for the Animal Enclosure Module") and requires minimum crew interaction to accurately monitor daily animal intake. The hardware is also designed to function in environmental conditions similar to those found in the Shuttle middeck during flight, and to provide sterile diet delivery while maintaining biocontainment and ensuring animals achieved ad-lib intake. The diet is fed in high-moisture form (60 to 65 percent water) and utilizes semipurified ingredients that allow flexibility in formulation. With this flexibility, single nutrients or nutrient ratios may be altered as experiment protocols require. The cohesive nature of the high-moisture diet makes it ideal for use in microgravity and minimizes waste.

A preliminary biocompatibility study, conducted during a mission simulation, compared conventional housing with the prototype hardware. Results indicated that all systems were equally capable of supporting normal rat growth and demonstrated the hardware's ability to allow ad-lib consumption to be monitored in a quantitative manner. CANDS evaluations in simulated micro- and hyper-gravity onboard a KC-135 further demonstrating the system's ability to maintain biocontainment and meet research objectives. The diet has been successfully tested when exposed to vibration profiles similar to those found in the Shuttle middeck.

A 28-day feeding study was performed using the high-moisture diet and an established purified diet, AIN-76A. Results showed that the high-moisture diet supported normal rat growth as well as AIN-76A. The present diet was formulated to meet National Research Council (NRC)

**ORIGINAL PAGE IS
OF POOR QUALITY**

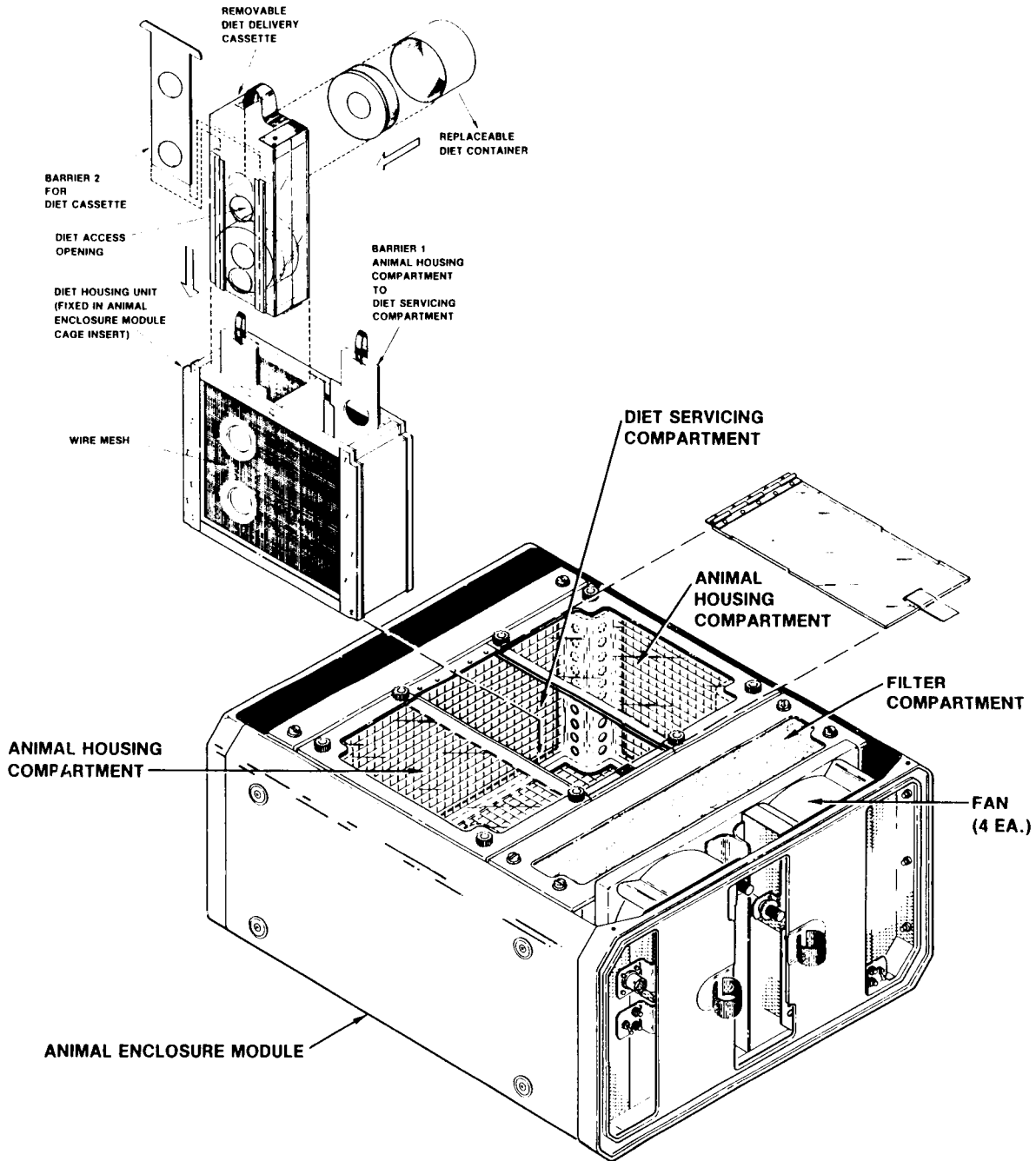
nutrient requirements for rats. A shelf-life (sterility and nutrient stability) study over 180 days showed that the diet remained sterile and within NRC requirements.

Upcoming studies will focus on: (1) Further characterizing rat performance when fed the present high-moisture diet formulation and when housed in the prototype hardware for extended periods of time, (2) simplification of hard-

ware to minimize crew interaction during flight, (3) collecting ground-based, baseline data for future comparison to animal performance in microgravity, (4) continuing the shelf-life study of different packaging systems, and (5) evaluating a diet packaging system to simplify ground-based activities.

Dr. W. M. Knott, 853-5142

MD-RES-L



Diet Delivery Concept for the Animal Enclosure Module

OPERATIONS



Telemetry Data Processing Using Microcomputers

The Hangar AE Telemetry Ground Station has three Raytheon Data Systems model 500 (RDS-500) minicomputers that are approximately 15 years old. These computers process telemetry data in several ways for various expendable launch vehicle programs. The data is displayed on cathode ray tube (CRT) displays, strip charts, and line printers. The RDS-500's are severely limited in memory size, and the requirements placed on these machines have outstripped their capability to do the task. All the software was written in assembly language, unique to these machines, and is not transportable. The age of the machines necessitated a switch to a state-of-the-art system, but at minimum cost.

The decision was made to switch to AMIGA microcomputers. While at first glance this may seem to be too small a machine to accomplish the task, some unique features of the AMIGA's made them ideally suited. The first advantage is cost. Microcomputers are very inexpensive. By using a networked system, as the need for computational power grows, additional computers can be added to the system at a relatively low cost. Secondly, the AMIGA's provide a capability to direct memory access (DMA) data into the computer central processing unit (CPU) memory without using any CPU cycle time. The older RDS-500's require the stealing of a machine cycle for every data word input, which uses a large amount of available machine cycle time. In the AMIGA, the entire cycle time is available for computational purposes. Thirdly, the basic computer is expandable to 9 megabytes of CPU memory instead of the 128-kilobytes capability of the RDS-500's. Fourthly, the AMIGA's are host to the "C" language. By converting all the software to "C," the software is transportable to newer machines as they become available. This conversion of the software to "C" is the greatest challenge and cost to the system.

The system is now on line, with the basic software modules working and the remaining ones

in development. The single AMIGA is capable of processing data and displaying it in the same manner as two RDS-500's. The system inputs data at a 250-kiloword rate, outputs 32 RS-170-compatible CRT displays, and has the capability of remoting the control of these displays anywhere. The system is baselined to support the Cosmic Background Explorer (COBE) mission on a Delta vehicle at Vandenberg Air Force Base in the summer of 1989.

A. J. Mackey, 853-9353

CV-DSD-1

Expendable Launch Vehicle (ELV) Payload Processing Historical Data Retrieval Study

Information about ELV payload processing at Cape Canaveral Air Force Station from 1977 to 1987 was collected in a data base and analyzed. The payloads were launched on several vehicles, but most were launched on either Delta or Atlas/Centaur. Seventy-six different launches are included in the data base, and the data was gathered from various official and unofficial documents and from interviews with engineers responsible for the processing. Both Government and private-sector payloads are included in the data base.

The analysis examined the processing in Payload Processing Facilities (PPF's), Hazardous Processing Facilities (HPF's), and at the launch pad. On the average, the larger payloads utilized PPF's about 50 percent longer than the smaller payloads and utilized the HPF's about 25 percent longer than the smaller payloads. At the launch pad, there was no difference in payload processing time. Forty-three percent of all payloads experienced problems during processing in the PPF's; this grew to 57 percent when only larger payloads were examined. The analysis also showed there was a one-in-four chance that a payload would experience a problem at the launch pad.

One objective of the analysis was to establish a data base for projecting facility utilization requirements. The analysis discovered that nearly 30 percent of all payloads required some period of quiescent storage. This was a significant statistic since it was usually an unplanned event. When launch delays were examined, the analysis showed nearly half of all payloads experienced a launch delay after arriving at the launch site. Weather was not a significant cause of launch delay, while payload or vehicle problems caused about half the launch delays.

The data base provides a good reference point for projecting facility requirements for future payloads. The data also shows that testing at the launch site is essential to mission success.

S. P. Green, 867-3374

CP-APO

Orbiter Spare Quantification Methods

An essential ingredient of successful operations at Kennedy Space Center (KSC) is Orbiter hardware availability. Availability of the hardware must not impose a constraint on the operations; to achieve this, an efficient and effective means of quantifying spares must be utilized.

An Orbiter is composed of over 200,000 line items; 50,000 of these are provisioned items. Three hundred line items make up 80 percent of the total cost of the provisioned items. Accurate sparing techniques for these items are essential.

In the past, the method used to quantify the requirement for spares was based on one formula, a probability of sufficiency (POS) equation:

$$P = e^{-K\lambda T} \sum_{n=0}^S \frac{(K\lambda T)^n}{n!}$$

P = Probability of having a spare available when needed.

K = Quantity per vehicle.

T = Repair turnaround time.

N = Number of spares on hand and due in.

λ = Number of failures per time.

The probability of having a spare available for those 300 most costly line items has been established by NASA Headquarters at 90 percent; in other words, a spare must be available nine out of ten times when needed.

This POS formula is based on four primary assumptions.

1. Individual failures of an item are independent and are a function of time.
2. The repair turnaround time (RTAT) for an item is constant.
3. The operating hours for an item are uniform in time.
4. The time between demands for an item has an exponential distribution during the normal operating period.

Due to the potential impact to KSC operations when a spare is not available, a study investigating the quantification technique for spares was conducted. In the study, each of the four primary assumptions was analyzed.

Assumption 1: This POS formula assumes that individual failures of an item are independent of each other and are a function of time (operating hours). Analysis of the failure history of various line items, however, showed that failures can be either time (operating hour) dependent or independent.

Some failures are directly related to the operating hours of the item, such as, the multiplexer/demultiplexer (MDM). For these time-dependent-type failures, one failure does not influence another failure; each individual failure is independent of the other failures.

A second category for failures is the time-independent, induced, or event-driven failures. These failures are caused by external factors on the item. The item is not designed to be subjected to these external factors during its normal operation. For example, the removal or installation of the attached hardware can cause damage to the cold-plate. Therefore, coldplate

failures are not dependent on operating hours but rather on events; thus, violating the first assumption of the standard POS formula.

Assumption 2: The POS formula also assumes the RTAT for an item is constant; however, since the RTAT, is dependent on the degree of the failure, variable RTAT's have been observed in the past. An estimate of the RTAT from the manufacturer of the item has traditionally been used in the formula. A more accurate estimate, which is based on actual data, is the average observed RTAT.

Assumption 3: Operating hours are assumed to be uniform in time; however, operating hours are dependent on numerous factors. The operating hours used in the formula are obtained from the mission planning office, which calculates the operating hours per flow. Based on historical data, a variety of factors influence operating hours, such as unanticipated retesting of items and changes in the flight rate. Therefore, operating hours have not been uniform in time and there is a high probability they will not be in the future.

Assumption 4: Typically, the life of an item can be characterized into three phases: burn-in, normal operating period, and wearout. The standard POS formula assumes the item has gone through the initial burn-in stage and is in the normal phase. It also assumes that the time between demands for the item has an exponential distribution during this phase. In actuality, however, time between demands can follow numerous distributions such as normal, exponential, gamma, Weibull, or its own unique distribution.

To determine which demand distribution is appropriate, each item must be analyzed. Demands of similar items can be combined to provide additional data points for analysis of a particular graph. These additional data points strengthen the accuracy of distribution determination.

Results: Results of the study showed that this POS formula is not always the best method to be used to quantify the requirements for spares since the four basic assumptions are not always followed; therefore, new alternative methods must be developed. For example, a method us-

ing a Monte Carlo simulation has been developed for items that do not follow the first POS formula assumption (in other words, those items that have induced or event-driven failures, such as the coldplate). This method involves four basic steps:

1. The event that caused the failure is determined.
2. Forecasting the number of times the event will occur in the future is performed.
3. The probability that the event will cause a failure is calculated.
4. The simulation program is implemented.

For the coldplate, the event that causes failures is the installation and removal of attached hardware. The number of future events is calculated as the maintenance demand rate for each attached piece of hardware multiplied by the historic operating hours. The number of problem reports written against the coldplate resulting in replacement is divided by the total number of events to yield the probability the event will cause a failure.

Finally, each future event is simulated by a computer program and by using random number generation, each event is determined as a failure or as a nonfailure. The total number of failures for all future events are calculated. The simulation is run a hundred times. The spare quantity necessary to achieve a 90-percent probability of sufficiency is obtained from the simulation runs.

Conclusions: The study showed that the POS formula is not always the appropriate technique to quantify spares. For each item, all the POS assumptions should be verified before implementing the POS technique. If an item's failures are determined to be event dependent, the Monte Carlo technique should be implemented. Additional methods and analysis of failure data are being developed and must continue to be developed to achieve the most effective and efficient means of quantifying spares.

M. M. Groh-Hammond, 867-5381 TL-FGP-4

Certification of a Microwave Landing System Using the Global Positioning System

Currently, there are seven operational Shuttle landing sites with two more sites planned. Each of these sites has one or two Microwave Landing Systems (MLS's); most having separate primary and backup systems. The accuracy of each MLS must be flight certified annually. To flight certify an MLS, an airplane flies into the area of coverage while being tracked by some location system, and the results are compared. The requirements for the location system include an accuracy of at least three times greater than the system being measured. The location system must be able to track a moving airplane and provide its position at least once per second. Finally, the system should be easily transportable since it will be moved to sites over three continents and islands, such as Guam and Hawaii.

Previously used techniques included a precision laser tracking system to record a plane's position during flight. Although the laser tracker was accurate to 0.001 degree in azimuth and elevation, it did have some limitations, including cost, size, weight, and susceptibility to damage during shipment. With the laser tracker, there was also a time limitation. Each test at a site took approximately four weeks including shipping and setup time; with seven sites to cover, it would take 28 weeks to complete all landing sites and had to be repeated annually.

A real-time display of landing system accuracy was developed utilizing the Global Positioning System (GPS). The Navstar/GPS satellite radio-based navigation system consists of a constellation of satellites orbiting the earth twice a day, monitor and control equipment, and user receivers. A user with a receiver is provided three-dimensional positioning, time, and velocity with an accuracy never before available. Currently, seven satellites provide position information a few hours each day. As the complete constellation of satellites (24) is launched, the user can receive nearly continuous position information worldwide.

In this configuration, two commercially available GPS receivers are used in a differential mode to determine a relative position between

an airplane and a reference location. A GPS reference station antenna is established above the MLS antennas. The GPS antenna receives L-band signals from at least four satellites. The received signals (nonclassified C/A code) are used to calculate the range to each satellite and then to calculate the receiver's location. The GPS receiver calculates and compares its position to a reference position entered before the test. The receiver then calculates a correction based on this comparison. This correction is broadcast once every two seconds over a 408-megahertz radio link to the airplane.

A similar receiver onboard the airplane receives signals from the same four satellites. The receiver calculates the relative position of the plane using the broadcast corrections to eliminate common mode errors.

Signals from the MLS are received from an antenna directly below the GPS antenna. Position outputs from the MLS and GPS receivers are compared in a Hewlett-Packard (HP) 9000 computer to provide a real-time display of angular errors while the airplane is in flight. These results are also digitally recorded for further processing.

The airplane flies a series of 8,000-foot radials along the runway centerline and up to a plus or minus 10-degree deviation from the centerline. To further evaluate the MLS area of coverage, approach guideslopes are flown from 4 to 1.5 degrees.

Errors of less than two meters in the relative position of the aircraft are observed using GPS during periods of good satellite geometry. This allows certification of the runway system alignment within 0.05-degree azimuth and elevation.

Transportation costs and test time have been significantly reduced by this configuration. Each Shuttle landing site was certified by the developed system. Because of the limited satellite coverage, each MLS system requires two to three days of flight tests. The test time will decrease as more satellites are launched.

The GPS receivers weigh only four pounds each. The receivers and all related equipment including the real-time display computer can be shipped with the test airplane instead of sepa-

rate shipments. A reduction in setup time is realized since each site now requires only two hours to install all the equipment.

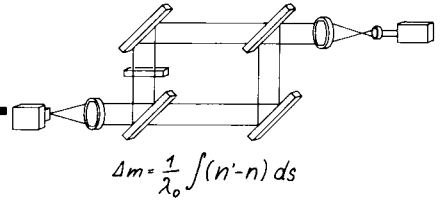
The current configuration allows the certification of other navigational aids such as LORAN or TACAN.

There will be considerable improvement to this configuration using GPS. GPS technology will improve as the system constellation and the number of users increase.

J. J. Kiriazes, 867-4068

TE-CID-3

FIBER OPTICS AND COMMUNICATIONS

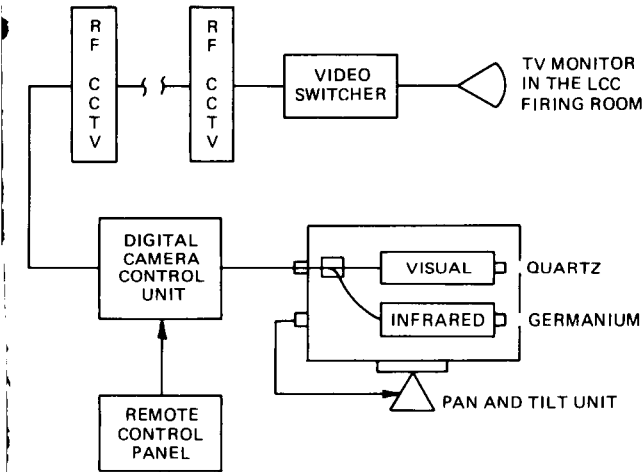


Hydrogen Detection Television Camera

A commercially produced dual imaging television camera was adapted for use in the Launch Complex 39 operational television (OTV) system to detect the presence of hydrogen fire in key locations. The basic system uses a thermal imaging camera and a standard visual camera with both images registered and overlaid to produce a standard RS-170 video output. The thermal imaging camera utilizes a noncooled pyroelectric vidicon sensitive from an 8- to 14-micron range to provide real-time thermal imaging at standard television rates. The visual camera uses a standard newvicon vidicon tube to provide the reference location of the superimposed hydrogen flame.

circuitry that operated dual lenses, allowed poling of both camera functions, and gave operators access to critical camera adjustments for better real-time performance. Adapting this unique thermal scanner and real-time visual imaging system into an imaging and display system suitable for distribution to KSC firing rooms will hopefully provide Launch Directors with an early warning of invisible fires.

The block diagram illustrates the basic system. The camera housing contains a visual camera, infrared (IR) scanner, power supplies, and interface connectors. The front plate incorporates two windows: a quartz window for the visual camera and a germanium window for the IR scanner camera. All the optical parts for the IR camera required germanium be used. The early version (used for STS-26R) of the camera system required two RS-170 video signals be fed back to the camera control unit where the two images were overlaid. The present version will overlay the two images in the camera head, thus requiring one RS-170 video path. The need for dual equalization and transmission is then eliminated. The digital camera control unit (DCCU) not only processes the video signal, but sends control voltage to both cameras by a multiconductor cable. The video combined signal is then sent over an RF closed circuit television (CCTV) cable link to the Launch Control Center (LCC) where it is distributed to the users in the Firing Room. The camera system is controlled from the LCC by an RS 232 circuit.



Hydrogen Detection Television Camera System

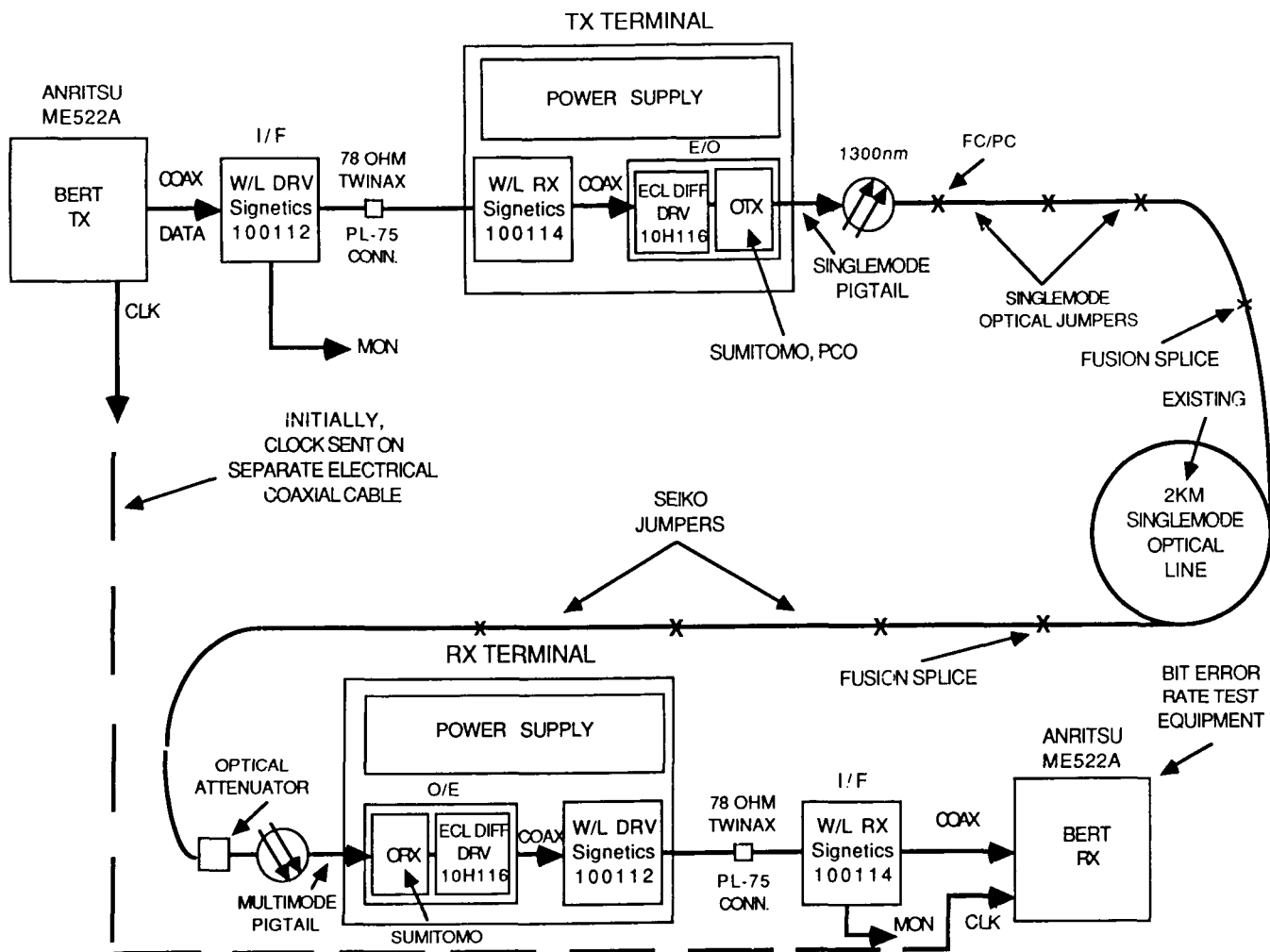
The camera was supplied in a specially designed housing which meets all the KSC electrical interface and environmental requirements. A custom digital camera control system [one camera control unit (CCU) that controls dual cameras] that allowed integration of the thermal imaging system into the OTV system was designed and implemented at Kennedy Space Center (KSC). This custom digital CCU contained

J. Kassak, 867-4548

DL-ESS-12

DC to 150-Megabits-per-Second Fiber Optic Link Development

Kennedy Space Center (KSC) has developed a fiber optic data link from DC to 150 megabits per second (Mb/s) to meet the requirement of



DC to 150 Mb/s Demonstration Link

space station module checkout in the Space Station Processing Facility and other facilities at KSC. The on-board fiber optic networks in the space station modules are 100 Mb/s fiber optic distribution data Interface (FDDI) for the data management system in each module and 150 Mb/s in the Communication and Tracking System of modules 1 and 2.

A demonstration link was developed and tested that is suitable for wideband transmission of digital data from DC to 150 Mb/s. The primary purpose of the link was to prove the feasibility of 150 Mb/s data rates over single mode and multimode fiber optic cable dependent on light source and distance.

For the initial test link in the laboratory, a single fiber optic channel was constructed for data

transmission with the clock signal being sent on a separate electrical coaxial cable. Currently, a duplicate fiber optic channel for clock transmission and a synchronizer circuit to retime the data and clock signal at the receiving terminal are being developed for use in the link.

Electrical interface circuits, utilizing 10KH and 100K ECL logic chips, were designed and bread-boarded to receive and transmit balanced and unbalanced data. These circuits were used to simulate patch panel connections and to provide an interface with the optical transmitter and optical detector.

The optical transmitter module was designed to have the capability to adapt three different light sources (1,300 nanometers); Sumitomo DM-87-2 laser diode, PCO DTX-13-L-200 laser

diode, and the Sumitomo DM-57-TA light emitting diode. The optical detector used was the Sumitomo DM-57-RA PIN photodiode module. The Sumitomo modules are DC-coupled to 250 Mb/s, and the PCO laser diode module is DC to 200 Mb/s (vendor specifications); these parameters provide wideband burst capability for the system. All modules were verified to be DC coupled and achieved data rates in excess of 250 Mb/s at a bit error rate (BER) of less than 1×10^{-9} . It was determined from the test data that the Sumitomo laser diode would have an effective range of 10 kilometers (km) and the PCO laser diode would have a range of 20 km. The Sumitomo light emitting diode could be used for multimode applications of less than 1 km. The minimum detectable level of the Sumitomo PIN photo detector was determined to be -24 dBm; slightly better than the manufacturer's specification of -20 dBm.

Currently, the test link is being upgraded to facilitate field testing in fiscal year 1989. The interface circuits are being refined, an activity detector circuit is being incorporated, an additional fiber optic clock channel is being added, a synchronizer circuit is being developed, and rack mountable transmitter/receiver terminal drawers are being manufactured to house the circuit boards and power supplies. For the field test, the transmitter/receiver terminal drawers will be installed in the Communication Distribution Switching Center (CDSC) at KSC and will use a single-mode fiber optic test loop from the CDSC to the Vehicle Assembly Building Repeater (VABR) and back, establishing a test circuit of about 13 km.

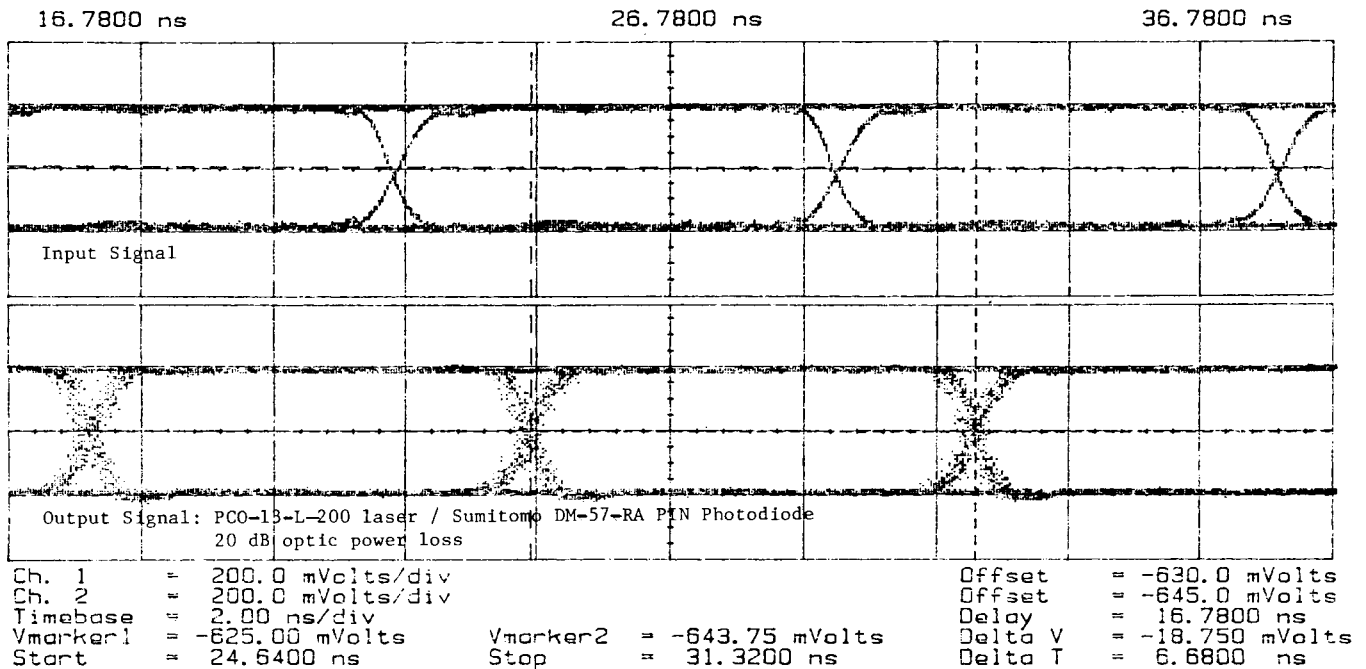
P. T. Huang, 867-4548

DL-ESS-12

Testing of the three optical sources revealed jitter percentages ranging from 6.17 to 8.50 percent at 150 Mb/s, with a free BER using an NRZ PRBS pattern. The recorded eye pattern measurements displayed consistent zero cross-over points and little waveform distortion.

Microwave Fiber Optic Link Study

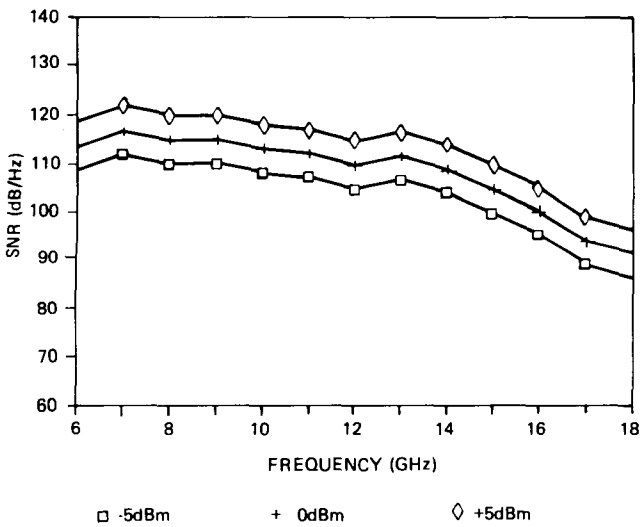
Kennedy Space Center had a contract [NAS10-11460, Small Business Innovative Research (SBIR) Phase I] with E-Tek for a feasibility and



Eye Pattern

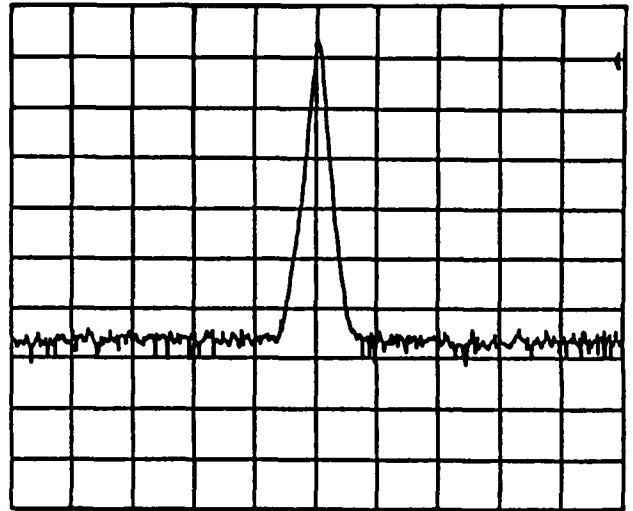
viability study of a microwave fiber optic link for C-band, X-band, and Ku-band antenna remoting application.

A prototype link (1.3-micrometer optic wavelength and 2-kilometer distance single-mode fiber) was fabricated and demonstrated. By using GTE's HFPD-15/L laser diode, PCO's pin photo detector, and a direct modulation scheme, the measured system signal-to-noise ratio achieved was 120 dB/Hz at 5 dBm optic output power.



Frequency Response of HFPD-15/L Laser Diode

RL 0.00 dBm
 ATTN 20 dB
 10.00 dB/DIV
 REFERENCE LEVEL
 0.00 dBm
 MKR NO. 1 FRQ 12.999 04 GHz
 2.60 dBm



12-GHz Signal Spectrum

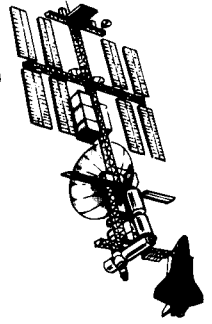
The laser diode was thermally stabilized and controlled using a precision constant-current supply designed and constructed by E-Tek. No impedance-matching network was employed between the photo detector and the post-detection amplifier. For linearity improvement, the impedance-matching circuit will be implemented into the system.

P. T. Haung, 867-4548

DL-ESS-1

ORIGINAL PAGE IS
 OF POOR QUALITY

TECHNOLOGY UTILIZATION



Alarm Processing and Diagnostic System Using NASA's Knowledge-Based Autonomous Test Engineer (KATE) Technology

A typical nuclear power plant has approximately 2,000 alarms and displays that were designed as aids to the operators; however, within minutes of a complex transient, hundreds of alarms may be activated which are more than can be optimally handled by the operator. Many of these alarms are irrelevant or contribute no significant new information to assist operators' diagnoses. The overabundance of alarms in a nuclear power plant during a transient has been identified by many electric utilities as an area in which the plant operators would like assistance. Therefore, it is desirable to develop an alarm processing and diagnostic system that could help the operator by prioritizing, simplifying, and filtering the alarms to emphasize the significant ones. The goal of this effort is to develop an alarm processing and diagnostic expert system based on technology already developed by NASA. This system will not only look at the status of alarms, but will also acquire real-time plant data from the plant process computers and then reason about the alarms and the plant data to determine which are significant alarms.

The primary objective of this project is to develop and deliver a fully functional alarm processing and diagnostic system that will receive enthusiastic acceptance from nuclear power plant control room operators. The system should reduce annunciator activity during plant transients and provide meaningful on-line advice to the operator concerning the priority of alarms.

Kennedy Space Center has developed the KATE expert system to help with Space Shuttle launch activities. KATE has the following capabilities: system monitoring, sensor signal validation, fault location and diagnosis, and automatic control reconfiguration. Using the KATE technology, this project will develop an alarm processing and diagnostic system for nuclear power plants. This system will have extensive

knowledge of the power plant, the physical processes in the plant, and the alarms. With the plant data (the status of the alarms and the knowledge of the plant), the system will prioritize the alarms for the operators. The knowledge and techniques developed for this advisory system could also be used to upgrade the plant alarm system. The combination of reasoning about the plant and the alarms will ensure a reliable identification of the significant alarms.

The second objective of this project is to deliver a model-based reasoning capability to the electric utility industry for use in developing a wide variety of monitoring, diagnostic, and control applications. To achieve this objective, the KATE system has been enhanced for widespread use. This includes additional capabilities, improved development interface, improved user interface, more efficient and structured coding, and comprehensive documentation. It is anticipated that this technology will be used not only for nuclear power plants but also for fossil power plants and for transmission and distribution systems.

The first phase of this project has documented the KATE technology, enhanced some of its capabilities, and developed a proof-of-concept demonstration of the alarm processing and diagnostics system. The proof-of-concept demonstration performs alarm prioritization on the reactor coolant pump seal injection system. The second phase, which is currently in process, will develop a full prototype system that will be tested on a full-scope training simulator of the power plant. The prototype system and its testing will be thoroughly documented to enable electric utilities to generate requirements and design specifications for an alarm processing and diagnostic system. These requirements and specifications will address both an advisory system and a system for upgrading the plant alarm

system. The displays for this system will take advantage of the human factors studies on alarm displays.

T. C. Davis, 867-3494

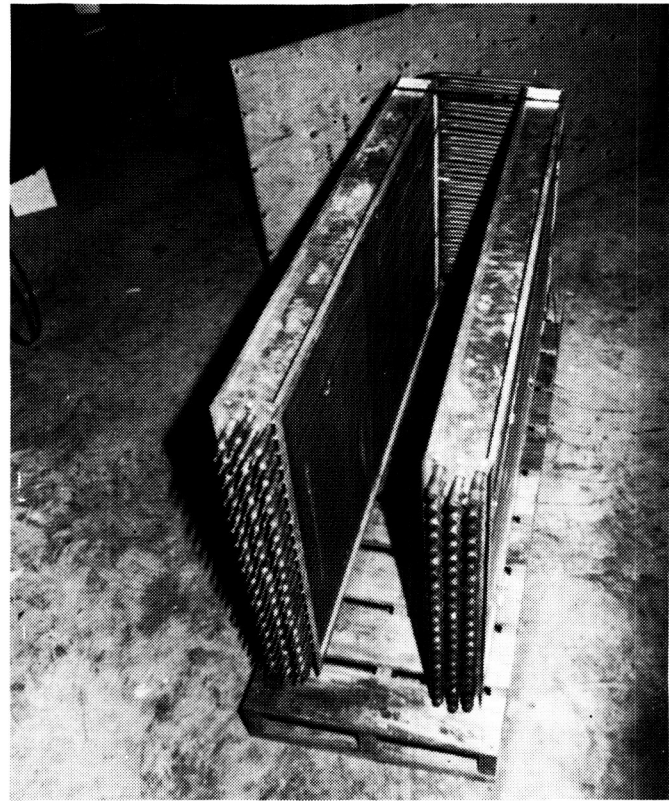
PT-AST

Feasibility Analysis of a High-Efficiency Dehumidifier/Air Conditioner Using Heat Pipes

The idea of using heat pipes between the supply air duct and the return air duct in conventional air conditioning units promises to be a cost-effective way to increase the latent heat removal capacity. This design feature is particularly attractive for subtropical climates where humidity control is essential to both industrial processes and human comfort.

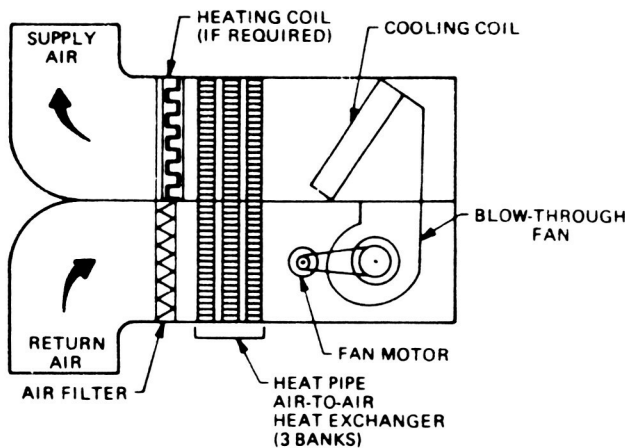
The unique aspect of the use of heat pipes is that this method allows efficient removal of sensible heat from the air approaching the evaporator and transfers the heat to the air that has passed through the evaporator, providing reheat. In essence, the heat pipes reduce the sensible load on the evaporator, drop the off-coil temperature, and significantly increase moisture removal. The goal of the project is to demonstrate a latent heat fraction of approximately 60 percent, as opposed to 20 to 30 percent which is typical of conventional units.

The principal contractor for this project is the Florida Solar Energy Center, which recently in-

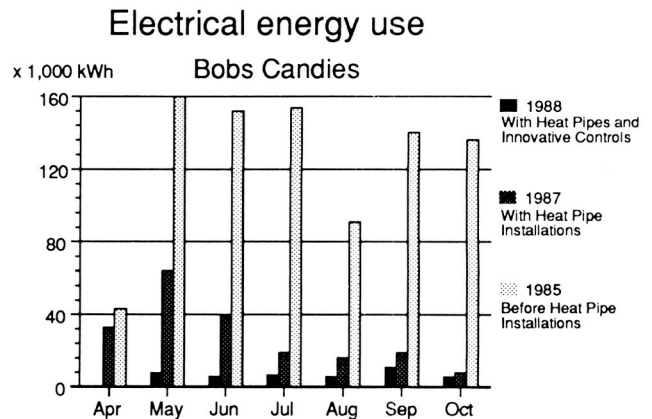


Prototype of a U-Shaped Heat Pipe

stalled a heat pipe in a warehouse for Bobs Candies in Albany, Georgia, as a demonstration project. The project, which is in cooperation with Georgia Power, has shown a 30 to 50 percent savings of electrical power. In other words, the cost of the project was recovered within the first year of operation.



Schematic of an Air Handling Unit With Three Banks of Heat Pipe Air-to-Air Exchange



Comparative Energy Use Before and After Installation of Heat Pipes and Innovative Controls

The next step of the project will be further detailed analysis to determine the actual breakdown of cost savings.

J. K. O'Malley, 867-3688

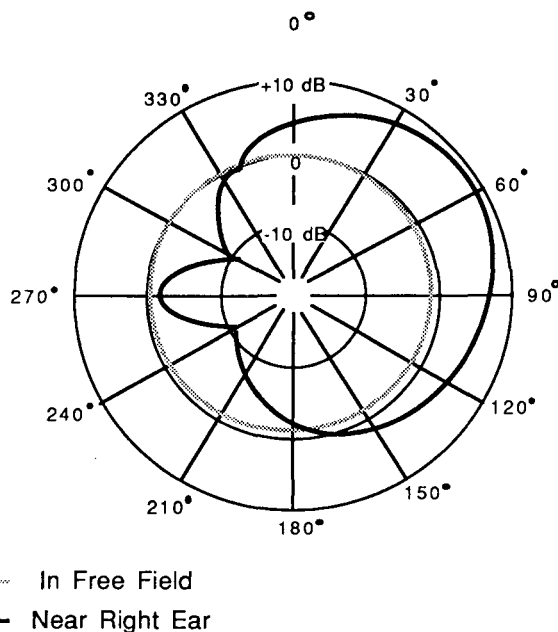
DF-FED-33

Development of a Digital Hearing Aid

The purpose of this project is to develop a digital hearing aid that will lead to improved performance of acoustic amplification for the hearing impaired. Digital hearing aid technology can provide the flexibility of adjustment and control of auditory signal processing required to better compensate for the patient's hearing impairment than is possible with conventional analog technology or even hybrid technology in which analog amplifiers and filters can be adjusted with digital logic.

A key factor in achieving an optimal fit for the patient is the acoustical interaction that occurs between the hearing aid and the patient. By incorporating the hearing aid into the fitting procedure and being able to adjust the parameters of the hearing aid remotely from a host computer (and audiometer) while the patient is wearing the aid, variables such as the acoustics of the earmold, ear, and head can be directly accounted. This allows adaptive fitting procedures to be implemented during testing that can vary the characteristics of the hearing aid.

One example of this acoustical interaction between patient and hearing aid is illustrated in the figure "Directional Sensitivity of Microphone in Free Field and Near Right Ear." The hatched curve shows the directional sensitivity of a hearing aid microphone for a 2,000-hertz tone for free field conditions. The solid curve illustrates how the directional sensitivity of the microphone is modified when it is positioned near the head at ear level. Other factors (such as the change in resonance of the ear canal when it is positioned near the head at ear level. Other factors (such as the change in resonance of the ear canal when it is occluded by the ear insert or the acoustic load imposed on the receiver by the ear impedance) also modify the transfer characteristic of the hearing aid. Although some of these factors are systematic, predictable, and time invariant and can be compensated for with fixed-filter shaping, others vary from patient to patient and



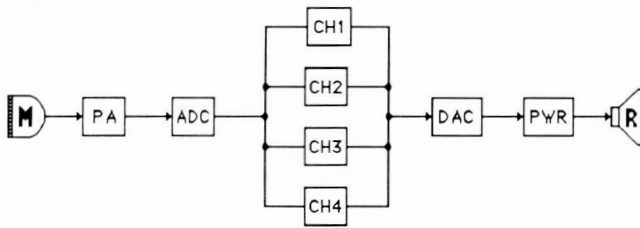
Directional Sensitivity of Microphone in Free Field and Near Right Ear

depend, in part, on the size and shape of the ear insert and its associated acoustic plumbing. These patient-dependent factors can be accounted for if the hearing aid has sufficient adjustment flexibility and if it can be worn and adjusted during the fitting procedure. There are also factors that vary over the short term; an example is sound leakage around the hearing aid back into the microphone, which can produce positive feedback and oscillation at certain frequencies.

The goal, therefore, is to develop a hearing aid that can be adjusted to compensate for a wide variety of hearing losses while taking into account all the factors that can corrupt the prescribed fit. A digital approach was chosen because of the flexibility of design that is afforded, which can include sophisticated adaptive signal processing algorithms. Low-power CMOS custom VLSI implementation has been employed to minimize power consumption. In order to use a typical hearing aid battery to power the digital hearing aid, the circuitry is being designed to operate at 1.2 volts and consume less than 2 milliwatts of power.

The figure "Functional Block Diagram of the Digital Hearing Aid" includes a microphone pre-amplifier and antialiasing filter that provides an input to the analog-to-digital converter (ADC).

ORIGINAL PAGE
BLACK AND WHITE PHOTOGRAPH



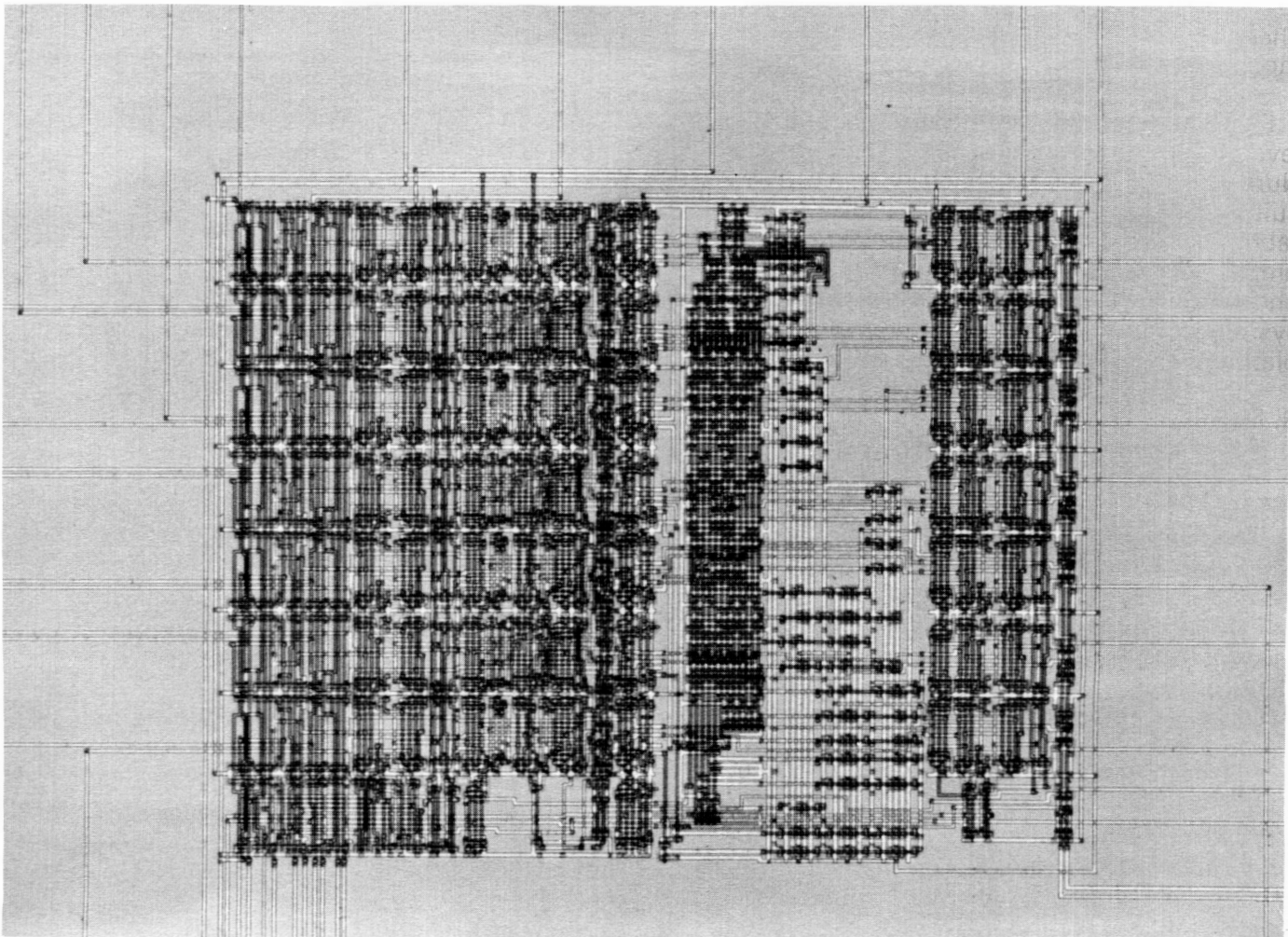
Functional Block Diagram of the Digital Hearing Aid

Following the ADC is a multichannel filter structure that is designed to provide independent adjustment of linear gain and maximum output over four different audio bands of frequencies. The control of maximum output is achieved with a minimum of harmonic distortion by incorporating a filter before and after the limiting opera-

tion. The multichannel filter structure is followed by a digital-to-analog converter (DAC) and power amplifier capable of driving the receiver (loud speaker) of the hearing aid.

Several algorithms have been designed to accommodate dynamically changing conditions of signal and ambient noise, thereby extending the operating range of the digital hearing aid over what can be achieved by conventional means. In addition, a serial port is included for communication between the hearing aid and host computer.

A key part of the multichannel filter structure is a basic cell, which is shown in the figure "Photomicrograph of Basic Multiply-Accumulate VLSI Cell," that performs the arithmetic for implementing one tap of a finite impulse response filter. This cell, which is a building block



Photomicrograph of Basic Multiply-Accumulate VLSI Cell

that can be used in constructing filter structures, includes a programmed logic array, coefficient registers, and various combinatorial logic circuitry. The cell is designed so it can be interconnected to create systolic digital filter arrays. A prototype version fabricated in CMOS consumed 10 microwatts when operated at 3 volts and a sampling rate of 12.5 kilohertz.

During 1988, progress has continued toward the ultimate goal of reducing the digital hearing aid to a VLSI chip set. The work has progressed in both the analog and digital sub-projects. The chip, whose design was started last year, has now been fabricated, tested, and incorporated into a desk-top system that employs four of the digital signal processing (DSP) chips to provide all 256 filter taps required for the four-channel DSP system. A printed circuit board version of the ADC and DAC circuitry has been completed and used in conjunction with the four-chip DSP to obtain a table-top, digital hearing aid system. The analog components were off-the-shelf commercial parts.

Further design innovations to increase the level of functional integration are in progress. Numerous analog functional building block circuits have been designed and submitted for fabrication. These include several operational amplifiers, charge pumps, comparators, current and voltage reference, and filters. A table-top system composed solely of custom circuits is planned to be built next.

R. M. Davis, 867-2780

PT-AST

EPCOT Project

The six hydroponic plant growth display racks installed in 1987 at EPCOT operated continuously during 1988. Visitors to the Land Pavilion were introduced to the plant growth methods currently being researched at NASA/KSC as a part of the Controlled Ecological Life Support System (CELSS) Breadboard Project. One of the six nutrient delivery systems was enhanced during 1988 with a state-of-the art computer control system that controls pH, flow, and temperature of the nutrient solution. This control system was the first prototype of a user-friendly menu-driven system that will be incorporated into the CELSS Breadboard Project as soon as it has been verified as operationally ready. The interaction with EPCOT has allowed NASA to evaluate this control system under operational conditions using researchers that are unfamiliar with the system to test it, to identify problems, and to generate growth data on selected crops.

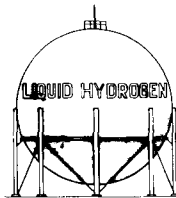
Future plans include the expansion of the nutrient delivery system control to all six tanks on the plant growth racks. This control system will allow research on plant pathogens in hydroponic systems to be initiated by researchers at EPCOT. The interaction between these researchers and the NASA staff will transfer some of this expertise to the CELSS Breadboard Project.

Dr. W. M. Knott, 853-5142

MD-RES-L

ORIGINAL PAGE IS
OF POOR QUALITY

CRYOGENICS



Two-Phase Pressure Drops in Developing and Fully Developed Pipe Flow of Dispersed Liquid/Vapor Mixtures Under Zero-Gravity Environment

The increased operating power needed for future space applications requires more efficient thermal transport techniques. Two-phase loops have been suggested for possible use on the Space Station and future spacecraft. In comparison with a single-phase loop, the two-phase system operates at considerably smaller flow rates and maintains a tighter temperature control with a still higher heat transfer coefficient. Design of the two-phase heat transfer systems for space applications requires a knowledge of the pressure drop and heat transfer under reduced gravity conditions.

Under a contract with Kennedy Space Center, the University of Illinois has performed a series of tests with equal density immiscible liquids to simulate zero-gravity (0-g) two-phase flow. The objective of the tests is to evaluate frictional pressure drop characteristics of developing and fully developed pipe flow of dispersed liquid/vapor mixtures under a 0-g environment. The findings are:

DEVELOPING FLOWS:

The displacement effect of bubbles of growing size and number in liquid/vapor flows at 0-g is simulated by the injection of benzoate at the pipe wall in a direction normal to the pipe axis. Experiments showed that the pressure drop in water/benzoate flows with wall injection of benzoate is the same as that in a water-only flow with an identical wall injection as long as the water/benzoate flow is dispersed. The pipe Reynolds number, Re , and the inlet and exit volume fraction of the benzoate, α_i and α_e , used in experiments are:

Re	Inlet α_i	Exit α_e , Percent
10,000	0	6.5, 18.9, 31.4, 39.9
15,000	0	5.8, 20.8, 30.5
25,000	0	3.5, 12.5, 18.3

The water/benzoate flow was found to consist of dispersed benzoate droplets, except for $\alpha_e = 31.4$ and 39.9 percent at $Re = 10,000$ for which the mixture flow was in the annular flow regime. In water-only flows, α_e is simply the ratio of the injected water flow rate to the total flow rate. The foregoing experimental finding combined with theoretical analysis leads to the conclusion that the two-phase pressure drop in steady, turbulent, developing flows of a liquid/vapor mixture with dispersed bubbles in straight conduits of constant cross section under 0-g is the same as that on earth, due to the liquid alone, but with wall injection of the liquid at a rate producing a displacement effect equal to that of bubbles of growing size and number.

FULLY DEVELOPED FLOWS:

Theoretical analysis is based on one-dimensional, area-averaged momentum and mass conservation equations. Experimental simulation is accomplished by using neutrally buoyant n-butyl benzoate drops in water. Pressure drop measurements have been made for the water benzoate flow covering:

1. Pipe Reynolds number (based on combined flow rate, hydraulic diameter, and kinematic viscosity of water): 15,000 to 84,000
2. Benzoate volume fraction: 0.006 to 0.35
3. Benzoate drop size: less than 1 to 30 millimeters

It was found that:

1. The two-phase frictional pressure gradient in a steady, fully developed, turbulent flow

of water containing neutrally buoyant benzoate droplets in a straight duct is the same as that due to water alone flowing at a volumetric rate equal to that of water and benzoate combined. This is true irrespective of the volume fraction and the size of drops as long as the flow is dispersed.

2. The dynamics of mixture flow containing neutrally buoyant dispersed phase is unaltered by changes in volume fraction and size of the dispersed phase. The power spectra of the flow-induced wall pressure fluctuations, due to water alone and due to the mixture flow of various volume fractions of the dispersed phase covering a wide range of drop sizes, exhibit only minor differences.

The conclusion reached from experimental findings combined with theoretical analysis is that the frictional pressure gradient in steady, fully developed, turbulent, liquid/vapor flow with dispersed bubbles in straight conduits of constant cross section under O-g is the same as that on earth, due to the liquid alone flowing at a volumetric rate equal to that of liquid and vapor combined.

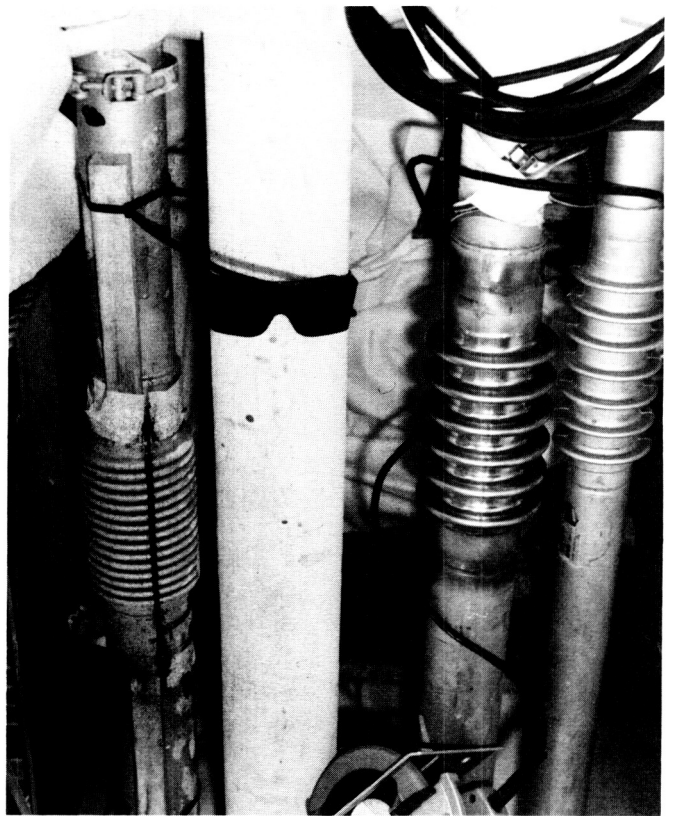
F. N. Lin, 867-4181

DM-MED-11

Clamshell Bellows Repair Technique With Hastelloy C-22 Material

In April 1987, the Fuel Cell Servicing System of Launch Complex 39B was found to have many of its 30 outer bellows leaking because of corrosion damage. The corrosion had been caused by hydrochloric acid generated from dew and rain reacting with the solid rocket booster (SRB) residue. The SRB dust contains aluminum particles that accelerate corrosion by deoxygenating the metal under the particles, eventually producing pitting corrosion.

The solution to the leaking bellows problem was to replace all the bellows in the system with a clamshell design. The clamshell technique allows a bellows to be installed on the vacuum-jacketed line in the field without cutting the inner line. The clamshell consists of a formed bellows which is bisected longitudinally. The clamshell bellows are put into place on the outer line with two longitudinal welds along the bellows and a circumferential weld at each end.



Clamshell Bellows Repair at Launch Complex 39B

(The convolute pitch must be approximately 1 inch or more to allow for the longitudinal weld.)

The stainless steel material of the previous bellows performed unacceptably in the corrosive environment of Kennedy Space Center. A new alloy was therefore needed for the thin-wall bellows application. An extensive corrosion study was conducted for 19 different alloys. The superior choice was determined to be Hastelloy C-22 (with a corrosion rate 50 times less than stainless steel and no tendency toward pitting corrosion). Hastelloy C-22 is easily welded to stainless steel and is the ideal corrosion-resistant alloy for the thin-wall bellows application.

The new clamshell method, combined with the use of the Hastelloy C-22 material, will allow the cryogenic piping designer to incorporate outer bellows without the concern of leaks due to corrosion. The repair technique and material combination will also provide dramatic reductions in maintenance.

W. I. Moore, 867-7777
J. E. Fesmire, 867-3313

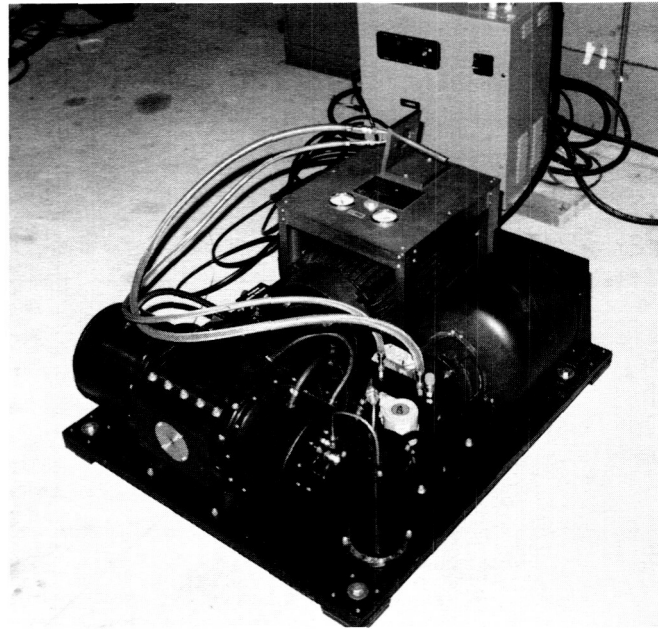
DM-MED-4
DM-MED-43

Temperature-Sensitive Variable-Area Joule-Thomson Expansion Nozzle and Cryocooler Development Program

A nitrogen cryogenic refrigerator having a variable area Joule-Thomson expansion valve capable of automatically adjusting with the temperature of the input nitrogen was developed for Kennedy Space Center under the Small Business Innovative Research (SBIR) program by General Pneumatics Incorporated Western Research Center.

The valve liquifies the nitrogen through isenthalpic expansion. The Joule-Thomson valve features a tapered annular expansion orifice, resulting in virtually clog-free operation because of a larger surface area. It uses dissimilar metals to vary the opening position.

The valve was mounted in a compression loop with a compressor, which provides the required nitrogen compression for water cooling prior to expansion. The device will be used in conjunc-



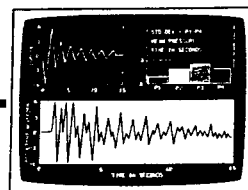
Joule-Thomson Expansion Nozzle and Cryocooler

tion with other cryogenic tests to be performed in the cryogenic laboratory.

F. S. Howard, 867-4181

DM-MED-1

ORIGINAL PAGE
BLACK AND WHITE PHOTOGRAPH



DIGITAL ELECTRONICS

Partial Payload Checkout Unit

The Partial Payload Checkout Unit (PPCU) is being developed at Kennedy Space Center for the Space Transportation System (STS) Payload Operations Directorate by the Engineering Development Directorate (DE). The PPCU is a UNIX-based system that will be used for interface and functional testing of partial payloads (non-Spacelab scientific payloads) prior to integration into the Orbiter. The PPCU will provide simulated Orbiter-to-payload interfaces and services. The PPCU will also provide simulated Payload Operations Control Center (POCC) services, including uplink commands and telemetry processing.

The PPCU is a distributed system consisting of five subsystems connected by four types of ethernet buses. The five subsystems are the Data Acquisition Subsystem (DAS), the Application Processor Subsystem (APS), the Display Processor Subsystem (DPS), the Archive and Retrieval Subsystem (ARS), and the Data Base Subsystem (DBS). This modular approach provides subsystem independence and allows any single subsystem to be upgraded without changes to other subsystems. The PPCU is also designed for system expansion and vendor independence. The custom, front-end interfaces are physically and logically separated from the generic system services and user interfaces. This allows for the maximum use of commercial off-the-shelf hardware and software.

The DAS front-end subsystem includes six Data Acquisition Modules (DAM's) and two Data Acquisition Processors (DAP's). A DAM consists of a VME chassis with a Motorola MVME147 single-board computer and one or more custom interface cards developed by DE. The custom cards which process and filter high-speed payload telemetry data are built around a parallel processing architecture using INMOS T800 transputers. Data and commands are passed between other subsystems and the DAM's through a DAP, which performs data concentration and command routing. The DAP is a Hewlett-Packard

(HP) 9000 Series 800 Model 825S computer. The DAM's and DAP's are connected by ethernet.

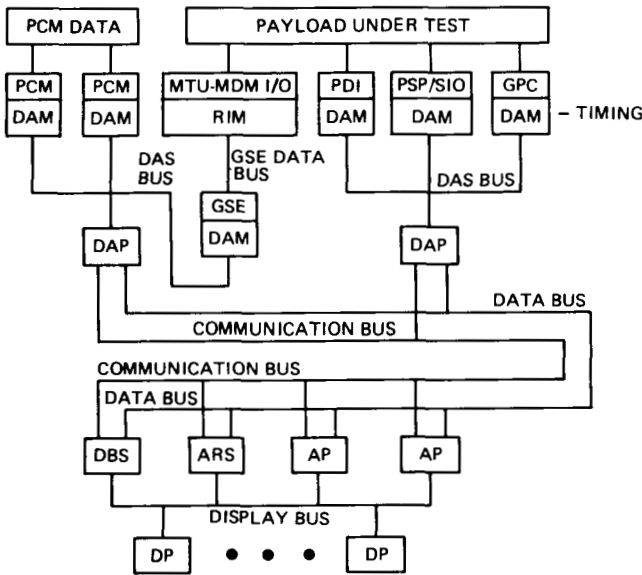
Telemetry data from the DAS is transmitted to other subsystems over an ethernet called the Data Bus. In order to support higher throughput, data is transmitted in only one direction over this bus. Commands and status messages are sent over another ethernet called the Communication Bus.

The APS consists of two Silicon Graphics IRIS-4Server-8 computers. The major functions of the APS include maintaining the measurement page set and system security, providing an environment for user application program execution, and supplying the interface between the display processors (DP's) and the DAS.

The DPS consists of six Silicon Graphics Personal IRIS 4D/20 workstations. The DP provides the user interface to the PPCU system. The DataViews software package by Visual Intelligence Corporation provides the windowing environment and the capability to link screen objects to incoming data measurements. The DPS is connected to the APS, DBS, and ARS through the Display Bus ethernet.

The ARS is an HP 9000 Series 800 Model 825S computer. The ARS archives all data packets from the Data Bus and the Communications Bus. The data is recorded on an optical disk for permanent storage and on a magnetic disk in a circular buffer for near-real-time retrieval.

The DBS is also an HP 9000 Series 800 Model 825S computer and utilizes the Informix-SQL relational database management software. The DBS hosts and provides configuration management for the system database and support software for all the subsystems. The DBS also builds the tables required for each subsystem and downloads these tables and system program loads during system initialization. In addition, the DBS performs retrieval and postprocessing of data archived by the ARS.



PPCU System

The PPCU represents the first system based upon this architecture. Future systems that will utilize the same architecture include the Space Station Test, Control, and Monitor System (TCMS) and the Space Shuttle Checkout, Control, and Monitor System (CCMS) II, which is part of the Launch Processing System. The commonality among these systems will allow the cost of spares, maintenance, and sustaining engineering to be shared among several programs. The users and operators will benefit since the systems will have a consistent user interface and set of system services.

R. M. Ferguson, 867-3811
J. E. Sudermann, 867-3466
E. G. Sherrill, 867-3646

DL-DSD
CS-EED-31
CP-FGO

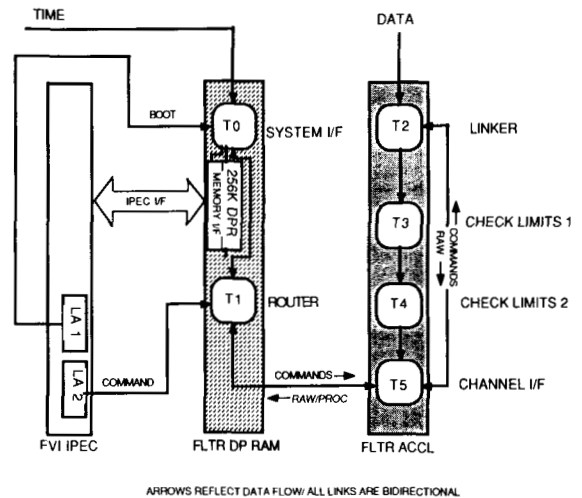
High-Speed Data Filter

The Engineering Development Directorate (DE) has developed a set of two VME cards as part of the Generic Checkout System (GCS) for the purpose of processing telemetry and data from flight or ground support equipment. The Filter Accelerator Card performs realtime processing of the data, which includes data compression, limit checking, linearization, engineering units conversion, and other data manipulations. The Filter Dual Port RAM Card provides an interface

from the filter function to the system through block of dual-ported memory.

The Filter Accelerator Card has four transputers, each with 256 kilobytes of dedicated fast static RAM. The transputers are connected by 20-megabit links in a pipelined array. In addition, the input transputer has a link connected to the output transputer of the pipe for the purpose of passing raw data for recording. It is in this pipeline that the data filtering occurs. The first transputer in the pipe links raw data to measurement descriptor tables; the second transputer processes discrete measurements and digitizes patterns; and the third processes analog measurements and those requiring format or engineering units conversion. The last transputer in the pipe handles channel interface function such as generating measurement identifiers for processed data that the Generic Checkout System can recognize and converting command requests from the system into measurement descriptor table (MDT) requests that the Filter Accelerator Card can process. Tables required by a particular process will reside in RAM of the responsible transputer. Filter Accelerator Card can be configured in parallel for processing additional channels simultaneously.

The Filter Dual Port RAM Card has two transputers, each with 256 kilobytes of dedicated fast static RAM. One transputer also has access to 256 kilobytes of static RAM dual ported to another microprocessor (Motorola 68010) on VME bus interface card. The first transputer



Configuration of Filter Function Cards

serves as a communications router for commands, raw data, and processed data for multi-channel configurations. The second transputer, serving as the system interface, maintains health status of the filter cards, builds time-stamped packets of raw, processed, and command response data and stores the packets into the dual port memory for subsequent transmission over the Ethernet network.

The design currently being implemented will be utilized as part of the Partial Payload Checkout Unit (PPCU) System to be installed in the cargo processing area of the Operations and Checkout Building at Kennedy Space Center. The system is expected to be installed and operational by January 1990 and will be used for verification and integration of payloads prior to installation in the Space Shuttle Orbiter.

R. B. Hanson, 867-3366

DL-DSD-12

Generic Checkout System (GCS)

As new programs such as Space Station evolve, there arises need for new control and monitor equipment to support development and operational phases. Current systems are either inadequate or overloaded. Existing control and monitor equipment supporting programs like the Shuttle also are in need of upgrade. Even though these programs utilize diverse technologies, there is much commonality in the control and monitor requirements. Rather than continue developing program-unique checkout systems, Engineering Development Directorate has elected to take advantage of the commonality between programs and develop a modular, general purpose, and upgradeable checkout system usable for new and old programs.

Based entirely on commercial, off-the-shelf components, a flexible and expandable architecture was developed. Strict adherence to standards has been followed for hardware, software, and protocols. A common operating system platform (UNIX) was also chosen for all processors, which provides a multivendor environment that can be easily upgraded and maintained. The system is composed of the following subsystems.

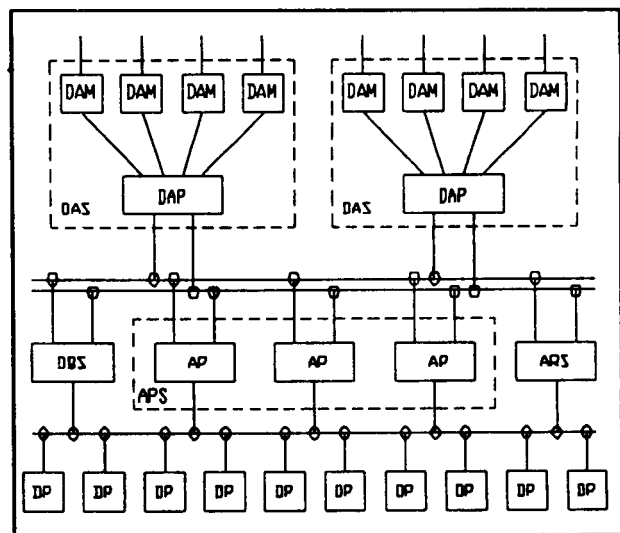
Data Acquisition Subsystem (DAS): The DAS consists of VME-based Data Acquisition Mod-

ules (DAM's) that do all common data dependant processing, such as linearization, significant change checking, and engineering units conversion with the aid of transputer-based data processing cards. Because of the VME standard, virtually any interface can be supported, most being available off-the-shelf. The DAM's are connected together and controlled by Data Acquisition Processors (DAP's). The DAP's provide a data concentration and broadcast function as well as reactive control sequence execution.

Application Processor Subsystem (APS): APS consists of one or more application processors (AP's) that act as a data buffer for user applications and displays. The data image is constantly updated and is available in shared memory for all users. The AP also provides access control for commands and data, allowing only authorized users access to proprietary data or to commands. The AP is a secure environment where only validated programs can be executed.

Archive and Retrieval Subsystem (ARS): The ARS is simply a recording subsystem that archives all data and commands that are processed by the system. It consists of one or more mini-computers with optical disk drives.

Display Processor Subsystem (DPS): The DPS consists of one or more color graphic workstations. They provide an object-oriented, real-time graphic interface to the user. This allows the user to interact without the typical software development burden. The user can also execute



Generic Checkout System

any type of local programs at the workstation without endangering the test article because of the access controls and prerequisites built into the AP.

Data Base Subsystem (DBS): The DBS consists of one or more large-scale minicomputers with a large amount of mass storage and optical disk drives. This subsystem provides all of the off-line support required to build the necessary measurement and command descriptor tables for the DAM's. It also provides all of the configuration management functions for the system. Data retrievals and analysis are also supported by the DBS.

R. D. Luken, 867-2977

DL-DSD-1

High-Speed Pulse Code Modulation (PCM) Processing System

As PCM data rates continue to increase, conventional circuits are becoming too slow and/or require too much physical space for efficient processing. The problem is being approached at the Kennedy Space Center by developing new designs based on large-scale integration (LSI) circuits. A new design being developed for payload processing utilizes a high-speed correlator integrated circuit, produced by the TRW Corporation for synchronizing pattern recognition, and

several Transputer integrated circuits, produced by the INMOS Corporation for high-speed parallel processing.

A prototype system was designed utilizing VME bus architecture running under the UNIX (AT&T Corporation) operating system that is capable of establishing frame and subframe synchronization and processing payload data at rates up to four million bits per second. The correlator integrated circuit replaces a large array of exclusive "or" gates and associated shift and storage registers with a single integrated circuit. The Transputers implement, with minimal external circuitry, a fast and powerful central processing unit (CPU) that, because of its inherent parallel processing capability, is ideally suited for processing PCM data. The Transputers expand processing capability almost linearly at approximately five million instructions per second (MIPS) per Transputer.

The design currently being developed will be used as part of the Partial Payload Checkout Unit (PPCU) system to be installed in the cargo processing area of the Operations and Checkout Building at Kennedy Space Center. The system is expected to be operational by January 1991 and will be used for verification and integration of payloads prior to installation into the Space Shuttle orbiter.

W. M. Prince, 867-3314

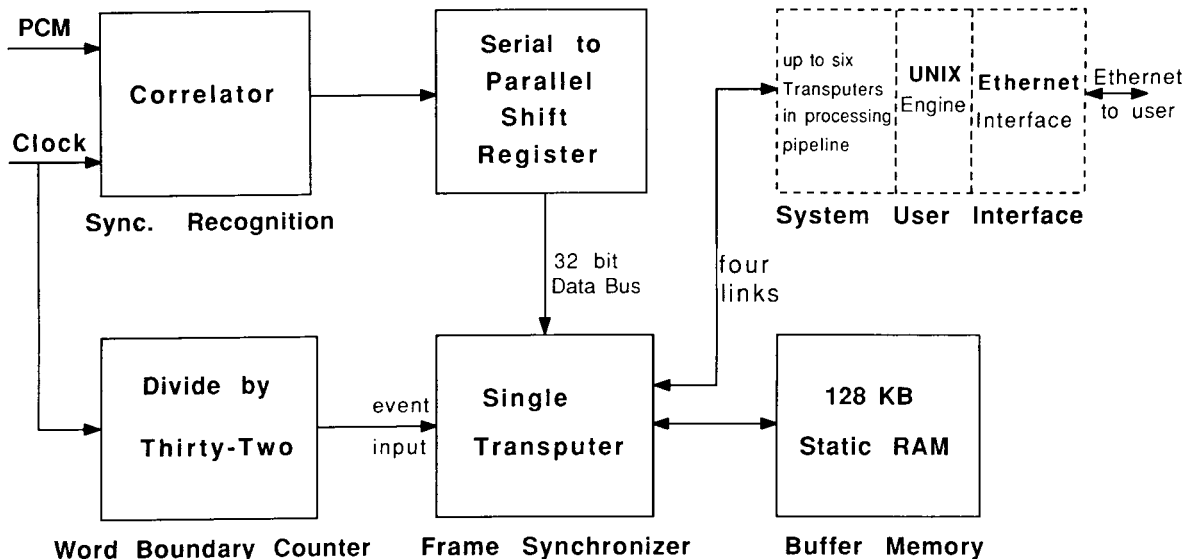
J. J. Escoffier, 867-3314

R. B. Hanson, 867-3366

DL-DSD-

DL-DSD-

DL-DSD-1



PCM Processing System

Manchester Interface for VME Bus

Tasked with developing a checkout system for Orbiter payloads [Partial Payload Checkout Unit (PPCU)], the Engineering Development Directorate at Kennedy Space Center developed a VME card set that communicates with a Manchester data bus. This card set was designed to be a general-purpose interface for Manchester data and meets the requirements for the Orbiter data bus and ground support equipment (GSE) data bus as defined for the PPCU.

The features of the card set are:

1. Stand-alone central processing unit (CPU) for front-end interface control
2. Variable number of bits from 8 to 24
3. Programmable synchronization on a word-by-word basis
4. Input/output program execution offloaded from front-end CPU

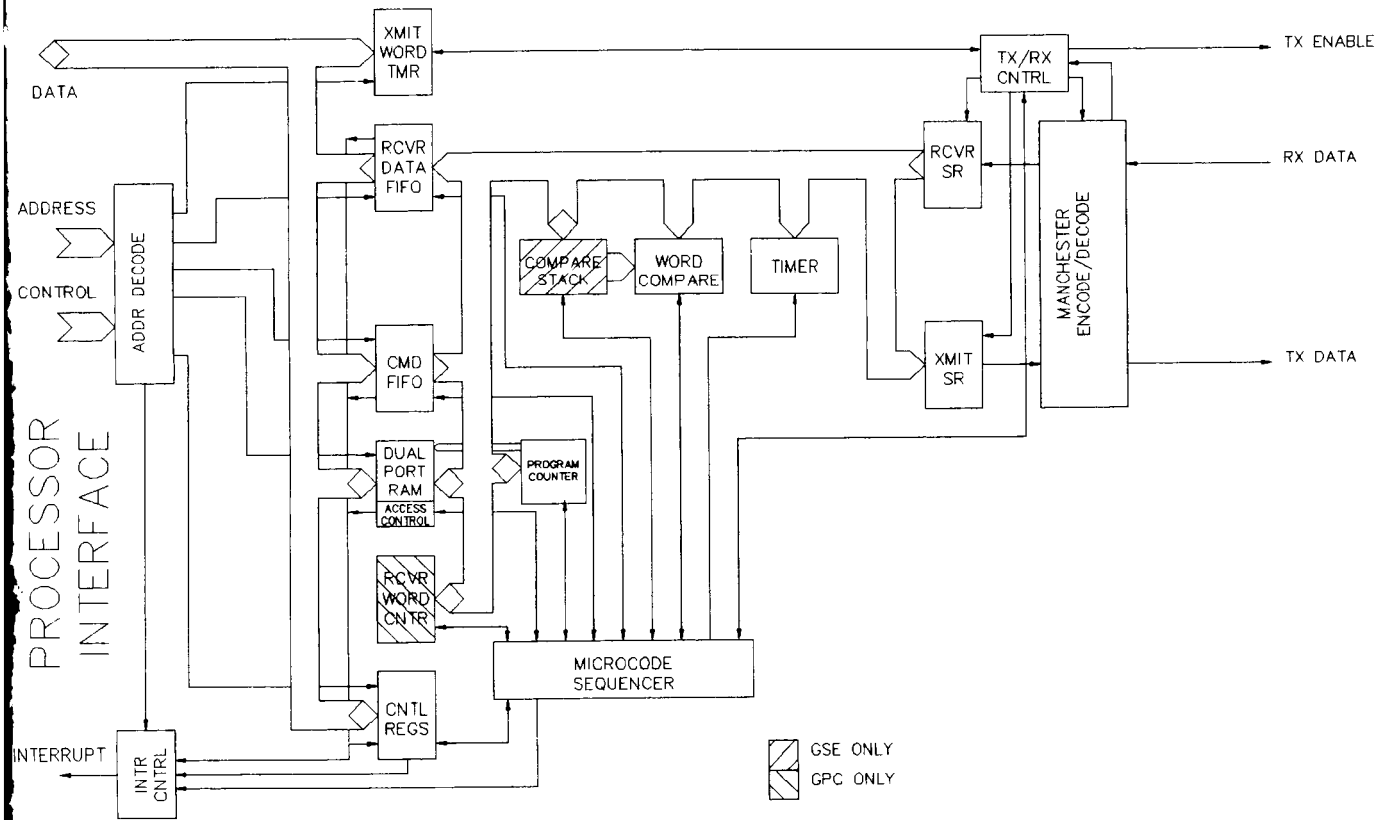
5. Timeout detection with timeout value changeable in real time
6. Input data compare and mask capability

The card set was developed using programmable gate arrays and programmable logic devices that allow maximum capability to be provided in a minimum of space. The gate arrays also allow some card functions to change during initialization if desired by the user.

The design currently being developed will be utilized as part of the PPCU system to be installed in the cargo processing area of the Operations and Checkout Building at the Kennedy Space Center. The system will be operational in January 1990 and will be used for verification and integration of payloads prior to installation into the Space Shuttle Orbiter.

J. M. Lunceford, 867-3842

DL-DSD-11



Manchester Data Bus Interface Card Block Diagram



MECHANISMS

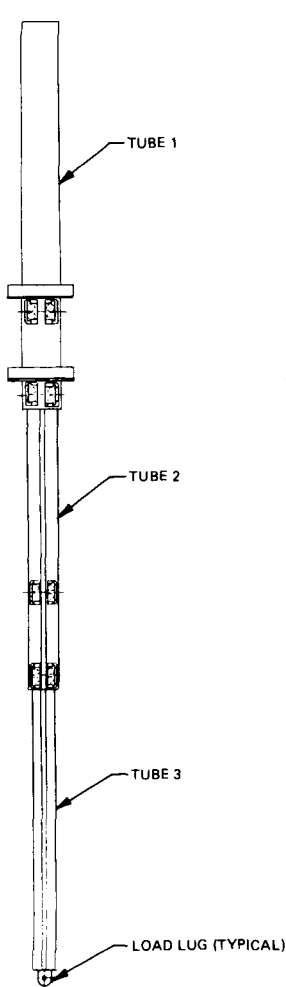
Telescoping Tube

Kennedy Space Center has been in the process of developing a telescoping tube to provide lateral and/or torsional support to access platforms and other equipment, such as the Orbiter Processing Facility payload bay access buckets and the Orbiter and platform wind restraints at the Mate/Demate Device. The telescoping tubes should have many future applications including support for fluid connections and servicing equipment.

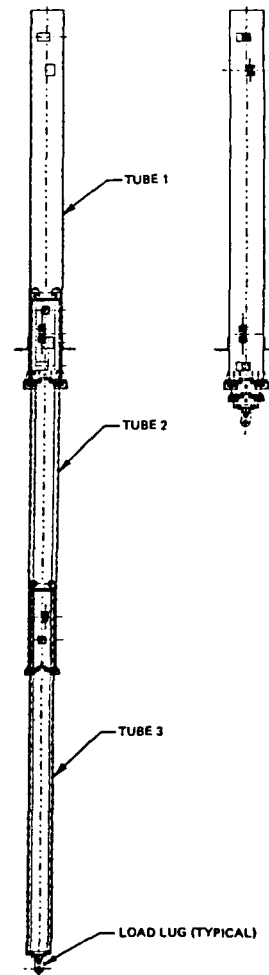
Two types of telescoping tubes have been designed and fabricated for testing. One tube (shown in the figure "Precision Telescoping Tube") is designed to support 500 pounds with high precision and stiffness. The other tube (shown in the figure "High-Strength Telescoping Tube") to support 1,500 pounds with low precision and stiffness. The telescoping tubes are presently being tested at the Launch Equipment Test Facility at the Telescoping Tube Test Fixture. Tests on the high-precision telescoping tube have met or exceeded the design criteria.

A. C. Littlefield, 867-7585

DM-MED-3



Precision Telescoping Tube



High-Strength Telescoping Tube

ORIGINAL PAGE IS
OF POOR QUALITY

TELESCOPING TUBE TEST FIXTURE

CONTROL ROOM

Launch Equipment Test Facility

0-2

PROJECT REFERENCE DATA

ITEM	RESPONSIBLE INDIVIDUAL	PARTICIPATING ORGANIZATION	NASA HEAD-QUARTERS SPONSOR*
<u>INSTRUMENTATION AND HAZARDOUS GAS</u>			
The Test and Evaluation of a Chemiluminescent Propellant Vapor Detection System	J.C. Travis, W.R. Helms 867-4438 DL-ESS-31	Naval Research Laboratory (Dr. J. Wyatt) (S. Rose-Pehrsson)	OSF
Remote Analysis of Monomethylhydrazine Using High-Flow Sampling	J.C. Travis, W.R. Helms 867-4438 DL-ESS-31	Naval Research Laboratory (S. Rose-Pehrsson) GEO Centers, Inc. (P. Taffe)	OSF
Evaluation of Electrochemical Hypergolic Fuel Vapor Detector Cells	J.C. Travis, W. R. Helms 867-4438 DL-ESS-31	Naval Research Laboratory (S. Rose-Pehrsson) GEO Centers, Inc. (K. Crossman)	OSF
Color Chemistry for Hydrazine Detection	J.C. Travis, W. R. Helms 867-4438 DL-ESS-31	Naval Research Laboratory (S. Rose-Pehrsson) GEO Centers, Inc. (P. Taffe)	OSF
Field Evaluation of a Quantitative Hydrazine Sampler	J.C. Travis, W. R. Helms 867-4438 DL-ESS-31	Naval Research Laboratory (S. Rose-Pehrsson) GEO Centers, Inc. (P. Taffe)	CDDP
Detection of Hypergolic Vapors Using Ion Mobility and Field Domain Ion Mobility Spectrometry	P.A. Mogan, W.R. Helms 867-4438 DL-ESS-31	Femtometrics, Inc. (Dr. W. D. Bowers)	OCP
Hydrogen Laser Monitoring System (HLMS)	M.A. Nurge, W.R. Helms 867-4438 DL-ESS-31	Spectral Sciences, Inc. (Dr. S. Adler-Golden)	OCP
Multispectral Imaging of Hydrogen Fires	J.D. Collins, W.R. Helms 867-4438 DL-ESS-31	Boeing Aerospace Operations, Engineering Support Contract (Dr. S. Gleaman) (Dr. R. Youngquist) (G. Rowe)	CDDF

ITEM	RESPONSIBLE INDIVIDUAL	PARTICIPATING ORGANIZATION	NASA HEAD-QUARTERS SPONSOR*
Remote Detection and Characterization of Fugitive Hydrogen by a Raman LIDAR System	M.A. Nurge, J.D. Collins, W.R. Helms 867-4438 DL-ESS-31	Computer Genetics Corporation (Dr. B. Caputo)	
Characterization of a Turbo-molecular-Pumped Magnetic Sector Mass Spectrometer	J.D. Collins, W.R. Helms 867-4438 DL-ESS-31	University of Puerto Rico at Mayaguez (Dr. N. K. Mehta)	OSF
Advanced Hazardous Gas Detection System (AHGDS)	J.D. Collins, W.R. Helms 867-4438 DL-ESS-31	Naval Research Laboratory (Dr. J. Wyatt)	OSF
Bidirectional Flow Meter	J.E. Fesmire 867-3313 DM-MED-43		OSF
Chemiresistors for the Detection of Hydrazine and Nitrogen Dioxide	J.D. Collins, W.R. Helms 867-4438 DL-ESS-31	Naval Research Laboratory (S. Rose-Pehrsson)	OSF
Toxic and Flammable Gas Detectors	P.A. Mogan, W.R. Helms 867-4438 DL-ESS-31	NASA, White Sands Test Facility (Dr. H. Johnson)	OSF
Colorimetric Hydrazine Dosimeter Badge for Personnel Monitoring	J.C. Travis, W.R. Helms 867-4438 DL-ESS-31	GMD Systems, Inc. (Dr. G. Moore)	OSF
Fast-Response Instrumentation Van	F.N. Lin 867-4181 DM-MED-11		OSF
<u>MATERIALS SCIENCE</u>			
Protective Coating Systems for Repaired Carbon Steel Surfaces	L.G. MacDowell 867-2906 DM-MSL-2		OSF
Study of Thermal Sprayed Metallic Coatings for Potential Application on Launch Complex 39 Structures	P.J. Welch 867-4614 DM-MSL-2		OSF

ORIGINAL PAGE IS
OF POOR QUALITY

ITEM	RESPONSIBLE INDIVIDUAL	PARTICIPATING ORGANIZATION	NASA HEAD-QUARTERS SPONSOR ³
Development of New Flooring Materials for Clean Rooms and Launch Site Facilities	C.J. Bryan 867-4344 DM-MSL-2		OCP
Conductive Organic Polymers As Corrosion Control Coatings	K. G. Thompson 867-4344 DM-MSL-2	Femtometrics, Inc. (Dr. W. D. Bowers)	OSF
Protective Coating Systems for the Space Transportation System (STS) Launch Environment	L.G. MacDowell 867-2906 DM-MSL-2		OSF
Ignition of Metals in High-Pressure Oxygen	C.J. Bryan 867-4344 DM-MSL-2		OSF
Permeability of Polymers to Organic Liquid and Condensable Gases	C.J. Bryan 867-4344 DM-MSL-2		OSF
Improved Bubble-Point Test Method	P.J. Welch 867-4614 DM-MSL-2		OSF
Electrically Conductive Polymer Applications	K. G. Thompson 867-4344 DM-MSL-2		OSF
Thermal Sprayed Cathodic Protection for Steel Structures	P.J. Welch 867-4614 DM-MSL-2		OSF
Corrosion of Convolute Metal Flexible Hoses	L.G. MacDowell 867-2906 DM-MSL-2		OSF
<u>ROBOTICS</u>			
Six-Degree-of-Freedom (6-DOF) Robot Target Tracking in KSC's Robotic Applications Development Laboratory	L. Shawaga 867-3402 DL-DSD-32		CDDF
Robotic Automation in the Controlled Ecological Life Support System (CELSS)	S.M. Hauss 867-4156 DM-MED-12		OSF

ORIGINAL PAGE IS
OF POOR QUALITY

ITEM	RESPONSIBLE INDIVIDUAL	PARTICIPATING ORGANIZATION	NASA HEAD-QUARTERS SPONSOR*
Robotics Applications Development Laboratory (RADL)	V. L. Davis 867-4156 DM-MED-12		OSF
<u>ATMOSPHERIC SCIENCE</u>			
Thunderstorm Weather Forecasting Expert System	A. E. Beller 867-3224 DL-DSD-22		OSF
Atmospheric Science Instrumentation Laboratory (ASIL)	R.P. Wesenberg 867-4438 DL-ESS-31		OSF
Clear-Air Wind-Sensing Doppler Radar	R.P. Wesenberg 867-4438 DL-ESS-31	University of Wisconsin, Stout Air Force Geophysical Laboratory	OSF
Lightning Tower Measurements System	R.P. Wesenberg 867-4438 DL-ESS-31	Boeing Aerospace Operations, Engineering Support Contract (P. M. Mulligan)	OSF
Lightning Hazard Detection and Warning	R.P. Wesenberg 867-4438 DL-ESS-31	University of Arizona Institute of Atmospheric Physics Boeing Aerospace Operations, Engineering Support Contract	OSF
Rocket-Triggered Lightning	W. Jafferis 867-4438 DL-ESS-31	Boeing Aerospace Operations, Engineering Support Contract (R. A. Sannicandro) (J. R. Stahmann)	OSF
Lightning-Induced Effects	W. Jafferis 867-4438 DL-ESS-31	Boeing Aerospace Operations, Engineering Support Contract (J. R. Stahmann) (R. A. Sannicandro) (M. W. Brooks)	OSF

ITEM	RESPONSIBLE INDIVIDUAL	PARTICIPATING ORGANIZATION	NASA HEAD-QUARTERS SPONSOR*
Electric Field Measurements Aloft	W. Jafferis 867-4438 DL-ESS-31	Boeing Aerospace Operations, Engineering Support Contract (J. R. Stahmann) New Mexico Institute of Mines and Technology (W. Weinn) University of Mississippi (T. Marshall) Embry-Riddle Aeronautical University (Christopher Phelps)	OSF
Numerical Weather Modeling	R.P. Wesenberg 867-4438 DL-ESS-31	R*SCAN Corporation ASTER Corporation	OCP
Measurement of Electro-magnetic Enhancement Due to Site Nonuniformities	L.M. Maier 867-4993 TE-CID-3		OSF
Atmospheric Science Field Laboratory (ASFL)	R.P. Wesenberg 867-4438 DL-ESS-31		OCP/ OSF
Solid State Instrumentation for Electric Field Detection of Lightning Potential	R.J. Wojtasinski 867-4993 TE-CID-3	Weather Corporation (R. Markson) (J. Goyaert) (B. Anderson)	OCP
<u>ARTIFICIAL INTELLIGENCE</u>			
Checkout, Control, and Monitor Subsystem (CCMS) Operations Analyst (OPERA) Expert System	A.E. Heard, P.P. Pinkowski 867-3926 TE-LPS-11	The MITRE Corporation (Dr. R. A. Adler) GTSI (R. B. Hasken)	OSF
Remote Maintenance Monitoring System	M. Lougheed, T. Ross 867-4946 TE-LPS-13A		OSF
Expert Mission Planning and Replanning Scheduling System	R.L. Pierce 867-3526 CS-ISO		OSF

ITEM	RESPONSIBLE INDIVIDUAL	PARTICIPATING ORGANIZATION	NASA HEAD-QUARTERS SPONSOR*
Automatic Test Expert Aid System Environment (AT-EASE)	M. Lougheed 867-4946 TE-LPS-13A		OSF
<u>BIOMEDICAL</u>			
Biological Flight Research Program: Chromosomes and Plant Cell Division in Space	Dr. W.M. Knott 853-5142 MD-RES-L		OSSA
Muscle Exercise Machine for Concentric Only Exercise	D.F. Doerr 867-3152 MD-ENG A.B. Maples, C.M. Campbell 867-4742 MD-ENG-A		OSSA
Human Physiology Research Projects: Blood Pressure Control	Dr. V.A. Convertino 867-4237 MD-RES-P		OSSA
Controlled Ecological Life Support System (CELSS) Breadboard Project	Dr. W.M. Knott 853-5142 MD-RES-L		OSSA
Environmental Monitoring Program	Dr. A.M. Koller 867-3165 MD-PLN Dr. W. M. Knott 853-5142 MD-RES-L	The Bionetics Corporation (Dr. C. R. Hinkle)	OSSA
Controlled Animal Nutrients Delivery System (CANDS)	Dr. W.M. Knott 853-5142 MD-RES-L		OSSA
<u>OPERATIONS</u>			
Telemetry Data Processing Using Microcomputers	A.J. Mackey, D.A. Brown 853-9353 CV-DSD-1	Computer Sciences Corporation (C. Mitchell)	
Expendable Launch Vehicle (ELV) Payload Processing Historical Data Retrieval Study	S.P. Green 867-3374 CP-APO		OSF

ITEM	RESPONSIBLE INDIVIDUAL	PARTICIPATING ORGANIZATION	NASA HEAD-QUARTERS SPONSOR*
Orbiter Spare Quantification Methods	M.M. Groh-Hammond 867-5381 TL-FGP-4		OSF
Certification of a Microwave Landing System Using the Global Positioning System	J.J. Kiriazes 867-4068 TE-CID-3 M.M. Scott 867-3475 DL-ESS-32	Lockheed Space Operations Company, Navigational Aids Group	OSF
<u>FIBER OPTICS AND COMMUNICATIONS</u>			
Hydrogen Detection Television Camera	J. Kassak 867-4548 DL-ESS-12	Lockheed Space Operations Company (D. Exley)	CDDF
DC to 150-Megabits-per-Second Fiber Optic Link Development	P.T. Huang 867-4548 DL-ESS-12		OSF
Microwave Fiber Optic Link Study	P.T. Huang 867-4548 DL-ESS-12		OCP
<u>TECHNOLOGY UTILIZATION</u>			
Alarm Processing and Diagnostic System Using NASA's Knowledge-Based Autonomous Test Engineer (KATE) Technology	T.C. Davis 867-3494 PT-AST	Electric Power Research Institute (J. Naser)	OCP
Feasibility Analysis of a High-Efficiency Dehumidifier/Air Conditioner Using Heat Pipes	J.K. O'Malley 867-3688 DF-FED-33	Florida Solar Energy Center (M. K. Khatter)	OCP
Development of a Digital Hearing Aid	R.M. Davis 867-2780 PT-AST	Central Institute for the Deaf, St. Louis, Missouri (A. M. Engebretson, D.Sc.) Washington University, St. Louis, Missouri (R. E. Morley, Jr., D.Sc.)	OCP

**ORIGINAL PAGE IS
OF POOR QUALITY**

ITEM	RESPONSIBLE INDIVIDUAL	PARTICIPATING ORGANIZATION	NASA HEAD-QUARTERS SPONSOR*
EPCOT Project	Dr. W.M. Knott 853-5142 MD-RES-L		OCP
<u>CRYOGENICS</u>			
Two-Phase Pressure Drops in Developing and Fully Developed Pipe Flow of Dispersed Liquid/Vapor Mixtures Under Zero-Gravity Environment	F.N. Lin 867-4181 DM-MED-11	University of Illinois (B.T. Chad)	OSF
Clamshell Bellows Repair Technique With Hastelloy C-22 Material	W.I. Moore 867-7777 DM-MED-4 J.E. Fesmire 867-3313 DM-MED-43		OSF
Temperature-Sensitive Variable-Area Joule-Thomson Expansion Nozzle and Cryocooler Development Program	F.S. Howard 867-4181 DM-MED-11		OCP
<u>DIGITAL ELECTRONICS</u>			
Partial Payload Checkout Unit	R.M. Ferguson 867-3811 DL-DSD J. E. Sudermann 867-3466 CS-EED-31 E.G. Sherrill 867-3646 CP-FGO		OSF
High-Speed Data Filter	R.B. Hanson 867-3366 DL-DSD-12		OSF
Generic Checkout System (GCS)	R.D. Luken 867-2977 DL-DSD-1		OSF

ITEM	RESPONSIBLE INDIVIDUAL	PARTICIPATING ORGANIZATION	NASA HEAD-QUARTERS SPONSOR
High-Speed Pulse Code Modulation (PCM) Processing System	W.M. Prince, J.J. Escoffier 867-3314 DL-DSD-1 R.B. Hanson DL-DSD-12		OSF
Manchester Interface for VME Bus	J.M. Lunceford 867-3842 DL-DSD-11		OSF
<u>MECHANISMS</u>			
Telescoping Tube	A.C. Littlefield 867-7585 DM-MED-31		OSF

- *OCP = Office of Commercial Programs
- CDDF = Center Director's Discretionary Fund
- OSF = Office of Space Flight
- OSSA = Office of Space Sciences and Applications

1. Report No NASA TM 100986		2. Government Accession No.		3. Recipient's Catalog No.	
4. Title and Subtitle Research and Technology 1988 Annual Report of the Kennedy Space Center				5. Report Date December 1988	
				6. Performing Organization Code PT-PMO	
7. Author(s)				8. Performing Organization Report No.	
				10. Work Unit No.	
9. Performing Organization Name and Address NASA John F. Kennedy Space Center Kennedy Space Center, Florida 32899				11. Contract or Grant No.	
				13. Type of Report and Period Covered Technical Memorandum 1988	
12. Sponsoring Agency Name and Address National Aeronautics and Space Administration Washington, DC 20546				14. Sponsoring Agency Code	
15. Supplementary Notes					
16. Abstract As the NASA Center responsible for assembly, checkout, servicing, launch, recovery, and operational support of Space Transportation System elements and payloads, Kennedy Space Center is placing increasing emphasis on the Center's research and technology program. In addition to strengthening those areas of engineering and operations technology that contribute to safer, more efficient, and more economical execution of our current mission, we are developing the technological tools needed to execute the Center's mission relative to future programs. The Engineering Development Directorate encompasses most of the laboratories and other Center resources that are key elements of research and technology program implementation, and is responsible for implementation of the majority of the projects in this Kennedy Space Center 1988 Annual Report. For further technical information about the projects, contact David A. Springer, Projects Management Office, DE-PMO, (407) 867-3035. Thomas M. Hammond, Technology Utilization Officer, PT-PMO, (407) 867-3017, is responsible for publication of this report and should be contacted for any desired information regarding the Center-wide research and technology program.					
17. Key Words (Suggested by Author(s)) Research and Technology			18. Distribution Statement Unclassified - Unlimited Subject Category 99		
19. Security Classif. (of this report) Unclassified		20. Security Classif. (of this page) Unclassified		21. No. of pages	22. Price